Division of Engineering Mechanics

STANFORD UNIVERSITY

Technical Report No. 148

MOVING CONTACT PROBLEMS OF A RIGID PROFILE ON A VISCOELASTIC BASE

by

J. N. Goodier and C. B. Loutzenheiser

July 1964

Prepared under Office of Naval Research

Contract Nonr 225(29)

(NR-064-241)

ABSTRACT

Two-dimensional steady-state solutions (suitable for computer evaluation) are given for moving normal contact loads (sliding or rolling) on the surface of a semi-infinite viscoelastic base, without restriction to simple profiles (e.g. circular cylinders) or to the simplest viscoelastic media (e.g. a single relaxation time, same behavior in shear and dilatation).

Examples worked out include (a) the rigid cylinder rolling on a material haveng 5 relaxation times; (b) the flat punch with corners rounded to eliminate infinite pressures. The results for (a) show that the variation of rolling resistance over a range of velocities becomes smoother with the greater number of relaxation times. The results for (b) show the dependence of the pressure peaks, near the ends of the contact, on the nature of rounding of the corners and the tilt of the punch.

Three dimensional solutions are considered for the purely viscous material. It is shown that there is a steady state for a base of finite thickness, but not for the semi-infinite base.

TABLE OF CONTENTS

NOTATION

References to the text are given in parentheses.

A	load or contact area (Fig. 1.1)
A_{jk}	coefficients in numerical procedure (eqn. 5.8a)
$B^*(t)$	creep function in dilatation (similar to Fig. 1.2)
$B(\tau)$	dimensionless form of $B^*(t)$ (eqn. 1.8b)
$B(k,\frac{1}{2})$	incomplete Beta function (p. 78)
C_k, D_k	coefficients in infinite series for displacement (eqns. 2.13, 2.14)
EEP	"equivalent elastic problem" (Sections 3.3, 3.4)
$Ei(x)$	exponential integral function (p. 56)
F^*	resultant horizontal force (eqn. 1.47, Fig. 1.8)
F	dimensionless form of F^* (eqns. 1.49, 1.51)
F_b	$= K_o/K_f > 1$
F_j	$= \mu_o/\mu_f > 1$
$G(x,y)$	function depending on the elastic surface displacement (eqn. 2.4, Fig. 2.1)
$G_\infty(y)$	$\lim_{x \to \infty} G(x,y)$
$H(t)$	unit step function (footnote 2, p. 8)
$I_o(x)$, $I_1(x)$	modified Bessel functions of the second kind
$J^*(t)$	creep function in shear (Fig. 1.2)
$J(\tau)$	dimensionless form of $J^*(t)$ (eqn. 1.8a)
$K_o(x)$, $K_1(x)$	modified Bessel functions of the second kind
K_o, K_f	initial, final elastic bulk modulus (eqn. 1.8b)
$K(\xi)$	kernel in integral for two-dimensional viscoelastic surface displacement (eqn. 1.42b)

N^*	total vertical load (Fig. 1.8)
N	dimensionless form of N^* (eqns. 1.48, 1.50)
N'	$= 2\rho N$, (eqn. 4.2b)
$P(x,y,z)$	potential function of pressure distribution (eqn. 1.2)
$P,Q;P_x,Q_x$	linear differential operators in viscoelastic stress-strain relations (eqns. 1.10a,b, 3.11)
$Q(\xi,\eta)$	dimensionless form of $q(x,y)$ (eqn. 1.29c)
$Q'(\xi)$	$= \rho Q(\xi)$, (eqn. 4.2a)
R	radius of rolling cylinder (Fig. 4.1)
$S_o(x)$	Struve's function
T^*	retardation time of viscoelastic material (p. 18)
T	characteristic time constant of viscoelastic material (p. 11)
U^*	vertical partical velocity (eqn. 1.38)
V	velocity of moving load or base (Figs. 1.1, 1.8)
$Y_o(x)$	Weber's Bessel function of the second kind
a	radius of circle (Sections 2.3, 2.4)
b	distance giving placement of contact surface (Fig. 3.1)
b_i	constants in model representation of viscoelastic material (p. 31)
d	length of flat portion of nearly flat punch (Fig. 5.4)
e_{ij}	deviator strains (p. 13)
e	dilatation (p. 13)
f	$= \int_0^\infty \gamma(\zeta)d\zeta$, constant of viscoelastic material

$g(\xi,\eta)$	dimensionless form of $G(x,y)$ (eqn. 2.10c)
h	Chapter II: thickness of finite layer (Fig. 2.11) Chapters IV,V: parameter in rolling cylinder problem (eqn. 4.11)
ℓ	actual length of contact region
m	ratio of Bessel functions (eqn. 4.16)
n	number of divisions of contact region (Chapter V)
$q(x,y)$	pressure distribution normal to surface (Fig. 1.1)
q_o, Q_o	constants representing magnitude of pressure
s	Laplace transform parameter (footnote, p. 17)
s_{ij}	deviator stresses (p. 13)
t	time
u_j	displacement components ($j = 1,2,3$)
u_z	vertical displacement at surface $z = 0$
v	$= u_z/VT$, dimensionless form of u_z
$w^*(x,y)$	function giving shape of contact surface (Section 3.1)
$w(\xi)$	dimensionless form of w^* in two-dimensional problem (eqn. 3.5b)
$w(\rho)$	dimensionless elastic surface displacement in Chapter II (eqn. 2.10b)
w_j	values obtained from $w(\xi)$ in numerical procedure (eqn. 5.8c)
x^*,y^*,z^*	cartesian coordinates fixed with respect to the base (Fig. 1.1)
x,y,z	cartesian coordinates fixed with respect to the load (eqn. 1.1)

α	small angle of tilt of rigid profile (Fig. 5.1)
β	$= b/VT$, dimensionless form of b (Fig. 5.1)
γ	Euler's constant = .5772157...
$\gamma(\zeta)$	characteristic creep function (eqn. 1.25)
δ	$= d/VT$, dimensionless form of d
δ_{ij}	Kronecker delta (footnote 2, p. 13)
$\delta(t)$	Delta function (footnote 2, p. 8)
ϵ_{ij}	total strain components (p. 13)
η	dimensionless coordinate; Section 5.5: ratio of rounded corner lengths (eqn. 5.24)
η^*	viscosity of purely viscous material (eqn. 2.1)
θ	$= \sigma_{kk}$; angle
θ_k	length of kth segment in numerical procedure
κ	$= K_o/\mu_o$
λ	$= \ell/VT$, dimensionless form of ℓ
μ_o, μ_f	initial, final elastic shear modulus
ν_o, ν_f	initial, final Poisson's ratio
ξ	$= x/VT$, dimensionless form of x
ρ	$= R/VT$, dimensionless form of R ; dimensionless radial coordinate (eqn. 2.10a)
σ_{ij}	stress components (p. 13)
τ	$= t/T$, dimensionless time (in Chapter II, defined by eqn. 2.10a)
ϕ	$= 2\rho\alpha$
χ	coefficient of friction (eqn. 1.53)
$\omega(\xi), \Omega_k(\xi)$	functions used in numerical procedure (eqns. 5.4b,d)

INTRODUCTION AND SUMMARY

Distributed loads moving over the surface of a deformable material are of frequent occurrence in engineering. Many technical operations involve a moving roller or slider. Impact of a high-speed jet on a moving surface, and certain cases of explosive loading and oblique impact equivalent to such jets[1], provide some of the less obvious examples. When the velocity of the load is small compared with stress-propagation speeds, inertia may be neglected and the problem treated as quasi-static. In this case, if the material is elastic the solution is the same as for the stationary load problem, but now carried along unchanged with the load. If, however, the stress depends not only on strain itself, but also on time derivatives of strain, the solution to the moving load problem has no such immediate relation to the corresponding stationary load solution.

In this investigation, a steady localized load moves at constant velocity in a straight line on the initially flat surface of a semi-infinite base. The base material is linearly viscoelastic, isotropic and homogeneous, with

---

[1] See, for example, Abrahamson [1][2].

[2] Numbers in brackets refer to the Bibliography.

stress-strain relations expressed in hereditary integral form (or as differential equations in special cases). It is free from body force, at constant temperature, and initially at rest and undisturbed. Inertia effects are neglected. The problems are considered with the usual assumptions of linear theory: infinitesimal strains, boundary conditions applied to the original undeformed surface.

The principal features of interest are:

(i) the possibility of a steady state when the load has been moving uniformly for a sufficiently long time;

(ii) the solution for such a steady state;

(iii) the rate of energy dissipation in the viscoelastic material.

A consequence of energy dissipation is that work is required to maintain the uniform velocity of a moving body applying the load, and the moving body encounters a resistance (e.g., rolling resistance).

The general problem of a moving load on a semi-infinite base is treated in Chapter I. It is shown that a steady state is always reached if the base is a solid, but there is no steady state if the base is a viscoelastic fluid. General expressions for surface displacement are developed, and some examples given. Moving loads on a purely viscous material are considered in Chapter II.

Specific results are given for a uniform circular load, showing the change in surface displacement with time. Although there is no steady state for a semi-infinite base, it is shown that for a base of finite thickness there is a steady state, its character depending on the way in which the lower boundary of the base is attached to its support.

The rest of the investigation is concerned with the steady state moving load problem resulting from the moving contact of a rigid body of given shape with the surface of a viscoelastic solid. The general theory of such contacts is considered in Chapter III. Further detailed analysis is limited to two-dimensional (plane strain) problems. The particular problem of a rolling rigid cylinder is considered in Chapter IV. Some results available in the literature, for materials of very restricted behavior, are examined and their limitations discussed. A numerical method for solving two dimensional moving contact problems is developed in Chapter V. The method, suitable for computer evaluation, can be used for very general contact profiles and any viscoelastic solid. Solutions are given for several rolling cylinder examples, illustrating the results for various materials over a range of contact times. Results for a material with five retardation times show that viscoelastic creep effects are much less pronounced, and the rolling resistance vs. velocity curve much smoother,

than for a simple material with a single retardation time. These results indicate that a single retardation time does not adequately characterize the behavior of actual materials in moving contact problems. Illustrative solutions are given also for a flat punch with corners slightly rounded. The pressure is everywhere finite, but there are sharp peaks at the ends of the contact. Results indicate how the pressure peaks depend on the nature of rounding of the corners and the tilt of the punch.

CHAPTER 1

GENERAL FEATURES OF MOVING LOAD PROBLEMS

The quasi-static problem of an arbitrary load moving uniformly on the initially flat surface of a semi-infinite linear viscoelastic base is considered in this chapter. In rectangular coordinates x^*, y^*, z^* fixed in the viscoelastic material, the base is taken as $z^* > 0$, with the surface $z^* = 0$. In this discussion, "load" refers to a pressure $q(x^*, y^*)$ applied normal to the surface over an area A. There are no tangential tractions and no other normal tractions applied to the surface. The load is moving at constant velocity V in a straight line parallel to the x^* axis (Fig. 1.1). For later convenience are introduced coordinates x, y, z moving with the load:

$$x = x^* - Vt \ , \ y = y^* \ , \ z = z^* \qquad (1.1)$$

where t is the time elapsed from some initial point.

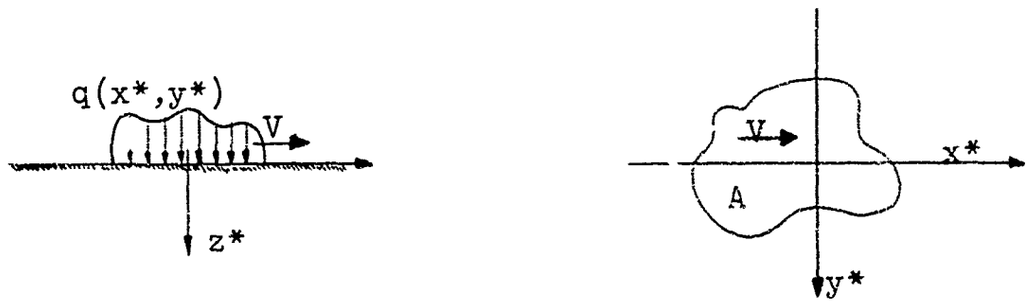

FIG. 1.1

1.1 Elastic Solution

The problem of a load on the surface of a semi-infinite elastic solid is the well-known Boussinesq problem, and the complete solution is readily available (see, for example, Love [22], p. 192). For the quasi-static moving load problem, the results are the same as for the load fixed, but carried along with the load. The moving load solution is thus the solution for the fixed load with x^* replaced by $x^* - Vt$, or expressed directly in x, y, z coordinates.

The elastic solution makes use of the potential of the pressure distribution:

$$P(x,y,z) = \frac{1}{2\pi} \iint_A \frac{q(x',y')}{r'} \, dx'dy' \qquad (1.2)$$

where $r' = \sqrt{(x-x')^2+(y-y')^2+ z^2}$ is the distance from a element at (x', y', 0) to the field point (x, y, z). In particular, the vertical displacement at the surface is

$$u_z^e (x, y, 0) = \frac{1-\nu}{\mu} P(x,y,0) \qquad (1.3)$$

where $u_z^e(x,y,z)$ is the displacement in the z direction (the superscript e indicates the elastic solution), ν is Poisson's ratio and μ the shear modulus of the elastic material. All displacements can be expressed in terms of $P(x,y,z)$ and $\int P(x,y,z)\, dz$, and from these the strains and stresses can be found.

In the two-dimensional problem of plane strain, the load does not vary with y, and extends infinitely far in the y direction. The problem can then be considered in the (x,z) plane, with a load q(x) (for a unit length in the y direction) applied over a segment of the x-axis of length ℓ. For convenience, this segment is taken as $0 \leq x \leq \ell$. The displacement u_z from the initially flat surface[1] is infinite (because as a three-dimensional problem the load is infinite), so displacement must be expressed relative to some arbitrary point on the surface. From (1.2),

$$P(x,0,0) = \frac{1}{2\pi} \int_0^{\ell} \int_{-\infty}^{\infty} \frac{q(x')}{\sqrt{(x-x')^2+(y')^2}} \, dx'dy'$$

$$= \frac{1}{\pi} \int_0^{\ell} q(x') \log|x-x'| dx' + \text{constant} \qquad (1.4)$$

Then,

$$u_z^e(x) = \Delta - \frac{1-\nu}{\mu} \frac{1}{\pi} \int_0^{\ell} q(x') \log|x-x'| dx' \qquad (1.5a)$$

where Δ is an arbitrary constant. The displacement relative to a point x_o on the surface is

$$u_z^e(x) - u_z^e(x_o) = \frac{1-\nu}{\mu} \frac{1}{\pi} \int_0^{\ell} q(x')[\log|x_o-x'| - \log|x-x'|]dx' \qquad (1.5b)$$

[1] u_z will always refer to the vertical displacement at the surface z = 0.

1.2 Linear Viscoelastic Materials

The stress-strain relations of viscoelastic materials are time dependent. At any instant they depend on the past history as well as the present state of the material. For any particular material, this time dependence is conveniently determined by a creep test. A constant stress is suddenly applied to an initially undisturbed specimen[1], and the resulting strain is measured. The function giving the strain variation with time for a unit applied stress is called the creep function, $J^*(t)$, of the material, i.e.,

$$\epsilon(t) = J^*(t) \quad \text{for}^2 \quad \sigma(t) = H(t)$$

$J^*(t)$ is necessarily zero for $t < 0$, since the material is initially undisturbed; $J^*(t)$ increases monotonically for $t > 0$.

A linear viscoelastic material has a ratio of stress to strain that is independent of the magnitude of the stress:

---

[1] Viscoelastic materials will always be considered initially undisturbed, with the load applied at $t = 0$; thus, $\epsilon(t) = \sigma(t) = 0$ for $t < 0$.

[2] $H(t)$ is the unit step function: $H(t) = \begin{cases} 0, & t<0 \\ 1, & t>0 \end{cases}$. Its derivative is the delta function, $\delta(t) = dH(t)/dt$, which has the properties

$$\delta(t) = 0 \text{ for } t \neq 0, \quad \int_{0^-}^{0+} \delta(t)f(t)dt = f(0).$$

$$\epsilon(t) = \sigma_o \, J^*(t) \quad \text{for} \quad \sigma(t) = \sigma_o \, H(t)$$

Many materials of practical interest can be considered linearly viscoelastic, at least for small enough applied stresses. This has the important consequence that the cumulative effect of several loadings is just the sum of the individual effects. The response to arbitrary time-varying stress is then obtained by superposition, leading to the hereditary integral stress-strain relation for linear viscoelastic materials:

$$\epsilon(t) = \int_0^t J^*(t-\tau) \, \frac{\partial \sigma(\tau)}{\partial \tau} \, d\tau \qquad (1.6)$$

If there are suddenly applied loads, the stress and strain histories will not be continuous functions of time, but will have jump discontinuities when these loads are applied. Treated in the classical manner, integrals such as (1.6) would need to be considered in several parts, with the effects of the jumps added as extra terms. It is more convenient to work with generalized functions--the step function and its derivatives--which take care of the effects of jump discontinuities without special consideration. This approach can be interpreted as the limiting case of rapidly-changing continuous functions. The use of generalized functions can, however, be established on a rigorous

mathematical basis[1]. If the discontinuity occurs at $t = 0$, the lower limit in integrals such as (1.6) is taken as 0^-, to include the effects of the jump. In this way, initial values of stress and strain functions and derivatives, taken at $t = 0^-$, are all zero for initially undisturbed materials. Initial values at $t = 0^+$ due to sudden loads at $t = 0$ are then accounted for by the generalized functions. This often eliminates the need for explicit evaluation of initial values of unknown functions, thus simplifying the solution of many viscoelastic problems. The use of generalized functions in viscoelastic problems is discussed by Corneliussen and Lee [5].

Viscoelastic materials fall into two general categories--solids and fluids. A viscoelastic solid has a finite upper limit to its creep after a long time. This means $J^*(t) \to 1/E_f$, a finite value, as $t \to \infty$. A viscoelastic fluid continues to creep without limit after a long time; thus $J^*(t) \to \infty$ as $t \to \infty$. The characterization of a viscoelastic material as solid or fluid depends on the extent of time appropriate to the particular problem. After a long enough time, a viscoelastic solid acts essentially as an elastic solid. The material exhibits its final elasticity, with final elastic modulus E_f. Most viscoelastic solids also have initial

---

[1] See Friedman [15] for the use of generalized functions in mathematical analysis, and for further references on the theoretical foundations.

elasticity. A suddenly applied stress produces an instantaneous response, then additional creep as time passes. In this case, $J^*(0^+) \equiv 1/E_o \neq 0$; E_o is the initial elastic modulus. If there is no initial elasticity, $J^*(0^+) = 0$. Representative creep curves are sketched in Fig. 1.2.

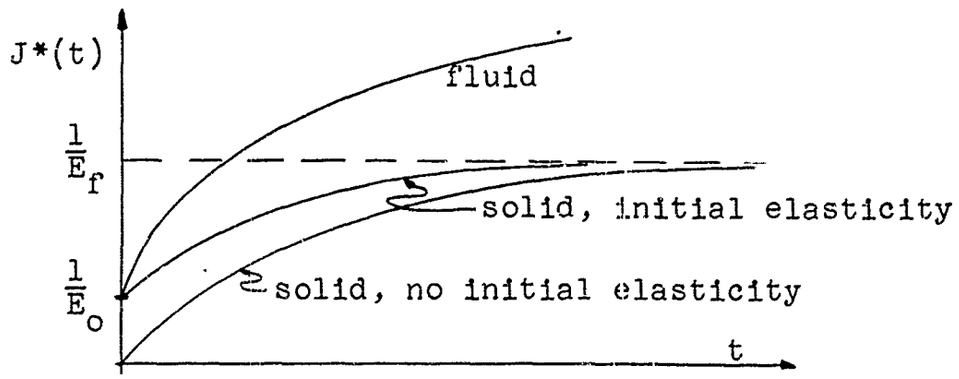

FIG. 1.2

It is convenient to express creep functions in non-dimensional form. An appropriate time parameter, T, is chosen. Viscoelastic materials may exhibit one or more characteristic retardation times, one of which can be used. Then, a non-dimensional time variable is taken as $\tau = t/T$. For a viscoelastic solid with initial elasticity, a dimensionless creep function is conveniently defined by $J(\tau) = E_o J^*(\tau T)$, and the final elastic response represented by $F = E_o\, J^*(\infty) = E_o/E_f$. Then, the stress-strain law (1.6) becomes

$$\epsilon(\tau) = \frac{1}{E_o} \int_{0^-}^{\tau} J(\tau-\zeta)\, \frac{\partial \sigma(\zeta)}{\partial \zeta}\, d\zeta \qquad (1.7)$$

with $J(0^+) = 1$, $J(\infty) = F$, $\tau = t/T$. This non-dimensional form based on an initial elastic response will be used in all that follows, unless otherwise noted.

The discussion so far has considered a one-dimensional state of stress and strain. In a general three-dimensional state, the response of a linear isotropic homogeneous viscoelastic material can be described by two independent creep functions. This is analogous to an isotropic elastic material where two elastic constants are sufficient. The two functions are conveniently taken as the shear creep function, $J^*(t)$, and the dilatation creep function, $B^*(t)$. For a material with initial elasticity, these are non-dimensionalized in terms of the initial elastic response and a common characterisitc time parameter T:

$$J(\tau) = 2\mu_o \, J^*(\tau T) \quad , \quad J(0^+) = 1 \tag{1.8a}$$

$$B(\tau) = 3K_o \, B^*(\tau T) \quad , \quad B(0^+) = 1 \tag{1.8b}$$

where μ_o is the initial elastic shear modulus and K_o is the initial elastic bulk modulus. If the material is a solid, with a final elastic response, the shear and dilatation creep functions will each approach a finite limit as $t \to \infty$. In this case, $J^*(\infty) = 1/2\mu_f$ and $B^*(\infty) = 1/3K_f$, where μ_f and K_f are the final elastic moduli. Then,

$$J(\infty) = F_j \quad ; \quad B(\infty) = F_b \tag{1.8c}$$

where $F_j = \mu_o/\mu_f > 1$, and $F_b = K_o/K_f > 1$.

General three-dimensional stress and strain is described in standard suffix notation[1], i,j taking on the values 1,2,3 corresponding to the coordinate axes $x_1 = x$, $x_2 = y$, $x_3 = z$.

Stress components: $\sigma_{ij}(x,y,z,t)$; $\theta = \sigma_{kk}$

Stress deviator components[2]: $s_{ij}(x,y,z,t) = \sigma_{ij} - \frac{1}{3}\theta\delta_{ij}$

Strain components: $\epsilon_{ij}(x,y,z,t)$; dilatation $e = \epsilon_{kk}$

Strain deviator components: $e_{ij}(x,y,z,t) = \epsilon_{ij} - \frac{1}{3} e\delta_{ij}$

Corresponding to (1.7), the stress-strain laws are[3]

$$e_{ij}(\tau) = \frac{1}{2\mu_o} \int_{o^-}^{\tau} J(\tau-\zeta) \frac{\partial s_{ij}(\zeta)}{\partial\zeta} \, d\zeta \; ; \tag{1.9a}$$

$$e(\tau) = \frac{1}{3K_o} \int_{o^-}^{\tau} B(\tau-\zeta) \frac{\partial\theta(\zeta)}{\partial\zeta} \, d\zeta \tag{1.9b}$$

---

1 The summation convention is used, so that repeated indices mean a sum of terms with index values 1, 2, 3.

2 δ_{ij} is the Kronecker delta symbol: $\delta_{ij} = 0$ for $i \neq j$, $\delta_{ij} = 1$ for $i = j$.

3 The stress-strain components are of course functions of the space variables (x,y,z) as well as time; this is not explicitly indicated.

For an elastic material the creep functions are just the step functions, $H(\tau)$. In this case, (1.9a,b) reduce to the stress-strain laws for an elastic body:

$$e_{ij} = \frac{1}{2\mu_o} s_{ij} \quad ; \quad e = \frac{1}{3K_o} \theta \tag{1.9c}$$

Mechanical models, made up of suitable combinations of springs and dashpots, can be used to represent viscoelastic materials. The load-deformation behavior of such models exhibits many of the important features of actual materials. By taking a large number of elements in a model, a particular material can often be approximated quite closely. The springs allow for storage and recovery of energy and the dashpots allow dissipation of energy that is characteristic of viscoelastic materials. In fact, molecular theories of viscoelasticity have been based on this type of model (see, for example, Bland [3]). For three-dimensional states, two such models would be necessary in general, to represent shear and dilatation. The advantage of using models is that the creep function can then be expressed in a simple analytic form, as a sum of exponential terms. This permits mathematical analysis of viscoelastic problems to be carried much further than would otherwise be possible, bringing to light significant features of the solution that are characteristic of actual materials.

Model representation permits a stress-strain law to be expressed as a linear differential equation, rather than the integral equation (1.7). This can be expressed

$$P(\sigma) = Q(\epsilon) \tag{1.10a}$$

where P and Q are linear differential operators of the form

$$P = \sum_{k=0}^{n} p_k \frac{\partial^k}{\partial t^k} \quad , \quad Q = \sum_{k=0}^{m} q_k \frac{\partial^k}{\partial t^k} \tag{1.10b}$$

p_k and q_k being constants for the particular model. In three-dimensional problems, two sets of operators are needed.

For shear $$P(s_{ij}) = Q(e_{ij}) \tag{1.11a}$$

and for dilatation $$P'(\theta) = Q'(e) \tag{1.11b}$$

More details and further references on viscoelastic models and their differential equations are given in Lee [20], Bland [3], and Kelly [18].

A convenient model to use is the general Voigt material. This is made up of a series of Kelvin elements (spring and dashpot in parallel), with a separate spring to represent initial elasticity if it is present (see Fig. 1.3). A model representing a viscoelastic fluid must also have a separate dashpot, giving unlimited creep under load. For each Kelvin element, the stress-strain law is of the form[1]

[1] A dot indicates the derivative with respect to time: $\dot{f}(t) = \partial f/\partial t$.

$\sigma = E(\epsilon + T\dot{\epsilon})$, where $T = \eta/E$ is the retardation time of the element. A Voigt material thus has n characteristic retardation times, one for each Kelvin element, with an initial elastic modulus E_o and a final elastic modulus $E_f = E_o + \sum_{k=1}^{n} E_k$. The simplest model that exhibits the initial response, delayed creep, and final elasticity characteristic of a viscoelastic solid is a Voigt solid with a single retardation time, called the standard linear (or three parameter) solid (see Fig. 1.3).

General Voigt Material (fluid)

(A Voigt solid has no free dashpot, i.e., $\eta_c = \infty$.)

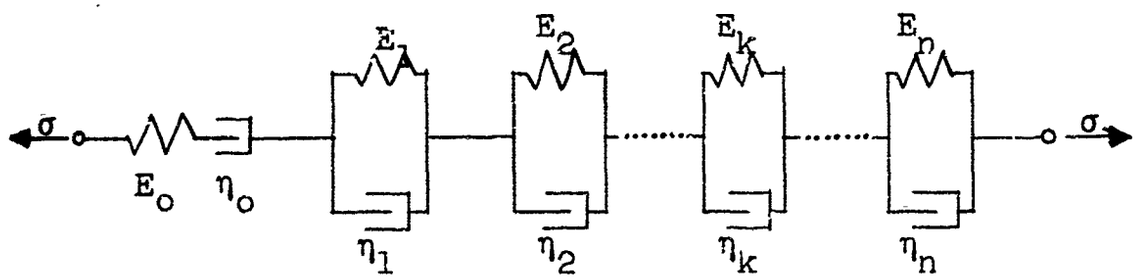

Standard linear solid

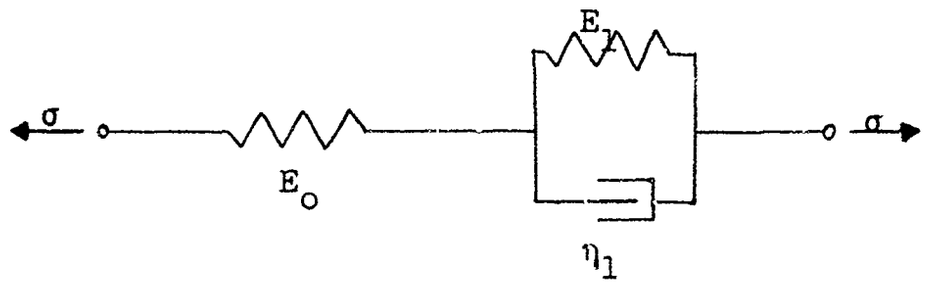

FIG. 1.3

More Kelvin elements with different retardation times can be added to give a more complex model that may in certain cases satisfactorily approximate a real material. However, real materials appear to have no discrete retardation times, so a model with a large number of elements is usually necessary to accurately represent an actual material over a long time span. The determination of constants to fit such a model to a test curve can be very tedious, and the result is still only an approximation. It is frequently more desirable to use the test curve directly in an integral law such as (1.9), which can be evaluated numerically. The approximation is then numerical rather than physical, and the resulting error can be estimated and controlled more readily.

The creep function for a model material can be determined directly from the differential law (1.10) by using the Laplace transform[1]. The linear differential operators P and Q become polynomials in s, so that (1.10) transforms to

$$\bar{P}(s)\ \bar{\sigma} = \bar{Q}(s)\ \bar{\epsilon} \qquad (1.12)$$

where

$$\bar{P}(s) = \sum_{k=0}^{n} p_k\, s^k \quad , \quad \bar{Q}(s) = \sum_{k=0}^{m} q_k\, s^k$$

---

[1] The Laplace transform of function f(t) is: $\bar{f}(s) \equiv \mathcal{L}\{f(t)\} \equiv \int_{0^-}^{\infty} e^{-st} f(t)dt$. It is taken in the generalized sense, starting at $t = 0^-$, to include the effects of discontinuities at $t = 0$.

From the definition of a creep function, $\epsilon(t) = J^*(t)$ when $\sigma(t) = H(t)$, thus $\bar{\epsilon}(s) = \bar{J}^*(s)$ when $\bar{\sigma}(s) = 1/s$. Then from (1.12),

$$\bar{J}^*(s) = \frac{1}{s}\,\frac{\bar{P}}{\bar{Q}} \tag{1.13}$$

For a general Voigt material (Fig. 1.3), the result is

$$\bar{J}^*(s) = \frac{1}{E_o}\cdot\frac{1}{s} + \frac{1}{\eta_o}\cdot\frac{1}{s^2} + \frac{1}{s}\cdot\sum_{k=1}^{n}\frac{1}{E_k + s\eta_k}$$

$$= \frac{1}{E_o}\cdot\frac{1}{s}\left[1 + \frac{1}{sT_o^*} + \sum_{k=1}^{n}\frac{f_k}{1 + sT_k^*}\right] \tag{1.14}$$

where $T_k^* = \eta_k/E_k$ is the retardation time of the k^{th} Kelvin element, $f_k = E_o/E_k$, and $T_o^* = \eta_o/E_o$. This model is a fluid material, because of the presence of the free dashpot with viscosity η_o. In a solid, there is no free dashpot, and this term in (1.14) is absent ($\eta_o = \infty$, $T_o^* = \infty$). From (1.14), the creep function is

$$J^*(t) = \frac{1}{E_o}\left[1 + \frac{t}{T_o^*} + \sum_{k=1}^{n} f_k(1 - e^{-t/T_k^*})\right]H(t) \tag{1.15a}$$

This has the initial response $J^*(0^+) = \frac{1}{E_o}$, and the long-time unlimited creep $J^*(t) \sim t/\eta_o$ as $t \to \infty$. With the η_o term absent, the solid has a final limiting value of creep $J^*(\infty) = 1/E_f = (1/E_o)(1 + \sum_{1}^{n} f_k)$.

In dimensionless form,

$$J(\tau) = [1 + \frac{\tau}{T_o} + \sum_{1}^{n} f_k(1 - e^{-\tau/T_k})]H(\tau) \qquad (1.15b)$$

where $\tau = t/T$, $T_k = T_k^*/T$ and T is a characteristic time parameter. Then, $J(0^+) = 1$, and $J(\infty) \equiv F = 1 + \sum_{k=1}^{n} f_k$. For a standard linear solid, $n = 1$, $T = T_1^*$. Then,

$$J(\tau) = 1 + f(1 - e^{-\tau}) \; ; \quad J(\infty) \equiv F = 1 + f$$

Most experimental data on actual viscoelastic materials, such as high polymers, provide information on the behavior in shear or simple tension. Very few tests have measured dilatation alone, so data for the creep curve $B(\tau)$ are frequently not available. In the absence of specific information, several assumptions of dilatational behavior have been made. Each may, in certain circumstances, be a good approximation to actual behavior[1]. The common assumptions are:

1) elastic dilatation, $B(\tau) = H(\tau)$

2) incompressible, $K_o = \infty$, $B(\tau) = 0$

3) similar behavior in shear and dilatation, $B(\tau) = J(\tau)$

In terms of Poisson's ratio, ν , which is discussed in the next section, 2) corresponds to $\nu = 1/2$, and 3) corresponds

[1] For further discussion, see Staverman and Schwarzl [29], Section 6d; Ferry [9], Chapter 18.

to $\nu = \nu_o$ = constant. Even when actual data are available, use of one of these assumptions may lead to significant simplifications in the analysis of a problem, without being too seriously in error.

1.3 Solution of Viscoelastic Moving Load Problems

Many problems in viscoelasticity can be solved by removing the time dependence with a Laplace transform[1], which reduces the viscoelastic problem to an "associated elastic problem" (Lee [19, 20]). Taking a Laplace transform of the viscoelastic stress-strain laws (1.9a,b) gives

$$\bar{e}_{ij} = \frac{1}{2\mu_o} s \bar{J}(s) \bar{s}_{ij} ; \quad \bar{e} = \frac{1}{3K_o} s \bar{B}(s) \bar{\theta} \qquad (1.16)$$

These are the same as the transforms of the elastic laws (1.9c) if μ_o is replaced by $\mu_o/s\bar{J}$ and K_o by $K_o/s\bar{B}$. If a Laplace transform of the boundary conditions is possible, the viscoelastic problem becomes an elastic problem in the transformed variables, with the elastic constants now functions of the transform parameter s. This is the associated elastic problem, and if its solution can be found, the viscoelastic solution is obtained by inversion of the Laplace transform.

---

[1] The Laplace transform is taken with respect to the dimensionless time $\tau = t/T$. The generalized transform, starting at $t = 0^-$, will always be used. In this way, initial conditions are all zero for an initially undisturbed material.

For an associated elastic problem to exist, it must be possible to transform the boundary conditions. There are two types of boundary conditions: tractions prescribed on a region R_1 of the boundary surface, and displacements prescribed on a region R_2 of the surface. If the regions R_1 and R_2 do not change with time (the quantities prescribed on them may vary with time, however), then a Laplace transform is possible. If R_1 or R_2 change with time, a Laplace transform of the boundary conditions is not generally possible, and the above method of solution is not applicable.

A procedure equivalent to solving the associated elastic problem (when it exists) is to solve the original viscoelastic problem as an elastic problem (with the same boundary conditions as the viscoelastic problem), take the Laplace transform of this solution, and replace the elastic constants by their appropriate viscoelastic analogues from (1.16). This is often much easier than solving the associated elastic problem directly; use can be made of existing solutions from the theory of elasticity. Frequently, the elastic solution is in the form of functions of space and time multiplied by rational functions of the elastic constants. The transformed viscoelastic solution is then a product of the transformed elastic solution and creep functions, and the inversion is just a convolution integral. In replacing the elastic constants according to (1.16), the

term $s\bar{J}$ (or $s\bar{B}$) occurs. This is the transform of $\dot{J}(\tau) \equiv dJ(\tau)/d\tau$ [or $\dot{B}(\tau) \equiv dB(\tau)/d\tau$]. The viscoelastic solution is thus a convolution of appropriate creep function derivatives with the elastic solution.

As an example, suppose an elastic solution has the form

$$g^e(x,y,z,\tau) = \frac{1}{\mu} f(x,y,z,\tau)$$

Taking Laplace transforms gives

$$\bar{g}^e(x,y,z,s) = \frac{1}{\mu} \bar{f}(x,y,z,s)$$

Replacing μ by $\mu_o/s\bar{J}$ gives the solution of the associated elastic problem, and inverting gives the viscoelastic solution

$$g(x,y,z,\tau) = \frac{1}{\mu_o} \int_o^\tau \dot{J}(\zeta)\, f(x,y,z,\tau-\zeta)d\zeta$$

Elastic solutions frequently contain Poisson's ratio, $\nu = (3K - 2\mu)/2(3K + \mu)$, which depends on both shear and dilatation properties of the material. In forming an associated elastic problem, ν is replaced by this same function of the transformed creep functions:

$$\nu \rightarrow \left(\frac{3K_o}{s\bar{B}} - \frac{2\mu_o}{s\bar{J}}\right)/2\left(\frac{3K_o}{s\bar{B}} + \frac{\mu_o}{s\bar{J}}\right) = \frac{3K_o s\bar{J} - 2\mu_o s\bar{B}}{2(3K_o s\bar{J} + \mu_o s\bar{B})} \qquad (1.17a)$$

This can be considered the transform of a viscoelastic Poisson's ratio, $\nu(\tau)$, which varies with time, so that

$$s\,\bar{\nu}(s) \equiv \frac{3K_o s\bar{J} - 2\mu_o s\bar{B}}{2(3K_o s\bar{J} + \mu_o s\bar{B})} \tag{1.17b}$$

Then, ν is replaced by $s\bar{\nu}(s)$ in the associated elastic problem.

From the initial and final value theorems of Laplace transforms (see, for example, Thomson [33]),

$$\nu(0^+) = \lim_{s\to\infty} s\bar{\nu}(s) = \frac{3K_o - 2\mu_o}{2(3K_o + \mu_o)} \equiv \nu_o \tag{1.18a}$$

where ν_o is the Poisson's ratio of the initial elastic response, and

$$\nu(\infty) = \lim_{s\to 0} s\bar{\nu}(s) \equiv \nu_f \tag{1.18b}$$

where ν_f is the final value of Poisson's ratio. If the material has a final elastic response, then its Poisson's ratio is $\nu_f = (3K_f - 2\mu_f)/2(3K_f + \mu_f)$. Using (1.8c) this becomes

$$\nu_f = \frac{1}{2}\,\frac{3K_o - 2\mu_o + 2\mu_o(F_j - F_b)/F_j}{3K_o + \mu_o - \mu_o(F_j - F_b)/F_j}$$

Thus, $\nu_f > \nu_o$ if $F_j > F_b$, and $\nu_f < \nu_o$ if $F_j < F_b$. If the material is fluid in shear and solid in dilatation, so that $J(\infty) = \infty$ while $B(\infty)$ is finite, then $\nu_f = 1/2$.

An example of a simple model that exhibits features similar to more general viscoelastic solids is one with standard linear solid behavior in shear, and elastic dilatation.

Then[1],

$$J(\tau) = [1 + f(1-e^{-\tau})]H(\tau) \; ; \; B(\tau) = H(\tau)$$

$$\bar{J}(s) = s\bar{J}(s) = 1 + \frac{f}{1+s} \; ; \; \bar{B}(s) = s\bar{B}(s) = 1$$

$$s\bar{\nu}(s) = \frac{3K_o[1 + f/(1+s)] - 2\mu_o}{2[3K_o[1 + f/(1+s)]+\mu_o}$$

$$= \nu_o\left[1 + \frac{9fK_o\mu_o}{(3K_o-2\mu_o)(3K_o+\mu_o)} \; \frac{1}{s + [1 + 3K_of/(3K_o+\mu_o)]}\right]$$

$$\nu(\tau) = \nu_o\left[1 + \frac{9fK_o\mu_o}{(3K_o-2\mu_o)(3K_o+\mu_o+3K_of)} [1-\exp(-\frac{3K_o+\mu_o+3K_of}{3K_o+\mu_o} \tau)]\right]H(\tau)$$

For example, if $K_o = (8/3)\mu_o$, then $\nu_o = 1/3$,
$\nu_f = (3+4f)/(9+8f)$,

$$\nu(\tau) = \frac{1}{3}\left[1 + \frac{4f}{9+8f} [1-\exp(-\frac{9+8f}{9} \tau)]\right]H(\tau)$$

For additional examples and discussion of Poisson's ratio, see Kelly [18], Freudenthal et al. [14].

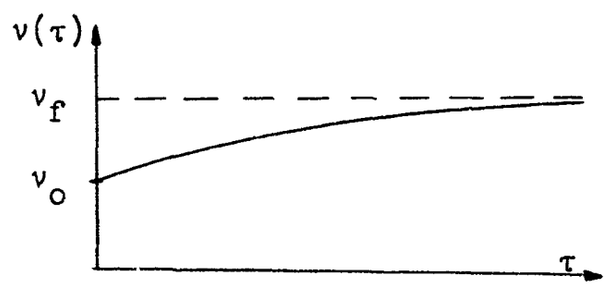

FIG. 1.4

[1] The retardation time T^* is taken as the time parameter T.

For the present problem of a given load moving on the surface of a semi-infinite base, boundary conditions on the surface z = 0 are

$$\sigma_z(x^*- Vt,y,0) = \begin{cases} -q(x^*-Vt,y) & \text{under the load} \\ 0 & \text{outside the load} \end{cases} \quad (1.19a)$$

$$\tau_{xz}(x^*,y^*,0) = \tau_{yz}(x^*,y^*,0) = 0 \quad \text{everywhere} \quad (1.19b)$$

Since the tractions at each point on the surface are known for all time, a Laplace transform of the boundary conditions is possible, and the problem can be solved as an associated elastic problem. The vertical surface displacement u_z (on z = 0) will be considered in detail. The same procedure can be used with the known elastic solution to find the viscoelastic displacements and stresses at all points in the semi-infinite material.

The elastic solution, as given in (1.2), (1.3), is

$$u_z^e(x^*- V\mathrm{T}\tau,y^*,0) = \frac{1-\nu}{\mu} P(x^*- V\mathrm{T}\tau,y^*,0) \quad (1.20)$$

$$P(x^*- V\mathrm{T}\tau,y^*,0) = \frac{1}{2\pi} \iint_A \frac{q(x',y')dx'dy'}{\sqrt{(x^*-V\mathrm{T}\tau-x')^2+(y^*-y')^2}}$$

The superscript e indicates the elastic solution. Taking a Laplace transform gives

$$\bar{u}_z^e(x^*,y^*,s) = \frac{1-\nu}{\mu} \bar{P}(x^*,y^*,s)$$

Replacing the elastic constants according to (1.16), (1.17a) gives the associated elastic solution

$$\bar{u}_z = \frac{1}{\mu_o} s\bar{J}(s)[1 - s\bar{\nu}(s)]\ \bar{P}(x^*,y^*,s) \qquad (1.21)$$

Inversion then gives the desired viscoelastic surface displacement.

Although (1.21) could be formally inverted as it stands, in the form of a convolution integral, the final result is seen more clearly by proceeding further. Let

$$\begin{aligned} J(\tau) &= [1 + J_1(\tau)]H(\tau) \\ B(\tau) &= [1 + B_1(\tau)]H(\tau) \end{aligned} \qquad (1.22a)$$

with

$$J_1(0) = B_1(0) = 0$$

Then

$$s\bar{J}(s) = 1 + s\bar{J}_1(s)\ ;\quad s\bar{B}(s) = 1 + s\bar{B}_1(s) \qquad (1.22b)$$

Also, let $\kappa \equiv K_o/\mu_o$ Then (1.18a) becomes

$$\nu_o = (3\kappa-2)/2(3\kappa+1) \qquad (1.23)$$

From (1.17b), after simplification,

$$1 - s\bar{\nu}(s) = (1-\nu_o)\left[1 - \frac{9\kappa}{3\kappa+4}\ \frac{s\bar{J}_1 - s\bar{B}_1}{3\kappa+1 + 3\kappa s\bar{J}_1 + s\bar{B}}\right] \qquad (1.24)$$

Then, using (1.22b) and (1.24),

$$\frac{1}{\mu_o} s\bar{J}(s)[1-s\bar{\nu}(s)] = \frac{1-\nu_o}{\mu_o}\left[1 + s\bar{J}_1 - \frac{9\kappa}{3\kappa+4} \cdot \frac{s\bar{J}_1 - s\bar{B}_1}{3\kappa+1+3\kappa s\bar{J}_1+s\bar{B}_1}(1+s\bar{J}_1)\right]$$

Now let $\gamma(\tau)$ be a new function such that

$$\bar{\gamma}(s) = s\bar{J}_1 - \frac{9\kappa}{3\kappa+4} \frac{s\bar{J}_1 - s\bar{B}_1}{3\kappa+1 + 3\kappa s\bar{J}_1+s\bar{B}_1}(1+s\bar{J}_1) \quad (1.25)$$

Then (1.21) can be written

$$\bar{u}_z = \frac{1-\nu_o}{\mu_o}[1 + \bar{\gamma}(s)]\,\bar{P}(x^*,y^*,s)$$

Inverting this gives the desired surface displacement

$$u_z(x^*,y^*,\tau) = \frac{1-\nu_o}{\mu_o} P(x^*-V\tau,y^*,0) + \frac{1-\nu_o}{\mu_o}\int_o^\tau \gamma(\zeta)P(x^*-V\tau+V\zeta,y^*,0)d\zeta$$

$$= u_z^e(x^*-V\tau,y^*) + \int_o^\tau \gamma(\zeta)\, u_z^e(x^*-V\tau + V\zeta,\, y^*)d\zeta$$

where u_z^e is the displacement due to the initial elastic response, given by (1.2,3) for a three-dimensional problem, and by (1.5b) for a two-dimensional (plane strain) problem. Expressed in coordinates moving with the load

$(x = x^* - V\tau,\ y = y^*)$,

$$u_z(x,y,\tau) = u_z^e(x,y) + \int_o^\tau \gamma(\zeta)\, u_z^e(x + V\zeta,y)d\zeta \qquad (1.26)$$

The explicit evaluation of u_z requires the function $\gamma(\tau)$. If the creep functions $J(\tau)$ and $B(\tau)$ can be expressed analytically, so that their Laplace transforms can be found, then direct inversion of (1.25) gives $\gamma(\tau)$. However, for actual materials, the creep functions cannot usually be expressed in simple analytic form, but are available only as curves or tabulated values from tests. Instead of the several approximations and considerable labor that may be needed to fit a curve with an analytic function, take its transform, then invert (1.25), it is better to obtain $\gamma(\tau)$ directly from the given data by a numerical procedure.

For this purpose, (1.25) can be written:

$$\bar{\gamma}(s)\left[1 + \frac{3\kappa s\bar{J}_1 + s\bar{B}_1}{3\kappa + 1}\right] = s\bar{J}_1 + \frac{1}{3\kappa+1}\,(3\kappa s\bar{J}_1 + s\bar{B}_1)\; s\bar{J}_1$$

$$- \frac{9\kappa}{(3\kappa+4)(3\kappa+1)}\,[s\bar{J}_1 - s\bar{B}_1 + s\bar{J}_1(s\bar{J}_1 - s\bar{B}_1)]$$

$$= s\bar{J}_1 - \frac{9\kappa}{(3\kappa+4)(3\kappa+1)}\,(s\bar{J}_1 - s\bar{B}_1) + \frac{3\kappa s\bar{J}_1 + 4s\bar{B}_1}{3\kappa+4}\; s\bar{J}_1$$

Inversion of this gives

$$\gamma(\tau) + \int_0^\tau \frac{3\kappa\dot{J}_1(\zeta) + \dot{B}_1(\zeta)}{3\kappa+1}\,\gamma(\tau-\zeta)\,d\zeta = \dot{J}_1(\tau)$$

$$- \frac{9\kappa}{(3\kappa+4)(3\kappa+1)}\,[\dot{J}_1(\tau) - \dot{B}_1(\tau)] + \int_0^\tau \frac{3\kappa\dot{J}_1(\zeta) + 4\dot{B}_1(\zeta)}{3\kappa+4}\,\dot{J}_1(\tau-\zeta)\,d\zeta \qquad (1.27)$$

This is a Volterra integral equation of the second kind for the unknown function $\gamma(\tau)$. It can be solved numerically by a finite difference method, requiring numerical values of the derivative of each creep function at intervals from 0 to τ. A procedure for solving such integral equations has been developed and discussed by Lee and Rogers [21]. Using a slight modification of their procedure, equation (1.27) can be solved numerically as follows: Let

$$\dot{M}(\zeta) = \frac{1}{3\kappa+1}\left[3\kappa\dot{J}_1(\zeta) + \dot{B}_1(\zeta)\right]$$

$$F(\tau) = \dot{J}_1(\tau) - \frac{9\kappa}{(3\kappa+4)(3\kappa+1)}(\dot{J}_1-\dot{B}_1) + \int_0^\tau \frac{3\kappa\dot{J}_1(\zeta)+4\dot{B}_1(\zeta)}{3\kappa+4}\,\dot{J}_1(\tau-\zeta)\,d\zeta$$

$M(\zeta)$ and $F(\tau)$ are known or can be found from the given creep functions $J(\tau)$ and $B(\tau)$. Then, (1.27) becomes

$$\gamma(\tau) + \int_0^\tau \dot{M}(\tau-\zeta)\gamma(\zeta)\,d\zeta = F(\tau)$$

Divide the time into intervals τ_i, $i = 1,2,\cdots, n+1$; $\tau_1 = 0$, $\tau_{n+1} = \tau$. Let $\gamma_{n+1} = \gamma(\tau_{n+1}) = \gamma(\tau)$. Then,

$$\gamma_1 = \gamma(0) = F(0) = \dot{J}_1(0) - \frac{9\kappa}{(3\kappa+4)(3\kappa+1)}\left[\dot{J}_1(0)-\dot{B}_1(0)\right]$$

$$\gamma_{n+1} = \frac{1}{1 + 1/2\, M(\tau_{n+1}-\tau_n)}\left\{F(\tau_{n+1}) - \frac{1}{2}M(\tau_{n+1}-\tau_n) + \frac{1}{2}\sum_{i=1}^{n-1}(\gamma_{i+1}+\gamma_i)\left[M(\tau_{n+1}-\tau_{i+1}) - M(\tau_{n+1}-\tau_i)\right]\right\}, n = 1,2,\ldots$$

In this way, $\gamma(\tau)$ can be evaluated in successive steps, starting from $\tau=0$. The time intervals can be varied as desired; equal intervals in log τ may be convenient.

The function $\gamma(\tau)$ will be qualitatively similar to $\dot{J}_1(\tau)$, as can be seen from (1.27). It is a monotonic decreasing function, concave upward. If the material is a solid, the creep functions approach asymptotically a limiting value; thus, $\dot{J}_1(\infty) = \dot{B}_1(\infty) = 0$, so $\gamma(\infty) = 0$. If the material is a fluid, the creep functions approach a linear function of time after a long time, so $\gamma(\infty) = \gamma_f > 0$. For a general Voigt model, from (1.15b),

$$\dot{J}_1(\tau) = \frac{1}{T_o} + \sum_1^n \frac{f_k}{T_k} e^{-\tau/T_k}$$

If the material is a solid, $T_o = \infty$, and $\dot{J}_1(\tau)$ decreases exponentially to zero. An actual material will have the same qualitative behavior for $\dot{J}_1(\tau)$, and thus for $\gamma(\tau)$. A representative sketch is shown in Fig. 1.5.

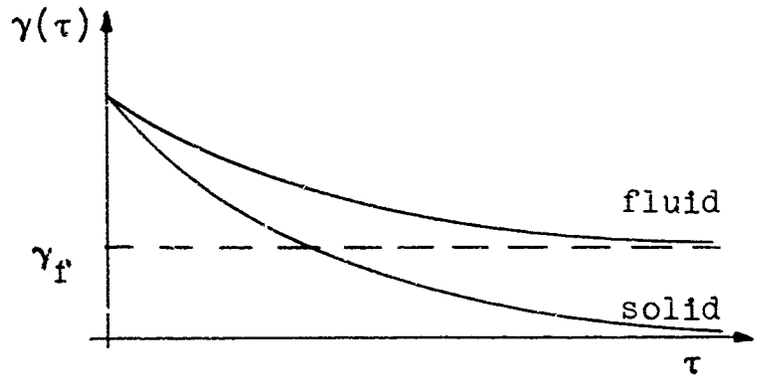

FIG. 1.5

If the material is assumed to have constant Poisson's ratio [$B(\tau) = J(\tau)$, or incompressible ($\nu = 1/2$)], then $\gamma(\tau) = \dot{J}_1(\tau)$. If the dilatation is assumed elastic, $\dot{B}_1 = 0$ in (1.27). As an example, for a material with standard linear solid behavior in shear and elastic dilatation,

$$J(\tau) = [1 + f(1-e^{-\tau})]\, H(\tau) \; ; \; B(\tau) = H(\tau) \qquad (1.28a)$$

$$\dot{J}_1(\tau) = f\, e^{-\tau} \quad , \quad \dot{B}_1(\tau) = 0$$

Inversion of (1.25) gives

$$\gamma(\tau) = \frac{f}{2(1-\nu_o)} \left[e^{-\tau} + \frac{3}{(3\kappa+1)2}\, e^{-(1 + \frac{3\kappa f}{3\kappa+1})\tau}\right] \qquad (1.28b)$$

$$\text{where} \quad \nu_o = \frac{3\kappa-2}{2(3\kappa+1)} \quad , \quad \text{or} \quad \kappa = \frac{2}{3}\,\frac{1+\nu_o}{1-2\nu_o}$$

For any material whose shear and dilatation behavior are represented by mechanical models, such as the general Voigt solid, $\gamma(\tau)$ will be a sum of exponentials, in the form $\gamma(\tau) = \sum_i f_i e^{-b_i \tau}$.

For further applications, it is desirable to express the surface displacement (1.26) in dimensionless form. This is most conveniently done by using as a characteristic length parameter the quantity VT. Then, the following dimensionless variables are introduced:

Coordinates: (moving with the load) $$\xi \equiv \frac{x}{VT}, \quad \eta \equiv \frac{y}{VT} \qquad (1.29a)$$

Displacement: $$v(\xi,\eta) \equiv \frac{u_z(x,y,0)}{VT} \qquad (1.29b)$$

Pressure: $$Q(\xi,\eta) \equiv \frac{1-\nu_o}{\mu_o} \frac{1}{\pi} q(x,y) \qquad (1.29c)$$

Using these, the elastic displacement is, from (1.20),

$$v^e(\xi,\eta) = \frac{1}{2} \iint_A \frac{Q(\xi',\eta')d\xi'd\eta'}{\sqrt{(\xi-\xi')^2 + (\eta-\eta')^2}} \qquad (1.30)$$

The viscoelastic result (1.26) then becomes:

$$v(\xi,\eta,\tau) = v^e(\xi,\eta) + \int_0^\tau \gamma(\zeta)\, v^e(\xi+\zeta,\eta)d\zeta \qquad (1.31)$$

For a general three-dimensional problem, using (1.30),

$$v(\xi,\eta,\tau) = \frac{1}{2} \iint_A Q(\xi',\eta')\Big[\frac{1}{\sqrt{(\xi-\xi')^2 + (\eta-\eta')^2}} + \int_0^\tau \frac{\gamma(\zeta)d\zeta}{\sqrt{(\xi-\xi'+\zeta)^2+(\eta-\eta')^2}} \Big] d\xi'd\eta' \qquad (1.32)$$

For a plane strain problem, from (1.5a),

$$v(\xi,\tau) - v(\xi_o,\tau) = \int_0^\lambda Q(\xi') \Big[\log \frac{|\xi_o-\xi'|}{|\xi-\xi'|} + \int_0^\tau \gamma(\zeta) \log \frac{|\xi_o+\zeta-\xi|}{|\xi+\zeta-\xi'|} d\zeta\Big]d\xi' \qquad (1.33)$$

where $\lambda = \frac{\ell}{VT}$ is the dimensionless length of the loaded region.

1.4 Steady State Solution

The stress and deformation patterns in the base change with time due to the delayed creep and recovery of viscoelastic materials. After a sufficiently long time, however, the transient effects may disappear, so that these patterns are unchanged with further passage of time. In this case, a steady state exists for an observer moving with the load. With respect to coordinates fixed in the base, functional dependence on time then occurs only in the combination $x^* - Vt$. In coordinates x,y,z moving with the load, there is no explicit time dependence. The question of whether and under what conditions a steady state occurs, and some of its consequences, will be considered in this section.

The viscoelastic solution (1.31) contains time explicity only as the upper limit of the integral. If this integral exists as $\tau \to \infty$, a steady state is reached, and is given by (1.31) with $\tau = \infty$. If the value of the integral increases without limit as $\tau \to \infty$, no steady state exists. Consider the integral in equation (1.31):

$$I(\tau) \equiv \int_0^\tau \gamma(\zeta)\, p^e(\xi+\zeta,\eta)\,d\zeta$$

$$= \frac{1}{2}\int_0^\tau \gamma(\zeta)\left[\iint_A Q(\xi',\eta')\,\frac{d\xi'd\eta'}{r'}\right] d\zeta \qquad (1.34)$$

where $r' = \sqrt{(\xi+\zeta-\xi')^2 + (\eta-\eta')^2}$

If $I(\infty)$ exists, there is a steady state. Let τ_o be a large but finite time. Then,

$$I(\infty) = I(\tau_o) + \int_{\tau_o}^{\infty} \gamma(\zeta)\left[\iint_A Q(\xi', \eta')\frac{d\xi' d\eta'}{r'}\right] d\zeta \qquad (1.35)$$

$I(\tau_o)$ is finite, so only the second term must be considered. Since ζ is always large in this integral, the integrand can be expanded in terms of ζ^{-1}:

$$\int_{\tau_o}^{\infty} \gamma(\zeta)\left[\iint_A Q \frac{dA}{r'}\right] d\zeta = \int_{\tau_o}^{\infty} \gamma(\zeta)\left[\frac{N_o}{\zeta} + \frac{N_1}{\zeta^2} + \ldots.\right] d\zeta \qquad (1.36a)$$

where N_o, N_1, ... are finite terms depending on (ξ,η) but not ζ. If the material is a viscoelastic solid, $\gamma(\zeta)$ decreases monotonically to zero as $\zeta \to \infty$. In this case, the integral (1.36a) is finite. Thus, $I(\infty)$ exists; a steady state is always reached when the semi-infinite material is a viscoelastic solid. If the material is fluid, $\gamma(\zeta)$ decreases monotonically to a constant value, γ_f, as $\zeta \to \infty$. Then, $\gamma(\zeta) = \gamma_f + \gamma_1(\zeta)$, where $\gamma_1(\zeta)$ decreases monotonically to zero as $\zeta \to \infty$ (see Fig. 1.6). The integral (1.36a) becomes

$$\int_{\tau_o}^{\infty} [\gamma_f + \gamma_1(\zeta)][\frac{N_o}{\zeta} + \frac{N_1}{\zeta^2} + \ldots]d\zeta = \int_{\tau_o}^{\infty} \frac{\gamma_f N_o}{\zeta} d\zeta + \int_{\tau_o}^{\infty} [\frac{\gamma_f N_1}{\zeta^2} + \ldots]d\zeta \qquad (1.36b)$$

The second integral is finite, but the first term integrates to $\gamma_f N_o [\log \zeta]_{\tau_o}^{\omega}$, which is unbounded, so $I(\infty)$ does not exist. Thus, a steady state is not reached when the material is a viscoelastic fluid.

If the problem is two-dimensional,

$$I(\tau) = \int_o^{\tau} \gamma(\zeta) \left[\int_o^{\lambda} Q(\xi') \log \frac{|\xi_o+\zeta-\xi'|}{|\xi+\zeta-\xi'|} \, d\xi' \right] d\zeta$$

For large ζ, the log term is expanded in powers of ζ^{-1} to give[1]

$$\log \frac{|\xi_o+\zeta-\xi'|}{|\xi+\zeta-\xi'|} = \log \left|1 + \frac{\xi_o-\xi'}{\zeta}\right| - \log \left|1 + \frac{\xi-\xi'}{\zeta}\right|$$

$$\sim \frac{\xi_o-\xi}{\zeta} \left[1 - \frac{\xi_o-\xi'+\xi-\xi'}{2\zeta} + \ldots.\right]$$

$$\text{as } \zeta \to \infty$$

Following the same procedure as before, an integral of the same form as (1.36) results. Thus, the conclusions are the same for the two- and three-dimensional cases: There is a steady state when the material is a solid; there is no steady state for a fluid.

For a viscoelastic fluid, where $\gamma(\zeta) = \gamma_f + \gamma_1(\zeta)$, the displacement (1.31) becomes

$$v(\xi,\eta,\tau) = v^e(\xi,\eta) + \gamma_f \int_o^{\tau} v^e(\xi+\zeta,\eta)d\zeta + \int_o^{\tau} \gamma_1(\zeta) v^e(\xi+\zeta,\eta)d\zeta$$

---

[1] The symbol $\sim$ means "asymptotically approaches"; i.e., $f(x) \sim g(x)$ as $x \to a$ means $\lim_{x\to\infty} |f(x)-g(x)| = 0$

The term with γ_f is due to the unlimited creep of the material, and this is what fails to reach a steady state. The fluid behaves after a long time as if it were purely viscous, as given by the term with γ_f. Thus, to decide if a steady state is reached for a general viscoelastic fluid, it is necessary to consider only an ideal viscous fluid. A viscoelastic fluid will have a steady state if and only if the ideal viscous fluid does.

The failure to reach a steady state when the base is a fluid has been shown here for a semi-infinite base. In this case there are no constraints or supports to prevent the displacement from increasing without limit as the fluid material undergoes unlimited creep. If the base was not semi-infinite, but a layer of finite thickness supported from below, the creep would be constrained and a steady state might result. This possibility will be considered in more detail in Chapter II.

When the material is a viscoelastic solid, the steady state solution is given by (1.31) with $\tau = \infty$:

$$v(\xi,\eta) = v^e(\xi,\eta) + \int_0^\infty \gamma(\zeta)\ v^e(\xi+\zeta,\eta)d\zeta \qquad (1.37)$$

The steady state is evident only to an observer moving with the load at velocity V; the coordinates (ξ,η) are also moving with the load. It is convenient to think instead

of a fixed load and coordinate system, with the semi-infinite base moving uniformly under the load, in the negative ξ direction (Fig. 1.6). A particle of the base comes from the right ($\xi = \infty$) and has been traveling horizontally for a long time. It continues to move with constant horizontal velocity V , but it also acquires a vertical velocity as it comes under the influence of the load. The path of the particle is deformed in the vicinity of the load, but the particle is eventually moving horizontally again far downstream. Particles initially on the surface remain on the surface, and undergo the vertical displacement $u_z(x^*-Vt,y^*) = u_z(x,y)$. The vertical velocity of surface particles is

$$U^* \equiv \frac{\partial u_z}{\partial t} = - V \frac{\partial u_z}{\partial x} = - V \frac{\partial v(\xi,\eta)}{\partial \xi} \qquad (1.38)$$

Thus, the vertical velocity of a particle on the surface is proportional to the slope of the deformed surface.

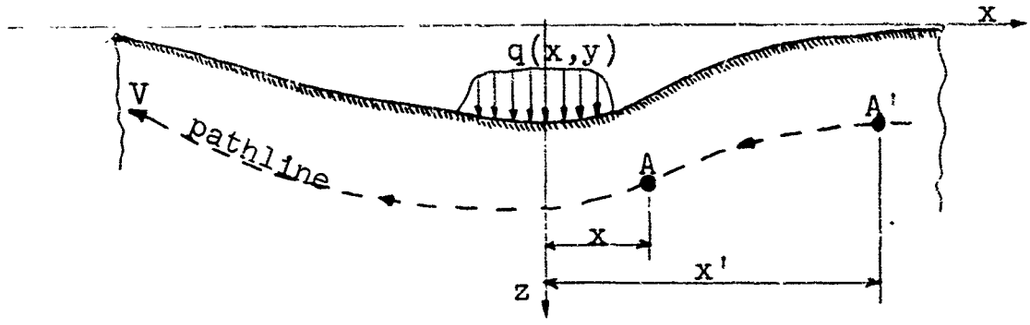

FIG. 1.6

When a steady state does exist, the resulting expressions for surface displacement (or any other displacement or stresses) can be found directly, without the necessity of considering time explicitly. Consider the load and coordinate system (x,y,z) fixed, and the viscoelastic base moving at constant velocity V in the negative x direction. For simplicity, a one-dimensional state of stress is considered. The argument is easily extended to shear components and dilatation in a general three-dimensional state.

An element A in the base, now at coordinate x, moves[1] on the pathline A'A (Fig. 1.6). Suppose while at x' it received a stress increment $d\sigma = [\partial\sigma(x')/\partial x']\, dx'$. This has influenced the element for a time $(x'-x)/V$, and the resulting strain increment is

$$d\epsilon(x) = \frac{1}{E_o} J\left(\frac{x'-x}{T}\right) d\sigma$$

Adding up all such increments from the initial position of the element at $x' = \infty$ to its present position a $x' = x$ gives the total strain

$$\epsilon(x) = \frac{1}{E_o} \int_{\infty}^{x} J\left(\frac{x'-x}{VT}\right) \frac{\partial\sigma(x')}{\partial x'}\, dx' \qquad (1.39)$$

---

[1] Deformations due to the applied load are infinitesimal and can be neglected, so the only motion is in the negative x-direction at velocity V.

The elements are coming from an undisturbed state, so that $\sigma(\infty) = 0$. Thus, integrating (1.39) by parts, and letting $\zeta = (x'-x)/VT$,

$$\epsilon(x) = \frac{1}{E_o} \int_o^\infty \sigma(x+VT\zeta)\ \dot{J}(\zeta)d\zeta \qquad (1.40)$$

This is the steady state equivalent of the stress-strain law (1.7). Similar laws, analogous to (1.9a,b), for shear and dilatation can be obtained in the same way. The stress-strain law (1.40) can be considered an operational extension of the elastic law $\epsilon(x) = 1/E_o\ \sigma(x)$, with $1/E_o$ replaced by $\dot{J}(\zeta)/E_o$ and the integration carried out as indicated in (1.40). In the same way, $(1-\nu_o)/\mu_o\ [\delta(\zeta) + \gamma(\zeta)]$ replaces $(1-\nu_o)/\mu_o$ in the elastic surface displacement (1.3), which leads to the viscoelastic steady state displacement[1]

$$u_z(x,y) = \frac{1-\nu_o}{\mu} \int_o^\infty [\delta(\zeta)+\gamma(\zeta)]P(x+VT\zeta,y)d\zeta$$

or,

$$u_z(x,y) = u_z^e(x,y) + \int_o^\infty \gamma(\zeta)u_z^e(x+VT\zeta,y)d\zeta$$

In dimensionless terms:

$$v(\xi,\eta) = v^e(\xi,\eta) + \int_o^\infty \gamma(\zeta)v^e(\xi+\zeta,\eta)d\zeta$$

which is identical to the previous result (1.37).

---

[1] This operation can be justified more rigorously using Fourier transforms in a way similar to the use of Laplace transforms in the preceding section.

The steady state solution for the surface displacement of a semi-infinite base is given by (1.32) or (1.33), with $\tau = \infty$. The result for the three-dimensional problem can be written

$$v(\xi,\eta) = \iint_A Q(\xi',\eta')K^*(\xi-\xi',\eta-\eta')d\xi'd\eta' \qquad (1.41a)$$

where

$$K^*(\xi,\eta) \equiv \frac{1}{2}\frac{1}{\sqrt{\xi^2+\eta^2}} + \frac{1}{2}\int_0^\infty \frac{\gamma(\zeta)d\zeta}{\sqrt{(\xi+\zeta)^2+\eta^2}} \qquad (1.41b)$$

For a two-dimensional problem,

$$v(\xi) - v(\xi_o) = \int_o^\lambda Q(\xi')[K(\xi_o-\xi')-K(\xi-\xi')]d\xi' \qquad (1.42a)$$

where

$$K(\xi) \equiv \log|\xi| + \int_o^\infty \gamma(\zeta)\log|\xi+\zeta|\,d\zeta \qquad (1.42b)$$

These results are for a viscoelastic solid with initial elasticity. The dimensionless terms ξ,η,v,Q are defined in (1.29), while $\gamma(\zeta)$ is obtained from the creep functions of the material by (1.25) or (1.27).

It is of interest to examine the surface displacement far away from the load. The loaded area will be taken to include the origin of the coordinate system. In the three-dimensional case, let $\rho^2 \equiv \xi^2 + \eta^2$ be very large; ρ is the (dimensionless) distance of a point on the surface from the origin. Then, as $\rho \to \infty$,

$$K^*(\xi,\eta) \sim \frac{1}{2\rho}\left[1 + \int_0^\infty \gamma(\zeta)d\zeta\right] - \frac{1}{2\rho^2}\,\xi \int_0^\infty \zeta\gamma(\zeta)d\zeta + \ldots$$

Thus, when $\xi^2 + \eta^2 \to \infty$,

$$v(\xi,\eta) \sim \frac{1}{\sqrt{\xi^2+\eta^2}} \cdot \frac{1}{2}\iint_A Q(\xi',\eta')d\xi'd\eta' \left[1 + \int_0^\infty \gamma(\zeta)d\zeta\right]$$

Using (1.25) and the final value theorem of Laplace transforms, it can be shown that

$$1 + \int_0^\infty \gamma(\zeta)d\zeta = \lim_{s\to 0}\left[1 + \bar{\gamma}(s)\right] = \frac{\mu_o}{1-\nu_o} \cdot \frac{1-\nu_f}{\mu_f} \qquad (1.43)$$

Then,
$$v(\xi,\eta) \sim \frac{1}{\sqrt{\xi^2+\eta^2}} \cdot \frac{1-\nu_f}{\mu_f} \cdot \frac{1}{2\pi}\iint_A q(\xi',\eta')d\xi'd\eta'$$

The total load, N^*, applied to the surface is

$$N^* = \iint_A q(x',y')dx'dy' = (VT)^2 \iint_A q(\xi',\eta')d\xi'd\eta'$$

Thus, far away from the load,

$$v(\xi,\eta) \sim \frac{1}{\sqrt{\xi^2+\eta^2}} \quad \frac{N^*}{2\pi(VT)^2} \quad \frac{1-\nu_f}{\mu_f} \quad , \text{ or}$$

$$u_z(x,y) \sim \frac{1}{\sqrt{x^2+y^2}} \quad \frac{N^*}{2\pi} \quad \frac{1-\nu_f}{\mu_f} \qquad (1.44)$$

This is the same displacement that would result from a concentrated load of magnitude N^* applied at the origin.

The result is that far from a localized pressure distribution moving on the surface of a viscoelastic solid, the surface displacement is the same as that for a concentrated load of the same total magnitude, acting at the origin on the surface of an elastic solid with the final elastic moduli of the viscoelastic material. This is true in any direction, whether ahead of or behind the moving load. The initially flat surface is deformed in the vicinity of the load, but gradually returns to its initial level after the load passes. Far enough away from the load, the actual pressure distribution has no effect; only the total load is significant.

In a two-dimensional problem, as $|\xi| \to \infty$,

$$v(\xi) - v(\xi_o) \sim \frac{1-\nu_f}{\mu_f} \frac{N^*}{\pi\sqrt{T}} [\log|\xi_o| - \log|\xi|] \qquad (1.45)$$

Here the result is the same as for a line load of the same total magnitude, $N^* = \int_o^\ell q(x')dx'$, per unit length in the y-direction. Again the base exhibits the final elastic behavior of the viscoelastic material. The surface levels far ahead of and behind the load are the same, and the slopes tend to zero as $|\xi| \to \infty$. For any two-dimensional (plane strain) problem, elastic or viscoelastic, the load is distributed on an area unbounded in the y-direction, and thus the total load is infinite. There is no lower boundary to the base to restrict the resulting deformation, so the displacement far from the load is infinite relative to points

near the load. The displacement must thus be expressed relative to an arbitrary point ξ_o near the load.

For the extremes of very large or very small velocity, the viscoelastic solution approaches as a limiting case the corresponding elastic solution. For $V = 0$, the viscoelastic material exhibits its final elastic response when a steady state is reached, and the result is the same as if it were an elastic solid with the final elastic behavior. For very large V, the load passes so fast that there is time only for the initial elastic response. Thus, as $V \to \infty$, the result is the same as if it were an elastic solid with the initial elastic behavior[1]. These results are confirmed from the limiting values of the surface displacement. Written out completely, the steady state solution is, from (1.41a,b)

$$u_z(x,y) = \frac{1-\nu_o}{\mu_o} \frac{1}{2\pi} \iint_A q(x',y') \left[\frac{1}{\sqrt{(x-x')^2+(y-y')^2}} + \int_o^\infty \frac{\gamma(\zeta)d\zeta}{\sqrt{(x+V\tau\zeta-x')^2+(y-y')^2}} \right] dx'dy' \qquad (1.46)$$

For $V = 0$, (1.46) becomes

$$u_z(x,y) = \frac{1-\nu_o}{\mu_o} \left[1 + \int_o^\infty \gamma(\zeta)d\zeta\right] P(x,y,0) = \frac{1-\gamma_f}{\mu_f} P(x,y,0)$$

[1] The solution in this case is no longer physically meaningful, because the problem cannot be treated as quasi-static. The limiting case may be approached, however, for relatively large velocities still within the restrictions of the quasi-static assumption.

This is the elastic solution (1.3), with elastic constants μ_f , ν_f of the final elastic response. For $V \to \infty$, the inner integral in (1.46) vanishes, so

$$u_z(x,y) = \frac{1-\nu_o}{\mu_o} P(x,y,0)$$

which is the elastic solution for the initial elastic response.

1.5 Energy Dissipation

When a perfectly elastic material is loaded, work done on the body as it deforms is stored internally as strain energy. If the body is subsequently unloaded, recovery takes place instantaneously. The strain energy is released and there is no net work done in a complete cycle. In a viscoelastic body, however, recovery takes place gradually after unloading, and not all of the stored energy is released. Energy is dissipated within the material during the loading and unloading process. Thus, net work must be done on a viscoelastic body, even though it may eventually return to its initial shape. The amount of work depends not only on the initial and final states, but on the history and rate of loading during the process. In a mechanical model of a viscoelastic material, the dashpot elements account for internal energy dissipation, while the springs provide for storage of free energy. The dissipation in actual materials is often attributed to "internal friction" or "elastic hysteresis losses."

Consider a moving load applied to some body in contact with the surface of base material. The contact is perfectly lubricated (or "frictionless") so there are no tangential surface tractions. The body would move at constant velocity with no resistance if the base were perfectly elastic. However, resistance is encountered with actual base materials, and a force is needed to maintain constant velocity. A common example is the resistance to rolling of a cylinder or sphere. Experimental evidence[1] indicates that rolling resistance is nearly independent of the roller material and of the lubrication between roller and base. Also, when the surface is well lubricated, resistance is nearly the same for rolling and sliding. This indicates the resistance is due to bulk properties of the base material and not to surface phenomena. Energy dissipation in the base material as it is deformed is the primary factor. Work must be done by the moving body to provide the energy dissipated in the base, and this accounts for the resistance to motion. In the alternate view adopted here, the base moves under a fixed load, and external work must be done on the base.

Since a viscoelastic material dissipates energy, the problem of a moving load on a viscoelastic base being considered in this chapter is one way to account for and predict resistance to moving loads. The initially flat surface

[1] Bowden and Tabor [4], Tabor [30,31], Tabor and Atack [32], Flom [10,11].

of the base is deformed by the load $q(x,y)$. Because there are no tangential stresses on the surface, the load must remain normal to the deformed surface. Consistent with other assumptions of the linear theory, the effect of the infinitesimal horizontal components of the load can be neglected compared to the vertical components. Thus, in solving the problem for stress and displacements, the load is considered to remain vertical and applied to the undeformed surface. To evaluate the energy dissipation, however, the horizontal component of the load and deformation of the surface must be considered.

At each point on the surface under the load there is a vertical component $q_v = q \cos\phi$ and a horizontal component $q_h = q \sin\phi$, where $\tan\phi = - \partial u_z/\partial x$ is the slope of the deformed surface (Fig. 1.7). With the restriction to small

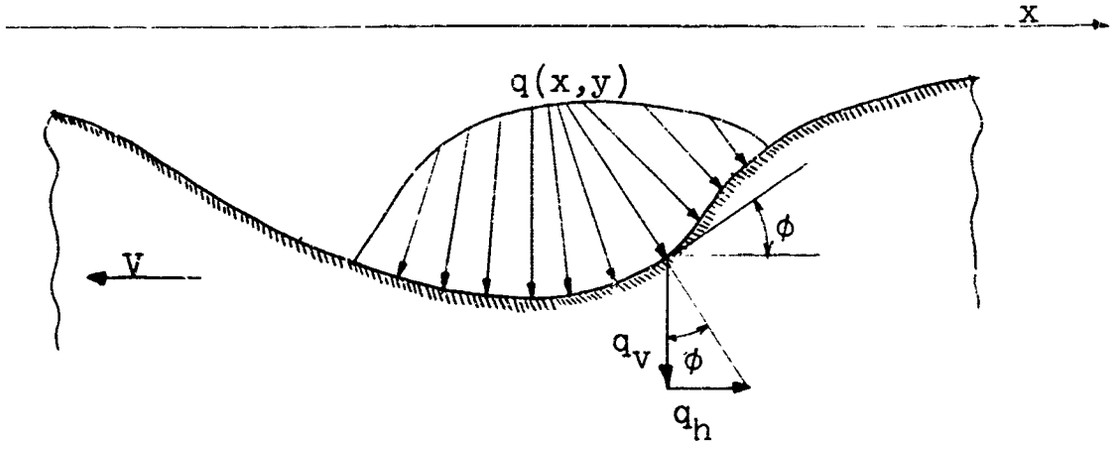

FIG. 1.7

slopes, the total vertical load is

$$N^* = \iint_A q(x,y)\, dx\, dy$$

The resultant horizontal force at the contact is

$$F^* = -\iint_A q(x,y)\, \frac{\partial u_z(x,y)}{\partial x}\, dx\, dy \qquad (1.47)$$

It is convenient to introduce dimensionless forces N and F, given in terms of the quantities of (1.29) by

$$N \equiv \frac{1-\nu_o}{\mu_o}\, \frac{1}{\pi}\, \frac{N^*}{(VT)^2} = \iint_A Q(\xi,\eta)\, d\xi\, d\eta \qquad (1.48)$$

$$F \equiv \frac{1-\nu_o}{\mu_o}\, \frac{1}{\pi}\, \frac{F^*}{(VT)^2} = -\iint_A Q(\xi,\eta)\, \frac{\partial v(\xi,\eta)}{\partial \xi}\, d\xi\, d\eta \qquad (1.49)$$

In a two-dimensional problem, the body is an infinite cylinder (not necessarily circular), with axis in the y direction. Then, N and F are forces per unit length, given by

$$N = \frac{1-\nu_o}{\mu_o}\, \frac{1}{\pi}\, \frac{N^*}{VT} = \int_o^\lambda Q(\xi)\, d\xi \qquad (1.50)$$

$$F = \frac{1-\nu_o}{\mu_o}\, \frac{1}{\pi}\, \frac{N^*}{VT} = -\int_o^\lambda Q(\xi)\, \frac{\partial v(\xi)}{\partial \xi}\, d\xi \qquad (1.51)$$

The force F^* is entirely a consequence of the viscoelastic behavior of the base. The deformation will not be symmetric, even for a symmetric load distribution, because the viscoelastic material experiences delayed recovery as it moves under the load. There will always be a horizontal resultant of the contact pressure, acting on the moving base (or body) opposite to the direction of motion. This will be shown in the two-dimensional case for simplicity (the three-dimensional case is similar). From (1.42a,b),

$$\frac{\partial v(\xi)}{\partial \xi} = -\int_0^{\lambda} Q(\xi') \left[\frac{1}{\xi - \xi'} + \int_0^{\infty} \frac{\gamma(\zeta)\, d\zeta}{\xi + \zeta - \xi'} \right] d\xi'$$

Substituting this in (1.51) gives:

$$F = \int_0^{\lambda}\int_0^{\lambda} Q(\xi)Q(\xi') \frac{d\xi\, d\xi'}{\xi - \xi'} + \int_0^{\lambda}\int_0^{\lambda} Q(\xi)Q(\xi') \int_0^{\infty} \frac{\gamma(\zeta)\, d\zeta}{\xi + \zeta - \xi'}\, d\xi\, d\xi'$$

The first term is the contribution from the initial elastic response:

$$F_o = \int_0^{\lambda}\int_0^{\lambda} Q(\xi)Q(\xi) \frac{d\xi\, d\xi'}{\xi - \xi'} \quad ; \quad \text{interchanging } \xi \text{ and } \xi' \text{ gives}$$

$$F_o = \int_0^{\lambda}\int_0^{\lambda} Q(\xi)Q(\xi') \frac{d\xi\, d\xi'}{\xi' - \xi} = -\int_0^{\lambda}\int_0^{\lambda} Q(\xi)Q(\xi') \frac{d\xi\, d\xi'}{\xi - \xi'} = -F_o$$

Thus, $F_o = 0$; there is no contribution from the elastic response. Then,

$$F = \iint_{oo}^{\lambda\lambda} Q(\xi)Q(\xi') \int_{o}^{\infty} \frac{\gamma(\zeta)d\zeta}{\xi+\zeta-\xi'} \, d\xi d\xi' \tag{1.52}$$

The horizontal force depends directly on the function $\gamma(\zeta)$ which characterizes the viscoelastic behavior of the material. For an elastic material, $\gamma(\zeta) = 0$, so $F = 0$.

At the contact, the force F^* acts to resist the motion, and can be referred to as a "resistance" or "friction" force. A convenient dimensionless measure of F^* is the coefficient of friction χ, given by

$$\chi \equiv \frac{F^*}{N^*} = \frac{F}{N} = \frac{\iint_A Q(\xi,\eta)(\partial v/\partial \xi)d\xi d\eta}{\iint_A Q(\xi,\eta)\, d\xi d\eta} \tag{1.53}$$

This coefficient varies with the velocity, total load, and load distribution. With the restriction to small slopes, $\partial u_z/\partial x = \partial v/\partial \xi \ll 1$, and thus $F^* \ll N^*$ ($\chi \ll 1$). This agrees with observed evidence; for example, resistance to rolling on hard surfaces is usually found to be very small.

For equilibrium, there must be resultant horizontal forces equal to F^* acting on the body and on the remote boundaries of the base (Fig. 1.8). These forces are needed to move the base and hold the body fixed (or, alternately, to move the body and hold the base fixed). Work is done

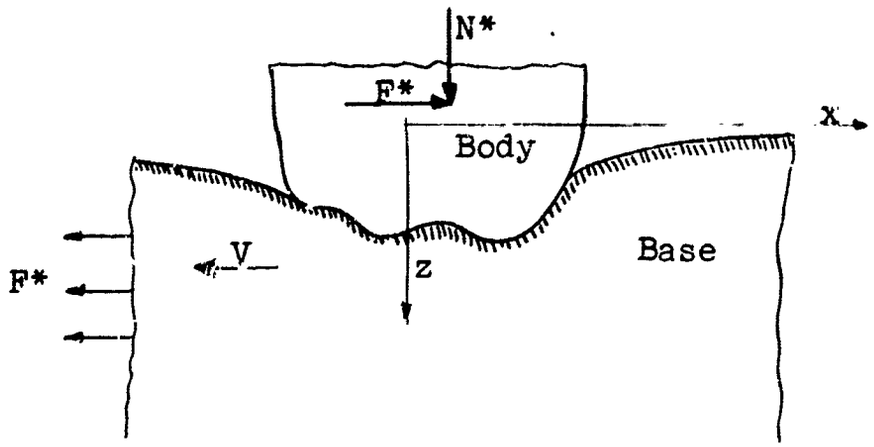

FIG. 1.8

on the base at its remote boundaries, at a rate

$$\dot{W} = VF^* = - V \iint_A q(x,y)(\partial u_z/\partial x)\, dxdy \qquad (1.54)$$

This equals the rate of energy dissipation within the viscoelastic base. No work is done at the contact, since particles are moving under the load at right angles to the direction of the load.

In the limiting cases of very fast or very slow velocity ($V \to 0$ or $V \to \infty$) it was shown in Section 1.4 that a viscoelastic solid behaves like an elastic solid, and the viscoelastic solution is the same as the elastic solution. As these limits are approached, it is a plausible expectation that energy

dissipation and resistance to motion will decrease to zero, since they are zero in the elastic problem. This is now shown to be the case. From (1.52),

$$F^* = \frac{1-\nu_o}{\mu_o} \frac{1}{\pi} \int_{oo}^{\ell\ell} q(x)q(x') \int_o^{\infty} \frac{\gamma(\zeta)d\zeta}{x+V\tau\zeta-x'} \, dxdx' \qquad (1.55)$$

For $V = 0$, this becomes

$$F^* = \frac{1-\nu_o}{\mu_o} \frac{1}{\pi} \int_o^{\infty} \gamma(\zeta)d\zeta \cdot \int_{oo}^{\ell\ell} q(x)q(x') \frac{dxdx'}{x-x'}$$

The double integral has been shown previously to be zero, so $F^* = 0$. For $V = \infty$, the integrand vanishes, so again $F^* = 0$. The resistance increases from zero as V increases from zero, and decreases to zero as V gets very large. It will have at least one maximum at some intermediate velocity. For a given load, N^* is fixed, so $\chi = F^*/N^*$ has the same behavior as F^*. The resistance to a given load, due to energy dissipation as the velocity varies can be seen best by plotting χ vs F; Fig. 1.9 shows how this might appear.

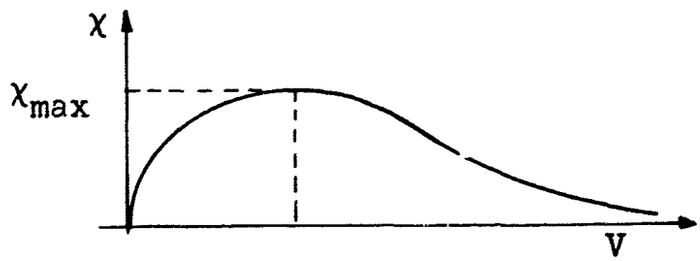

FIG. 1.9

There is an alternate view of the way in which work is done on the moving viscoelastic base. The load $q(x,y)$ is taken as strictly vertical on the deformed surface. Particles under the load have a vertical velocity $U^* = - V \partial u_z/\partial x$ (1.38) in the direction of the load. Thus, a load element qdA does work at a rate

$$d\dot{W} = U^* q(x,y)dA = - V \left(\frac{\partial u_z}{\partial x}\right) q(x,y)dA$$

The total rate of work done is then

$$\dot{W} = - V \iint_A \left(\frac{\partial u_z}{\partial x}\right) q(x,y)\, dxdy$$

This is (in the linear theory) the same result as before (1.54). But here the work is done at the contact of load and base; no work is done at the remote boundaries. Thus, the source of energy is quite different from before. This alternate view gives rise to difficulties in physical interpretation. The vertical pressure is not normal to the deformed surface, so there are tangential stresses. This contradicts the assumption of a perfectly frictionless contact, since the base and load are in relative motion.

1.6 Examples of Moving Loads

The results given so far in this chapter apply to any load distribution and any linear viscoelastic material. Some

examples of particular loads are now considered. The material used will be a general Voigt solid. This adequately represents characteristics of actual materials such as polymers[1], while allowing results to be expressed in analytical form. For such a material,

$$\gamma(\zeta) = \sum_{i=1}^{m} f_i e^{-b_i \zeta} \tag{1.56}$$

The steady state surface displacement (1.37) is then

$$v(\xi,\eta) = v^e(\xi,\eta) + \sum_{i=1}^{m} f_i \int_0^\infty e^{-b_i\zeta}\, v^e(\xi+\zeta,\eta)\,d\zeta \tag{1.57}$$

Integrating by parts gives

$$v(\xi,\eta) = \left(1 + \sum_{i=1}^{m} \frac{f_i}{b_i}\right) v^e(\xi,\eta) + \sum_{i=1}^{m} \frac{f_i}{b_i}\, v^v(\xi,\eta;b_i) \tag{1.58a}$$

where

$$v^v(\xi,\eta;b) \equiv \int_0^\infty e^{-b\zeta}\, \frac{\partial v^e(\xi+\zeta,\eta)}{\partial\zeta}\, d\zeta \tag{1.58b}$$

The elastic part of the displacement gives no contribution to the resisting force. Thus,

$$F = -\sum_{i=1}^{m} \frac{f_i}{b_i}\, F^v(b_i) \tag{1.59a}$$

---

[1] Ferry [9] and Tobolsky [34] give creep or relaxation data for many polymers, with discussions of their properties and references to original literature.

where

$$F^v(b) = \iint_A Q(\xi,\eta)\, \frac{\partial v^v(\xi,\eta;b)}{\partial \xi}\, d\xi d\eta \qquad (1.59b)$$

The results (1.58), (1.59) are sums of terms which are identical except for the value of the constants f_i and b_i; there is one term for each exponential in (1.56). In the examples to follow, only a single term is indicated, and the functions $v^v(\xi,\eta;b_i)$ and $F^v(b_i)$ are evaluated for an arbitrary value of b. The results thus presented correspond to a single term in (1.56), i.e., $\gamma(\zeta) = f\, e^{-b\zeta}$. A more general model is then easily treated as a sum of terms, as indicated in (1.58), (1.59).

Even when the material behavior is expressed in the simple analytic form (1.56), the surface displacement in a general three-dimensional problem cannot usually be given in simple terms. This is evident even in the most elementary case, that of a concentrated load at the origin (Example A). Therefore, the other examples will be two-dimensional (plane strain) problems, for which results can be given in relatively simple expressions.

A) Three Dimensions Concentrated Load

$$Q(\xi,\eta) = 2\delta(\xi)\delta(\eta)$$

$$v^e(\xi,\eta) = \frac{1}{\sqrt{\xi^2+\eta^2}}$$

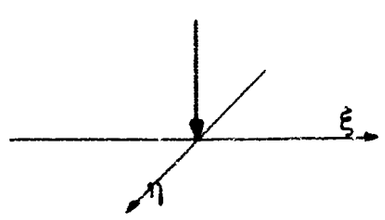

$$v(\xi,\eta) = \frac{1}{\sqrt{\xi^2+\eta^2}} + f\int_0^\infty \frac{e^{-b\zeta}d\zeta}{\sqrt{(\xi+\zeta)^2+\eta^2}} \qquad (1.60)$$

The integral in (1.60) has no simple evaluation in the general case; some special cases are given.

For $\eta = 0$:

$$v(\xi,0) = \frac{1}{\xi} - fe^{b\xi}\, E_1(-b\xi) \quad , \quad \xi > 0$$

$$= \infty \quad , \quad \xi < 0$$

as $\xi \to +\infty$, $\quad v(\xi,0) \sim \frac{1}{\xi}\left(1 + \frac{f}{b}\right) - \frac{f}{b}\frac{1}{\xi}\left(\frac{1}{b\xi} - \frac{2}{b^2\xi^2} \ldots\right)$

For $\xi = 0$:

$$v(0,\eta) = \frac{1}{|\eta|} + f\frac{\pi}{2}\left[S_o|b\eta| - Y_o|b\eta|\right]$$

Y_o is Weber's Bessel function of the second kind, order zero.

S_o is Struve's function of order zero.

as $|\eta| \to 0$, $\quad v(0,\eta) \sim \frac{1}{|\eta|} - f\frac{\pi}{2}\log|b\eta|$

as $|\eta| \to \infty$, $\quad v(0,\eta) \sim \left(1 + \frac{f}{b}\right)\frac{1}{|\eta|} - f\frac{1}{(b|\eta|)^3}\left[1 - \frac{9}{(b\eta)^2} + \ldots\right]$

The surface displacement is infinite at the origin and all along the negative ξ axis; at all other points it is finite. Some typical surface profiles are sketched in Fig. 1.10.

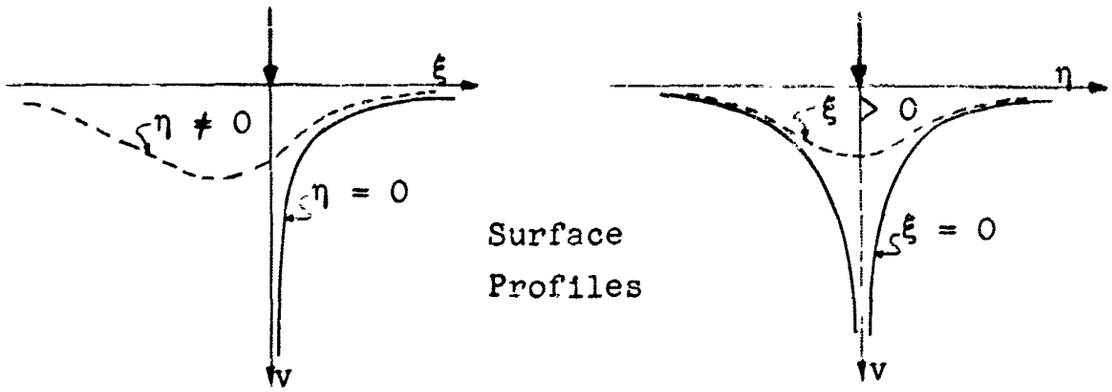

Parallel to ξ-axis Parallel to η-axis

FIG. 1.10

B) Two Dimensions Concentrated Load

$$Q(\xi) = \delta(\xi)$$

$$v^e(\xi) - v^e(\xi_o) = \log\left|\frac{\xi_o}{\xi}\right| , \quad \xi_o \text{ arbitrary}$$

$$v(\xi) - v(\xi_o) = \left(1 + \frac{f}{b}\right) \log\left|\frac{\xi_o}{\xi}\right| + \frac{f}{b}\left[e^{b\xi}E_1(-b\xi) - e^{b\xi_o}E_1(-b\xi_c)\right] \tag{1.61}$$

$$E_1(-x) \equiv -\int_x^\infty \frac{e^{-t}}{t}\,dt \quad \text{is the Exponential Integral.}$$

$$\text{as } |\xi| \to 0 , \quad v(\xi) - v(\xi_o) \sim \log\left|\frac{\xi_o}{\xi}\right|$$

$$\text{as } |\xi| \to \infty , \quad v(\xi) - v(\xi_o) \sim \left(1 + \frac{f}{b}\right) \log\left|\frac{\xi_o}{\xi}\right|$$

A surface profile is sketched in Fig. 1.11.

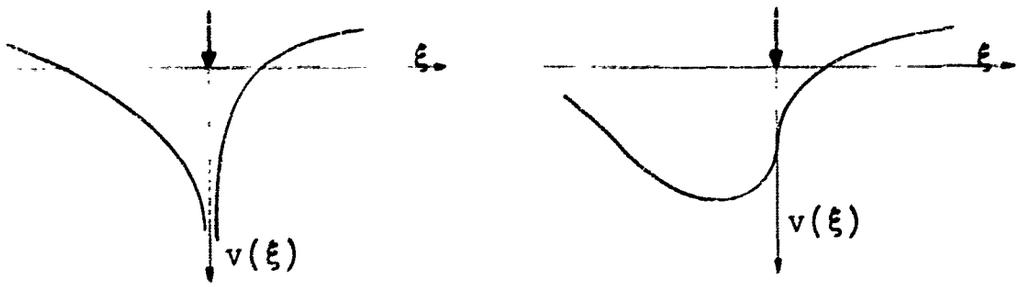

Example B Kelvin solid

FIG. 1.11

A concentrated load is an idealized case which is useful for some considerations, and the results can serve as a fundamental solution to be integrated for more general problems. At distances far from the load, the results for any distributed load are nearly the same as those for a concentrated load. Near the load, however, the actual distribution is significant. A concentrated load is a singularity which has an infinite displacement at the point of application. The elastic displacement under a concentrated load is also infinite. Thus all points of the viscoelastic surface that have passed under the load retain infinite displacement. In the two-dimensional problem, the concentrated load is actually a line load; the singularity is not quite as pronounced. The displacement immediately under the load is infinite, due entirely to the initial elastic response. However, points that have passed under the load have recovered to a finite displacement. If there is no initial elasticity, the displacement in the two-dimensional problem is finite even under the

load. For example, a model with a single Kelvin element gives:

$$v(\xi) - v(\xi_o) = \log \left|\frac{\xi_o}{\xi}\right| + e^{b\xi}\, E_1(-b\xi) - e^{b\xi_o} E_1(b\xi_o);$$

for $\xi=0$ $\quad v(0) - v(\xi_o) = \gamma + \log \xi_o - e^{b\xi_o}\, E_1(-b\xi_o)$

A sketch of this displacement profile is shown in Fig. 1.11.

A distributed load can be considered an integral of a concentrated load. The singularity is no longer present, and displacement under the load is finite. Two simple cases of distributed loads are given in examples C) and D) as two-dimensional problems. The resisting force and coefficient of friction are evaluated in these examples, along with the surface displacement.

C) Two Dimensions Uniform Load

$$Q(\xi) = Q_o \quad , \quad 0 < \xi < \lambda$$

$$N = Q_o\, \lambda$$

$$v^e(\xi) - v^e(0) = Q_o\, [(\xi-\lambda)\log|\xi-\lambda| - \xi\log|\xi| + \lambda \log \lambda]$$

$$\frac{1}{Q_o}[v(\xi) - v\,0)] = (1 + \frac{f}{b})[(\xi-\lambda)\log|\xi-\lambda| - \xi\log|\xi| + \lambda \log \lambda]$$

$$+ \frac{f}{b^2}[\log(b|\xi-\lambda|) - e^{b(\xi-\lambda)}E_1\{-b(\xi-\lambda)\} - \log b|\xi| \qquad (1.62)$$

$$+ e^{b\xi}E_1(-b\xi) - \log b\lambda + e^{-b\lambda}E_1(b\lambda) - \gamma\,]$$

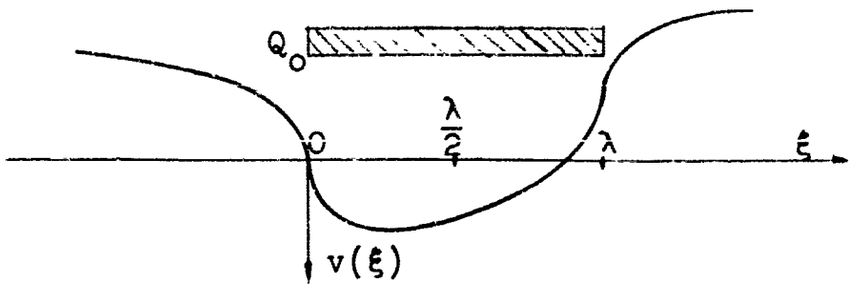

Sketch of displacement

The low point (where $\partial v/\partial \xi = 0$) always occurs for $0 < \xi < \frac{\lambda}{2}$. The slope $\partial v/\partial \xi$ is infinite at $\xi = 0$ and $\xi = \lambda$.

$$F = -\int_0^\lambda Q_o \frac{\partial v}{\partial \xi} d\xi = Q_o[v(0) - v(\lambda)]$$

$$\chi = \frac{F}{N} = Q_o \frac{2f}{b} h_1(b\lambda) \qquad (1.63)$$

where $h_1(x) = \frac{1}{2x}[2\gamma + 2 \log x - e^x E_1(-x) - e^{-x} E_1(x)]$

as $x \to 0$, $h_1(x) \sim \frac{x}{2}(2 - \gamma - \log x + \frac{x}{2} + \dots) \to 0$

as $x \to \infty$, $h_1(x) \sim \frac{1}{x}(\log x + \gamma - \frac{1}{x^2} - \frac{6}{x^4} \to 0$

See Fig. 1.12.

$\gamma = .577216..$, Euler's constant

D) Two Dimensions Elliptical Load

$$Q(\xi) = \frac{8}{\pi} \frac{N}{\lambda^2} \sqrt{\xi(\lambda-\xi)}, \quad 0 < \xi < \lambda$$

$$\frac{\lambda^2}{4N} [v^e(\xi) - v^e(0)] = -\xi^2 + \lambda\xi, \quad 0 < \xi < \lambda$$

$$= -\xi^2 + \lambda\xi + |\xi - \frac{\lambda}{2}| \sqrt{\xi(\xi-\lambda)}$$

$$- \frac{\lambda^2}{4} \cosh^{-1} |\frac{2\xi}{\lambda} - 1|, \quad \xi < 0, \ \xi > 1$$

$$\frac{\lambda^2}{4N} [v(\xi) - v(0)] = (1 + \frac{f}{b}) (-\xi^2 + \lambda\xi)$$

$$+ \frac{f}{b^2}[-2\xi + \lambda e^{-b\lambda/2} (e^{b\xi}-1)K_1(\frac{b\lambda}{2})], \quad 0<\xi<\lambda \qquad (1.64)$$

$$= (1 + \frac{f}{b})(-\xi^2+\lambda\xi + |\xi - \frac{\lambda}{2}| \sqrt{\xi(\xi-\lambda)}$$

$$- \frac{\lambda^2}{4} \cosh^{-1}|\frac{2\xi}{\lambda} - 1|$$

$$+ \frac{f}{b^2} [-2\xi + \lambda e^{-b\lambda/2}(e^{b\xi} - 1)K_1(\frac{b\lambda}{2})$$

$$- \frac{1}{2} b\lambda^2 e^{b(\xi-\lambda/2)} \int_{\pm 1}^{2\xi/\lambda-1} \sqrt{u^2-1}\, e^{-b\lambda u/2}\, du]$$

lower limit of integral is $\begin{cases} +1 \text{ for } \xi > \lambda \\ -1 \text{ for } \xi < 0 \end{cases}$

Slopes are finite at

$$\xi = 0,\ \lambda$$

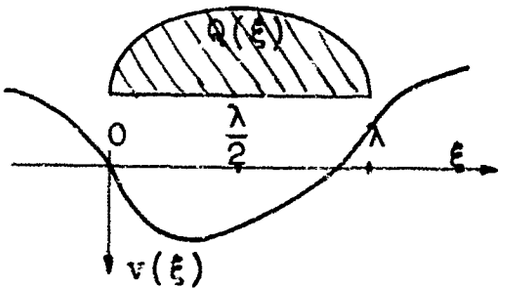

Sketch of displacement

Low point occurs for

$$0 < \xi \leq \frac{\lambda}{2}$$

$$\chi = f\ N\ \frac{8}{(b\lambda)^2}\left[1 - 2K_1\left(\frac{b\lambda}{2}\right)I_1\left(\frac{b\lambda}{2}\right)\right] = \pi\ Q_m\ \frac{f}{b}\ h_2\left(\frac{b\lambda}{2}\right)$$

where $\quad h_2(x) = \frac{1}{x}\left[1 - 2K_1(x)\ I_1(x)\right]$

as $\quad x \to 0\ ,\quad h_2(x) \sim \frac{x}{2}\ (.6159 - \log x) \to 0$

$$x \to \infty\ ,\quad h_2(x) \sim \frac{1}{x}\left(1 - \frac{1}{x} + \ldots\right) \to 0$$

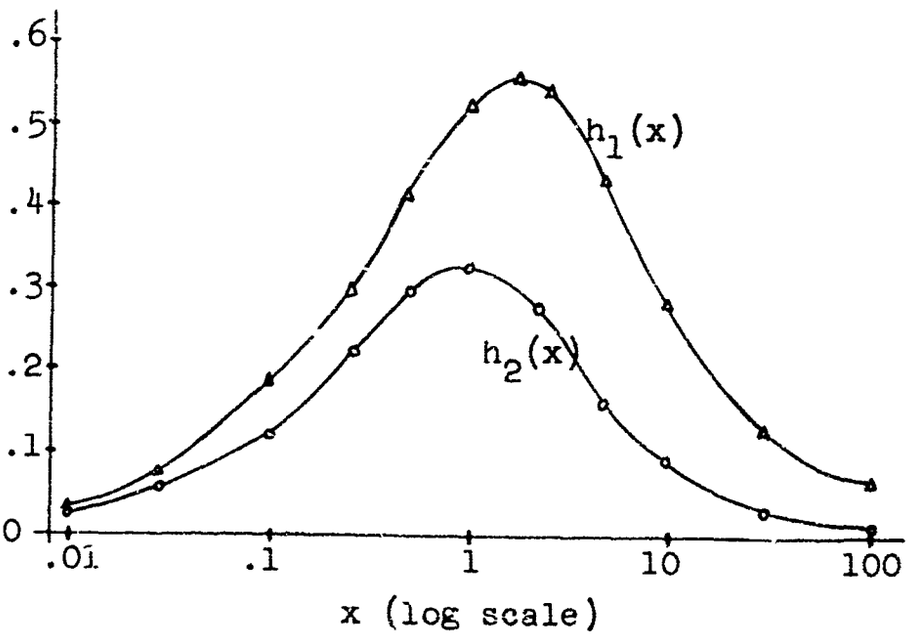

FIG. 1.12

Some results of examples C) and D) indicate general conclusions that apply to other distributed loads. The displacement relative to $\xi = 0$, $v(\xi) - v(0)$, is everywhere finite in the vicinity of the load, and increases like $-\log|\xi|$ as $|\xi| \to \infty$. Example C) has a discontinuity in the pressure, a sudden jump from zero to Q_o, at each end of the loaded area. This results in an infinite slope $\partial v/\partial \xi$ at each end where the jump occurs. This is a general result; if there is a finite jump in the load at $\xi = \xi_o$, the slope will contain a term $\log|\xi - \xi_o|$, and will thus be infinite at ξ_o. In example D), the pressure is continuous and goes to zero at the ends; the slope is finite everywhere. In each example, the pressure distribution is symmetric about the center of the loaded area ($\xi = \lambda/2$). However, the displacement is not symmetric because of delayed recovery in the moving viscoelastic base. The low point in the surface profile will always be displaced downstream from the center of the load. The velocity is conveniently represented in dimensionless form by $VT/\ell = 1/\lambda$. The variation of resistance with velocity for a given load is then shown by a plot of χ vs $1/\lambda$. For the two examples, this variation is indicated by the plots of $h_1(x)$ and $h_2(x)$ in Fig. 1.12. Each example shows that χ increases from zero, reaches a single maximum, and then decreases to zero again, as the velocity goes from 0 to ∞.

CHAPTER II

MOVING LOADS ON A PURELY VISCOUS MATERIAL

The problem of a load moving on the surface of a purely viscous material is considered in this chapter. By "viscous material" is meant an ideal incompressible viscous fluid, in which stress is linearly related to strain rate. This is a special case of the general viscoelastic fluid considered in Chapter I. Such materials as dough or road asphalt may sometimes be treated as purely viscous. Even metals may be considered viscous fluids when subject to high speed impact (Abrahamson [1]). The problem is treated as one of slow steady motion of a very viscous fluid, so that inertia forces are negligible and linear theory can be used. As in Chapter I, the load $q(x,y)$ will be normal pressure on the initially flat surface $z = 0$ of a base of infinite extent (see Fig. 1.1).

The principal interest will again be the surface deformation as the load moves with constant velocity V in the x direction. The base is undisturbed for $t < 0$, and the load is applied at $t = 0$. The resulting deformation will vary with time due to both the motion of the load and the viscous nature of the base. The relative simplicity of the purely viscous material allows solution of some three-dimensional problems. These give some idea of the much

greater difficulties encountered in the same problems with a general viscoelastic material. In Section 1.4 it was shown that the question of a steady state for a general viscoelastic fluid can be answered by considering the same problem for a purely viscous material. In particular, since there is no steady state for a semi-infinite base, the possibility of a steady when the base is a viscous layer of finite thickness is considered.

2.1 General Solution for Viscous Base

For an incompressible viscous fluid with viscosity η^*, the relations between stress and strain are

$$s_{ij} = 2\eta^* \dot{e}_{ij} \quad , \quad \dot{e} = 0 \tag{2.1}$$

For an incompressible elastic solid, with $\nu = \frac{1}{2}$,

$$s_{ij} = 2\mu\, e_{ij} \quad , \quad e = 0 \tag{2.2}$$

In a quasi-static problem with prescribed tractions on the boundaries, equilibrium and boundary conditions are the same for elastic and viscous materials at any instant of time. Also, for an elastic material $\epsilon_{ij} = 1/2(u_{i,j} + u_{j,i})$, while for a viscous material $\dot{\epsilon}_{ij} = 1/2(\dot{u}_{i,j} + \dot{u}_{j,i})$. Comparison of these relations makes evident the "viscous analogy" for slow motion of a viscous fluid: the viscous solution is the

same as the incompressible elastic solution with μ replaced by η^*, $\nu = 1/2$, and strains replaced by strain rates. In particular, elastic displacements become viscous velocities. This viscous analogy corresponds to the use of the associated elastic problem for general viscoelastic materials.

In moving load problems, the surface displacement for an incompressible elastic material is $u_z^e(x^*-Vt,y^*)$ in coordinates (x^*,y^*) fixed with the base, where $u_z^e(x^*,y^*) = (1/2\mu)\, P(x^*,y^*)$ is the displacement for the same load at rest. Thus, from the viscous analogy

$$\frac{\partial}{\partial t}\, u_z(x^*,y^*,t) = \frac{1}{2\eta^*}\, P(x^*-Vt,y^*)$$

Since the surface is undeformed at $t = 0$, $u_z(x^*,y^*,0) = 0$. The viscous displacement is then

$$u_z(x^*,y^*,t) = \frac{1}{2\eta^*} \int_0^t P(x^*-Vt',y^*)dt'$$

Changing to coordinates (1.1) moving with the load

$$u_z(x,y,t) = \frac{1}{2\eta^*} \int_0^t P(x+ Vt - Vt')\, dt'$$

$$u_z(x,y,t) = \frac{1}{2\eta^* V} \int_x^{x+Vt} P(x',y)\ dx' \qquad (2.3)$$

In these coordinates, it will be more convenient to think of the load at rest (with the origin included inside the loaded area), and the base moving under it with velocity V in the negative x-direction. The base may be either semi-infinite or a layer of finite thickness.

The general solution for surface displacement is given by equation (2.3). This can be expressed in terms of a function $G(x,y)$, defined by

$$G(x,y) \equiv \frac{1}{2\eta^* V} \int_0^x P(x',y)\, dx' \qquad (2.4)$$

Since $P(x',y)$ is (except for a constant factor) the elastic displacement for the given load distribution, $G(x,y)$ represents the area between the initial and deformed surfaces of an elastic base, from $x' = 0$ to $x' = x$, in a slice parallel to the x-axis at the given value of y (see Fig. 2.1). Then

$$u_z(x,y,t) = G(x+Vt,y) - G(x,y) \qquad (2.5)$$

The term $G(x+Vt,y)$ represents a "wave" moving with the base. The other term $G(x,y)$ is a displacement of the same shape, fixed relative to the load. The difference of these terms gives the net displacement, which varies with time as the "wave" is carried downstream (see Fig. 2.2). If the area under the complete elastic curve is finite, so that

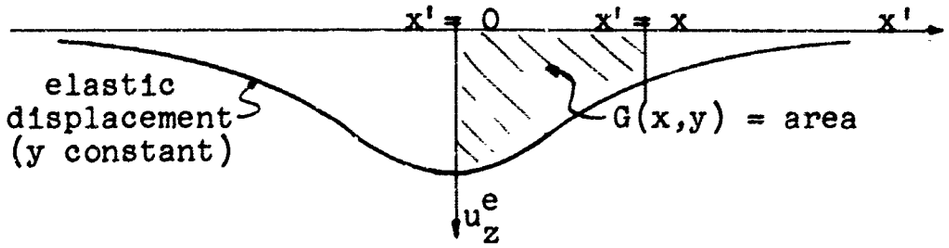

FIG. 2.1

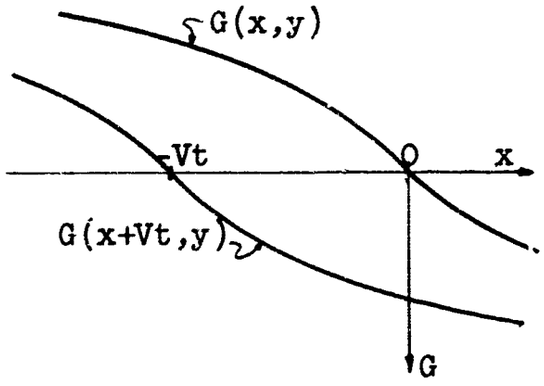

FIG. 2.2

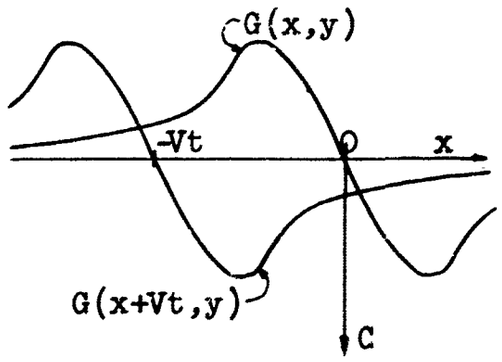

FIG. 2.3

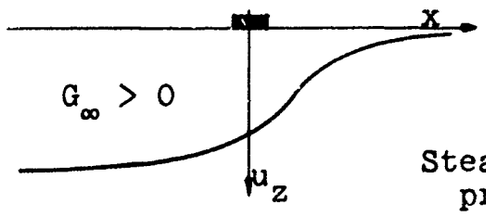

FIG. 2.4a

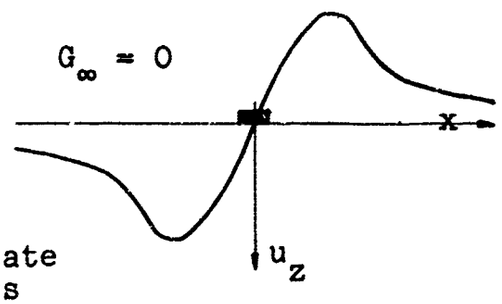

FIG. 2.4b

Steady state profiles

$G(\infty,y)$ has a finite value, $u_z(x,y,t)$ approaches a limiting value as $t \to \infty$, and there is a steady state. If $G(\infty,y)$ is infinite, there is no steady state.

When the elastic displacement is always positive (this is the case for a semi-infinite base), $G(x,y)$ is a monotonic increasing function as shown in Fig. 2.2. When the base is a layer of finite thickness, the elastic displacement may be negative (rise above the initial surface) at some distance from the load. Then, $G(x,y)$ will have the form shown in Fig. 2.3. Let $G_\infty(y) \equiv \lim_{x \to \infty} G(x,y)$; there is a steady state if this limit exists. If $G_\infty > 0$, the steady state displacement is $u_z(x,y) = G_\infty(y) - G(x,y)$. The result is a depression of finite depth extending infinitely far downstream from the load, and zero displacement far upstream from the load (Fig. 2.4a). In the case shown in Fig. 2.3, it is possible to have $G_\infty = 0$. Then, the steady state is $u_z = -G(x,y)$. The displacement is zero far from the load in any direction, and a definite localized hump is left near the load (Fig. 2.4b).

When the load is symmetric with respect to the y-axis, so that $q(x,y) = q(-x,y)$, the elastic displacement will be symmetric (thus even in x): $P(x,y) = P(-x,y)$. Then, the function G will be antisymmetric (odd in x): $G(x,y) = -G(-x,y)$. In this case,

$$u_z(-x-Vt,y) = G(-x,y) - G(-x-Vt,y)$$

$$= -G(x,y) + G(x+Vt,y)$$

$$= u_z(x,y)$$

Thus, the viscous displacement will be symmetric with respect to a line parallel to the y-axis, halfway between the fixed origin (x=0) and the point on the base originally at the origin (x = -Vt). This line of symmetry, to be called the trough line, is then $x = -Vt/2$. It moves downstream at half the velocity of the base material. The displacement along the trough line is

$$u_z(-\tfrac{1}{2}Vt,y,t) = 2G(\tfrac{1}{2}Vt,y) \qquad (2.6)$$

If $G(x,y)$ is a monotonic function, this is the maximum displacement for given y and t (see Fig. 2.5).

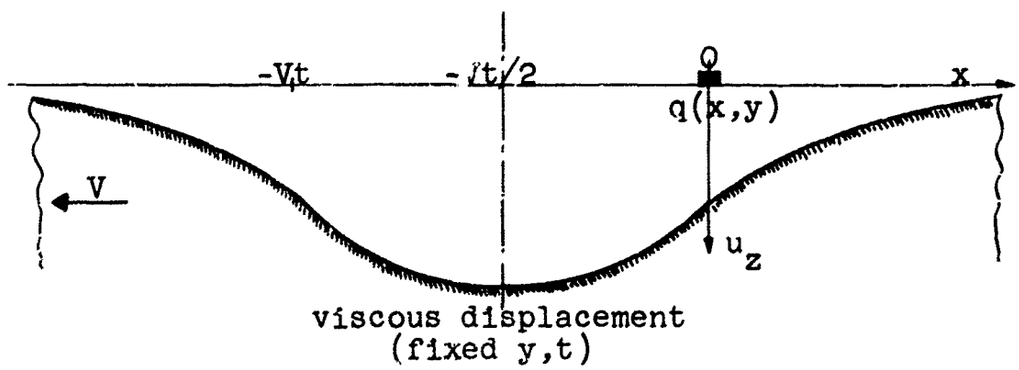

FIG. 2.5

2.2 Three-Dimensional Problem, Concentrated Load

For a pressure $q(x,y)$ on a semi-infinite base, the displacement function is

$$P(x,y) = \frac{1}{2\pi} \iint_A \frac{q(x',y')\,dx'dy'}{\sqrt{(x-x')^2+(y-y')^2}}$$

The displacement is always positive [for $q(x,y) > 0$], with a maximum near the load, and approaches zero far from the load (see Fig. 2.1 for typical profile). For large $r = \sqrt{x^2+y^2}$, $P(x,y)$ is nearly the same as for a concentrated load, i.e., $P(r) \sim \frac{N}{2\pi r}$ as $r \to \infty$, where $N = \iint_A q(x,y)dxdy$. Thus, the function $G(x,y)$ is nearly the same far from any distributed load as for a concentrated load N at the origin. It is useful, therefore, to consider the case of a concentrated load in some detail.

For a load N at the origin,

$$P(x,y) = \frac{N}{2\pi}\,\frac{1}{r} = \frac{N}{2\pi}\,\frac{1}{\sqrt{x^2+y^2}}$$

Then, from (2.4)

$$G(x,y) = \frac{N}{4\pi\eta^*V} \int_0^x \frac{dx'}{\sqrt{x'^2+y^2}} = \frac{N}{4\pi\eta^*V} \cdot \log\left[\frac{x+\sqrt{x^2+y^2}}{|y|}\right]$$

From (2.5),

$$\frac{4\pi\eta^* V}{N}\ u_z(x,y,t) = \log\left[\frac{x+Vt+\sqrt{(x+Vt)^2+y^2}}{x+\sqrt{x^2+y^2}}\right] \qquad (2.7)$$

For a given y, $G(\infty,y)$ is infinite, confirming the conclusion in Chapter I that there is no steady state. At any point on the surface, as $t \to \infty$,

$$\frac{4\pi\eta^* V}{N}\ u_z(x,y,t) \sim \log Vt - \log(x+\sqrt{x^2+y^2} + \log 2 + \frac{x}{Vt} + \ldots \qquad (2.8)$$

Thus, the displacement increases without limit as $t \to \infty$. It can be shown that the vertical velocity $\partial u_z/\partial t$ of the surface approaches zero, and the surface slopes ($\partial u_z/\partial x$, $\partial u_z/\partial y$) approach finite values as $t \to \infty$.

For a given finite time, the displacement (2.7) is positive everywhere; it approaches zero far from the load, as $|x|$ or $|y| \to \infty$. Thus, appreciable surface deformation occurs only in the vicinity of those points on the surface that have passed under or near the load. The displacement is symmetric about a trough line at $x = -Vt/2$, as discussed in Section 2.2. The maximum displacement at any given y and t is, from (2.6)

$$u_z\big|_{max} = \frac{N}{2\pi\eta^* V}\ \log\left[\frac{\sqrt{(Vt)^2+4y^2}-Vt}{2|y|}\right] = \frac{N}{2\pi\eta^* V}\ \tanh^{-1}\left[\frac{1}{\sqrt{1+(2y/Vt)^2}}\right] \qquad (2.9)$$

Because the load is concentrated at a point, the elastic displacement is infinite at that point. The viscous displacement is thus infinite at all points that have passed directly under the load, i.e., for $y = 0$, $-Vt < x < 0$. The contour lines of constant displacement at a given time are ellipses, with common foci at the initial and present load positions: $y = 0$; $x = 0, -Vt$. The contour ellipse for $(4\pi\eta^*V/N)u_z = D$ has a constant eccentricity $\epsilon = (e^D-1)/(e^D+1)$, and an expanding major axis $Vt/2\epsilon$. Figure 2.6 shows typical profiles and a plan view of the surface for a concentraced load.

Except near points that have passed under the load, the results for a distributed load (symmetric about the y-axis) are qualitatively similar to those for the concentrated load. The general shape of the surface is like a shallow bowl, with displacements decreasing monotonically in any direction from the low point at $y = 0$, $x = -Vt/2$. The surface approaches its initial flat position far away from the loaded regions. As time goes on, the displacement increases without limit, but at a continually slower rate. For the semi-infinite base, there is no localized "hump" formed near the load, but rather a downstream depression that is continually deepening and moving away from the load. The contours of constant displacement will be simple closed curves, symmetric about the trough line. To demonstrate these results for a specific distributed load, an example will be considered in the next section.

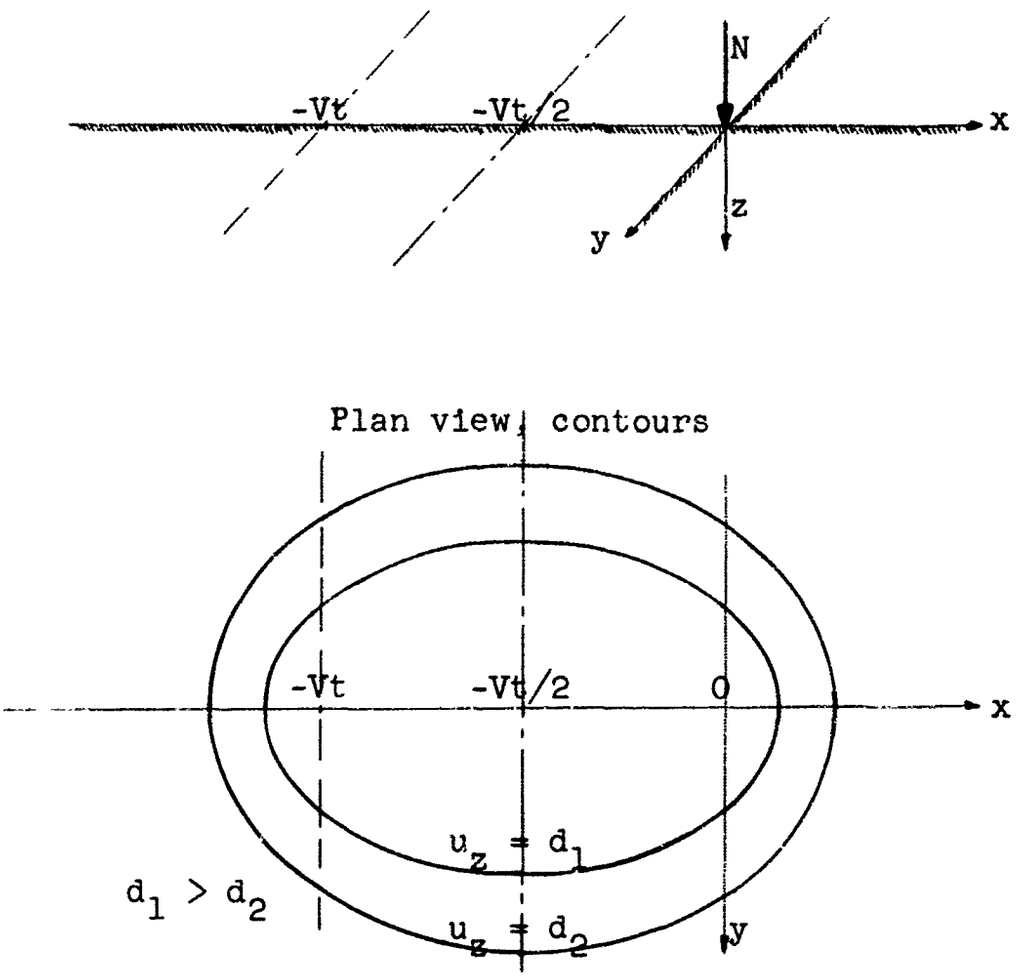

FIG. 2.6

Surface displacement, fixed t (eqn. 2.7)

2.3 Uniform Pressure on a Circular Area

As a three-dimensional example of a distributed load, a uniform pressure q_o acts on a circle of radius a. Then,

$$q(x,y) = q(r) = q_o \quad , \quad 0 \leq r \leq a$$

where $r = \sqrt{x^2+y^2}$. The viscous base is semi-infinite. The following dimensionless quantities are used:

$$\xi = \frac{x}{a} \ , \ \eta = \frac{y}{a} \ , \ \rho = \frac{r}{a} = \sqrt{\xi^2+\eta^2} \ , \ \tau = \frac{Vt}{a} \tag{2.10a}$$

$$w(\rho) = \frac{2\mu}{q_o a} \ u_z^e(r) \tag{2.10b}$$

$$g(\xi,\eta) = \frac{2\eta^* V}{q_o a^2} \ G(x,y) \tag{2.10c}$$

$$v(\xi,\eta,\tau) = \frac{2\eta^* V}{q_o a^2} \ u_z(x,y,t) \tag{2.10d}$$

The elastic displacement can be expressed in several ways. The most convenient form for use here is derived using the Hankel Transform (Sneddon [28], p. 469), and gives

$$w(\rho) = \int_o^\infty J_1(u) \ J_o(\rho u) \ \frac{du}{u} \tag{2.11}$$

This integral is a special case of the Weber-Schaftheitlin discontinuous integral (Watson [35], p. 398), and has the series form

$$\int_0^\infty J_1(u)\ J_o(\rho u)\ \frac{du}{u} = {}_2F_1\left(\tfrac{1}{2}, -\tfrac{1}{2}\ ;\ 1\ ;\ \rho^2\right),\ \rho \le 1$$

$$= {}_2F_1\left(\tfrac{1}{2}\ ,\ \tfrac{1}{2}\ ;\ 2\ ;\ \frac{1}{\rho^2}\right),\ \rho \ge 1$$

$$= \frac{2}{\pi}\ ,\quad \rho = 1 \qquad (2.12)$$

where

$${}_2F_1\ (a,b;\ c;\ x) = 1 + \sum_{k=1}^{\infty} \frac{\Gamma(a+k)}{\Gamma(a)}\ \frac{\Gamma(b+k)}{\Gamma(b)}\ \frac{\Gamma(c)}{\Gamma(c+k)}\ \frac{x^k}{k!}$$

is the hypergeometric function. Thus,

$$w(\rho) = 1 - \sum_{k=1}^{\infty} C_k\ \rho^{2k}\ ,\ \rho \le 1$$

$$= \frac{1}{2\rho} + \sum_{k=1}^{\infty} D_k\ \rho^{-(2k+1)}\ ,\ \rho \ge 1$$

$$= \frac{2}{\pi}\ ,\qquad \rho = 1 \qquad (2.13)$$

where

$$C_k = \frac{1}{\pi}\ \frac{[\Gamma(k+\frac{1}{2})]^2}{(k!)^2(2k-1)}\ ;\quad D_k = \frac{1}{2\pi}\ \frac{[\Gamma(k+\frac{1}{2})]^2}{(k!)^2(k+1)} = \frac{2k-1}{2(k+1)}\ C_k \qquad (2.14)$$

(Numerical values of C_k and D_k are given in Table 2.1 at the end of the chapter.) A profile of the elastic displacement is sketched in Fig. 2.7.

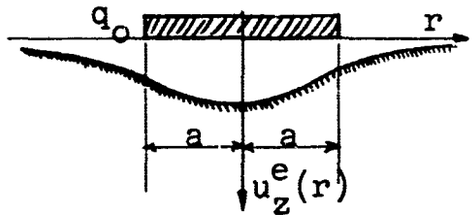

FIG. 2.7

Since $P(x,y) = 2\mu\, u_z^e(r) = q_o a\, w(\rho)$, (2.4) and (2.10c) give

$$g(\xi,\eta) = \int_0^{\xi} w\left(\sqrt{\zeta^2+\eta^2}\right)\, d\zeta \qquad (2.15)$$

and (2.5) and (2.10d) give

$$v(\xi,\eta,\tau) = g(\xi+\tau,\eta) - g(\xi,\eta) \qquad (2.16)$$

The function $g(\xi,\eta)$ is independent of any physical parameters, so the numerical values need be determined only once for all problems of uniform circular load. Then, the viscous displacement at any point on the surface for any time is

$$u_z(x,y,t) = \frac{q_o a^2}{2\eta^* V}\left[g\left(\frac{x+Vt}{a}\,,\,\frac{y}{a}\right) - g\left(\frac{x}{a}\,,\,\frac{y}{a}\right)\right]$$

Because there are two different expressions (2.13) for $w(\rho)$, one for $\rho \leq 1$ and one for $\rho \geq 1$, there is more than one form of $g(\xi,\eta)$ evaluated from (2.15). Since $g(\xi,\eta) = -\,g(-\xi,\eta)$ and $g(\xi,\eta) = g(\xi,-\eta)$, it is sufficient to evaluate $g(\xi,\eta)$ for (ξ,η) in the first quadrant only. There are three forms for $g(\xi,\eta)$, one for each of the three regions shown in Fig. 2.8. Numerical values of $g(\xi,\eta)$ can be determined from the expressions which follow. Some values are given in Fig. 2.9, and contour lines are sketched in.

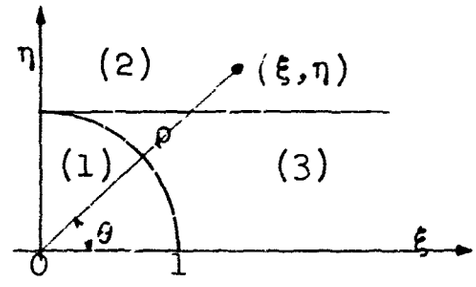

FIG. 2.8

(1) $\underline{\rho \leq 1}$, $0 \leq \eta \leq 1$, $0 \leq \xi \leq \sqrt{1-\eta^2}$

$$g(\xi,\eta) \equiv g_1(\xi,\eta) = \int_0^{\xi} [1 - \sum_{k=1}^{\infty} C_k(\zeta^2+\eta^2)^k] d\zeta$$

$$= \xi - \sum_{1}^{\infty} C_k \int_0^{\xi} (\zeta^2+\eta^2)^k \, d\zeta$$

Let $$I_k^1(\xi,\eta) \equiv \int_0^{\xi} (\zeta^2+\eta^2)^k \, d\zeta = \xi\eta^{2k} \sum_{j=0}^{k} \binom{k}{j} \frac{1}{2j+1} \left(\frac{\xi}{\eta}\right)^{2j} \tag{2.17a}$$

$$I_k^1(\xi,0) = \frac{1}{2k+1} \, \xi^{2k+1} \tag{2.17b}$$

Then

$$g_1(\xi,\eta) = \xi - \sum_{k=1}^{\infty} C_k \, I_k^1(\xi,\eta) \tag{2.18a}$$

$$g_1(\xi,0) = \xi - \sum_{1}^{\infty} \frac{C_k}{2k+1} \, \xi^{2k+1} \tag{2.18b}$$

(2) $\underline{\rho \geq 1}$, $\underline{\eta \geq 1}$

$$\zeta(\xi,\eta) \equiv g_2(\xi,\eta) = \int_0^{\xi} \left[\frac{1}{2\sqrt{\zeta^2+\eta^2}} + \sum_{k=1}^{\infty} D_k(\zeta^2+\eta^2)^{-(k+\frac{1}{2})} \right] d\zeta$$

$$= \frac{1}{2} \log \frac{\xi+\rho}{\eta} + \sum_{k=1}^{\infty} D_k \int_0^{\xi} (\zeta^2+\eta^2)^{-(k+\frac{1}{2})} \, d\zeta$$

Let $$I_k^2(\xi,\eta) \equiv \int_0^{\xi} (\zeta^2+\eta^2)^{-(k+\frac{1}{2})} \, d\zeta \, , \quad (\eta \geq 1) \tag{2.19a}$$

With the substitution $\zeta = \eta \cot \phi$, this becomes

$$I_k^2 (\xi,\eta) = \eta^{-2k} \int_{\theta}^{\pi/2} \sin^{2k-1} \phi \, d\phi \qquad (2.19b)$$

where $\theta = \tan^{-1} \frac{\eta}{\xi}$ (see Fig. 2.8).

For numerical evaluation, this can be expressed in terms of the incomplete Beta function $B_x(a,b)$. With $x = \sin^2\theta$ $(0 \leq \theta \leq \frac{\pi}{2})$,

$$\int_0^{\theta} \sin^{2k-1} \phi \, d\phi = \frac{1}{2} B_x (k,\tfrac{1}{2})$$

Then, (2.19b) becomes

$$I_k^2 (\xi,\eta) = \frac{1}{2} \eta^{-2k} [B_1(k,\tfrac{1}{2}) - B_x(k,\tfrac{1}{2})] \qquad (2.19c)$$

Values of $B_x(k,\frac{1}{2})$ are tabulated in Pearson [28] for $x = 0(.01)1.00$, $k = 1(1)50$.

As $\xi \to \infty$, $I_k^2(\xi,\eta) \sim \frac{1}{2} \eta^{-2k} B_1(k,\frac{1}{2}) - \frac{1}{2k} \xi^{-2k} + \frac{2k+1}{4(k+1)} \eta^2 \xi^{-(2k+2)} \ldots$

As $\xi \to 0$, $I_k^2(\xi,\eta) \sim \xi \eta^{-(2k+1)} - \frac{2k+1}{6} \eta^{-(2k+3)} \xi^3 + \ldots$

Using (2.19a,c),

$$g_2(\xi,\eta) = \frac{1}{2} \log \frac{\xi+\rho}{\eta} + \sum_{k=1}^{\infty} D_k I_k^2 (\xi,\eta) \qquad (2.20a)$$

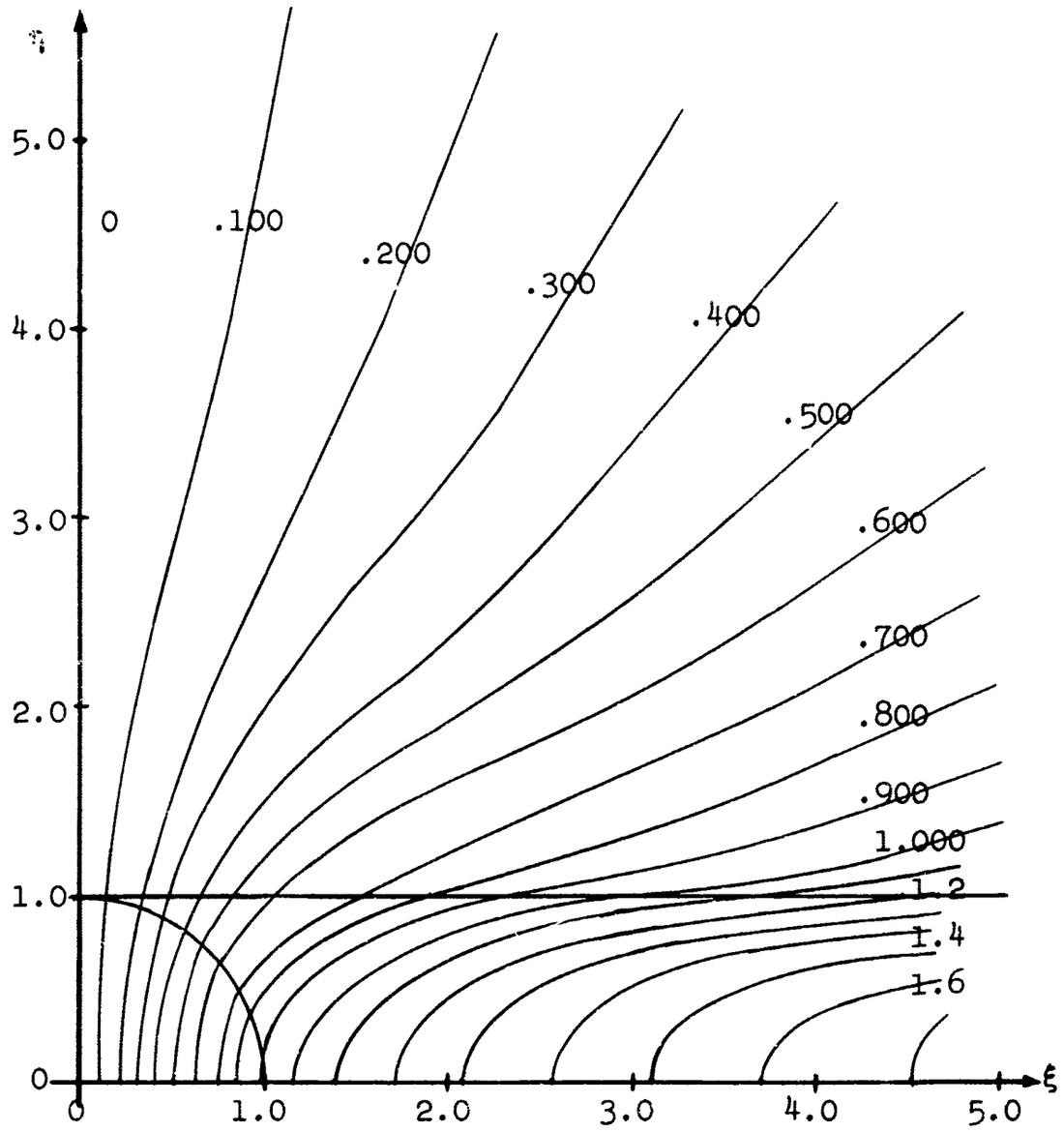

Lines of constant $g(\xi,\eta)$

for uniform circular load

$$g(-\xi,\eta) = -g(\xi,\eta) \quad ; \quad g(\xi,-\eta) = g(\xi,\eta)$$

FIG. 2.9

or

$$g_2(\xi,\eta) = -\frac{1}{2}\log\tan\frac{\theta}{2} + \frac{1}{2}\sum_{k=1}^{\infty} D_k \eta^{-2k}[B_1(k,\tfrac{1}{2}) - B_x(k,\tfrac{1}{2})] \qquad (2.20b)$$

where $x = \sin^2\theta$.

For a given θ, as $\rho \to \infty$, $g_2 \sim -\frac{1}{2}\log\tan\frac{\theta}{2} + \frac{1}{16}\frac{\cos\theta}{\sin^2\theta}\rho^{-2} + \ldots$

(3) $\underline{\rho \geq 1}$, $\underline{0 \leq \eta \leq 1}$, $\xi \geq \sqrt{1-\eta^2}$

$$g(\xi,\eta) \equiv g_3(\xi,\eta) = \int_0^{\sqrt{1-\eta^2}} w(\sqrt{\zeta^2+\eta^2})\,d\zeta + \int_{\sqrt{1-\eta^2}}^{\xi} w(\sqrt{\zeta^2+\eta^2})\,d\zeta$$

$$= g_1(\sqrt{1-\eta^2},\ \eta) + \int_{\sqrt{1-\eta^2}}^{\xi} \left[\frac{1}{2\sqrt{\zeta^2+\eta^2}} + \sum_{k=1}^{\infty} D_k(\zeta^2+\eta^2)^{-(k+\frac{1}{2})}\right]d\zeta$$

Let $I_k^3(\xi,\eta) \equiv \int_{\sqrt{1-\eta^2}}^{\xi} (\zeta^2+\eta^2)^{-(k+\frac{1}{2})}\,d\zeta$, $(\eta \geq 1,\ \xi \geq \sqrt{1-\eta^2})$

$$= \frac{1}{2}\eta^{-2k}\,[B_{\eta 2}(k,\tfrac{1}{2}) - b_{s2}(k,\tfrac{1}{2})] \qquad (2.21a)$$

where $s = \eta/\rho$

$$I_k^3(\xi,0) = \frac{1}{2k}\,(1 - \xi^{-2k}) \qquad (2.21b)$$

As $\xi \to \infty$, $I_k^3(\xi,\eta) \sim \frac{1}{2}\eta^{-2k}B_{\eta 2}(k,\tfrac{1}{2}) - \frac{1}{2k}\xi^{-2k} + \ldots$

Then, $$g_3(\xi,\eta) = g_1(\sqrt{1-\eta^2},\eta) + \frac{1}{2}\log\left(\frac{\xi+\rho}{1+\sqrt{1-\eta^2}}\right) + \sum_{k=1}^{\infty} D_k I_k^3(\xi,\eta) \qquad (2.22a)$$

$$g_3(\xi,0) = 1 - \sum_{k=1}^{\infty}\left(\frac{C_k}{2k+1} - \frac{D_k}{2k}\right) - \sum_{k=1}^{\infty}\frac{D_k}{2k}\xi^{-2k} + \frac{1}{2}\log\xi \qquad (2.22b)$$

As $\xi \to \infty$ for a given η, both g_2 and g_3 behave like $1/2 \log \xi$ and increase without limit. This again confirms that there is no steady state.

There are several regions of the surface, each having a different expression for the displacement $v(\xi,\eta,\tau) = g(\xi+\tau,\eta) - g(\xi,\eta)$, because of the different forms of g. These regions are shown in Fig. 2.10a for $0 < \tau < 2$, and Fig. 2.10b for $\tau > 2$. Displacements are symmetric about the ξ axis and the trough line $\xi = -\tau/2$, so only the quadrant $\eta > 0$, $\xi > -\tau/2$ is considered.

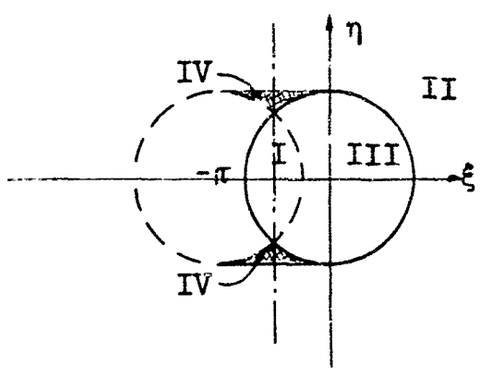

FIG. 2.10a

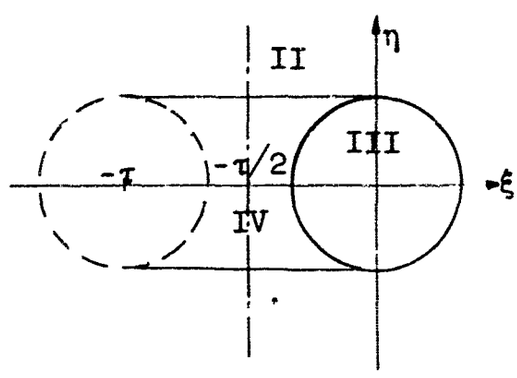

FIG. 2.10b

I. Points always under the load (beginning at $\tau = 0$).

$$v(\xi,\eta,\tau) = g_1(\xi+\tau,\eta) - g_1(\xi,\eta)$$

II. Points never under the load.

$$v(\xi,\eta,\tau) = g_2(\xi+\tau,\eta) - g_2(\xi,\eta) \quad \text{for} \quad \eta \geq 1$$

$$= g_3(\xi+\tau,\eta) - g_3(\xi,\eta) \quad \text{for} \quad \eta \leq 1$$

(Both cases give the same analytic expression.)

III. Points originally outside the load which have moved under it.

$$v(\xi,\eta,\tau) = g_3(\xi+\tau,\eta) - g_1(\xi,\eta)$$

IV. Point originally outside the load which then moved under it and are now outside again.

$$v(\xi,\eta,\tau) = g_3(\xi+\tau,\eta) + g_3(|\xi|,\eta)$$

Displacements and slopes are continuous across the boundaries of these regions. The maximum displacement occurs at $\xi = -\tau/2$, $\eta = 0$:

$$v_{max} = 2g(\tfrac{\tau}{2},0) = \tau\left[1 - \Sigma \frac{C_k}{2k+1} \left(\frac{\tau}{2}\right)^{2k}\right], \quad 0 \leq \tau \leq 2$$

$$= 2\left[1 - \Sigma\left(\frac{C_k}{2k+1} - \frac{D_k}{2k}\right)\right] - 2\Sigma \frac{D_k}{2k} \left(\frac{\tau}{2}\right)^{-2k} + \log \frac{\tau}{2}, \quad \tau \geq 2$$

The resulting deformed surface is smooth, with finite displacement everywhere for finite τ. As $\tau \to \infty$, $v(\xi,\eta,\tau) \sim \frac{1}{2} \log \tau$ at all points on the surface. The general description in the last paragraph of Section 2.2 applies in particular to this problem, and conclusions given there can be verified directly from this section. At any finite time, the displacement far from the load is nearly the same as for a concentrated load $N = q_o \pi a^2$.

2.4 Base of Finite Thickness

When the base is semi-infinite, the viscous material flows without limit due to the vertical velocity resulting from the load on the surface. There is no lower boundary to the base, so the vertical displacements continue to increase with time and no steady state is reached. If, however, the base had a lower boundary, so that flow is constrained at some depth below the surface, vertical displacements would not increase indefinitely. It seems quite likely on physical grounds that this situation would lead to a steady state when the base is moving horizontally under the load. The base of finite thickness does of course represent a real situation more closely than does the semi-infinite base. The thickness of the base is thus a critical factor for establishment of a steady state in problems of this type, when the base is a fluid material

To investigate this situation more closely, the base will be considered as a layer of constant finite thickness h, but extending infinitely far in the x and y directions. As before, the load $q(x,y)$ is applied to the otherwise free surface $z = 0$, and the viscous layer moves with velocity V in the negative x direction (Fig. 2.11). The bottom of the layer, $z = h$, rests on a rigid support, so that vertical velocity and displacement are prevented. One condition is thus

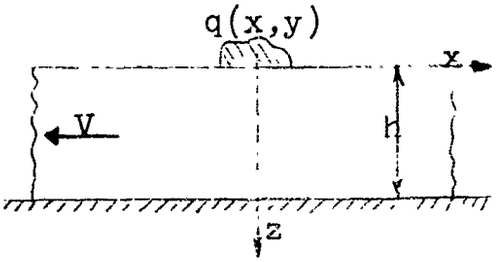

FIG. 2.11

$$\dot{u}_z(x,y,h) = 0 \quad \text{on} \quad z = h \tag{2.23}$$

The way in which the layer is supported at the lower boundary is quite important. The two extremes are considered here; other possibilities will fall in between. One extreme is rigid attachment so that tangential displacements are prevented. This gives the conditions (for a moving base)

$$\dot{u}_z(x,y,t) = -V, \quad \dot{u}_y(x,y,h) = 0 \quad \text{on } z = h \tag{2.24a}$$

The other extreme is no attachment (i.e., frictionless support), so there will be no tangential stresses. Then,

$$\tau_{yz} = (x,y,h) = \tau_{xz}(x,y,h) = 0 \quad \text{on} \quad z = h \tag{2.24b}$$

The problem of an axisymmetric load will be considered in more detail. The results for other distributed loads would be qualitatively similar. The load is $q(r)$ on a circle of radius a. The dimensionless quantities (2.10a-d) are used. Also, let $q(r) = q_o\, Q(\rho)$, where $Q(\rho)$ is dimensionless and q_o is some measure of the load magnitude. Following the analysis of Sneddon [28], the incompressible elastic solution is determined using Hankel Transforms. The resulting surface displacement is

$$w(\rho) = \int_0^\infty \bar{Q}(u)\; J_o(\rho u)\; F(\lambda u)\; du \tag{2.25}$$

where $\lambda = \frac{h}{a}$ and

$$\bar{Q}(u) \equiv \int_0^1 Q(\rho)\; J_o(\rho u)\; \rho\; d\rho \tag{2.26}$$

For a uniform load q_o, $Q(\rho) = 1$ and $\bar{Q}(u) = \frac{J_1(u)}{u}$.

The function $F(\lambda u)$ depends on the method of support. For rigid attachment (2.24a)

$$F(x) = \frac{\cosh x \sinh x - x}{x^2 + \cosh^2 x} \tag{2.27}$$

$$\sim \frac{2}{3} x^3 \left(1 - \frac{9}{5} x^2 + \ldots\right) \quad \text{as } x \to 0$$

$$\sim 1 - 2(1+2x+2x^2)e^{-2x} + \ldots \quad \text{as } x \to \infty$$

For frictionless support (2.24b)

$$F(x) = \frac{2 \sinh^2 x}{2x + \sinh 2x} \qquad (2.28)$$

$$\sim \frac{1}{2} x \left(1 - \frac{1}{45} x^4 + \ldots\right) \text{ as } x \to 0$$

$$\sim 1 - 2(1 + 2x)e^{-2x} + \ldots \text{ as } x \to \infty$$

In both cases, $F(x)$ increases monotonically from zero and approaches 1 asymptotically as x goes from 0 to ∞. For a semi-infinite base, $\lambda = \infty$ and $F(\lambda u) = 1$ in each case. Then, for a uniform load, (2.25) reduces to (2.11).

From the elastic displacement (2.25), equation (2.15) gives

$$g(\xi,\eta) = \int_0^{\xi} \left[\int_0^{\infty} \bar{Q}(u)\, F(\lambda u)\, J_0\left(\sqrt{\zeta^2+\eta^2}\, u\right) du \right] d\zeta \qquad (2.29)$$

The possible steady state depends on $g_\infty(\eta) \equiv \lim_{\xi \to \infty} g(\xi,\eta)$. Letting $\xi \to \infty$ in (2.29), and using

$$J_0\left(\sqrt{\xi^2+\eta^2}\right) = J_0(\xi)\, J_0(\eta) + 2 \sum_{k=1}^{\infty} J_k(\xi) J_k(\eta)$$

$$\int_0^{\infty} J_k(u\xi)\, d\xi = \frac{1}{u}$$

the ζ integration in (2.29) can be carried out. This gives

$$g_\infty(\eta) = \int_0^{\infty} \bar{Q}(u)\, F(\lambda u) \left[J_0(u\eta) + 2 \sum_{k=1}^{\infty} J_k(u\eta)\right] \frac{du}{u} \qquad (2.30)$$

The integrand of (2.30) is finite, continuous, and behaves like $u^{-(m+1/2)}$ $(m \geq 1)$ as $u \to \infty$. Although (2.30) cannot be evaluated analytically, it can be verified that $g_\infty(\eta)$ has a finite value. Thus, the base of finite thickness <u>does</u> reach a steady state.

The nature of the steady state depends on the value of $g_\infty(\eta)$, as discussed in Section 2.1. This would require a numerical evaluation of the integral (2.30), or of the surface displacement and the area it encloses. For frictionless support, $F(\lambda u)$ of equation (2.28) can be approximated by exponential terms (Sneddon [28]), and the resulting integrals can be evaluated. This gives $g_\infty(\eta) > 0$ for any η , thus indicating a steady state with a finite depression downstream (Fig. 2.4a).

The two-dimensional problem can be treated in the same way. The elastic displacement can be determined using Fourier transforms. The result is similar to the axisymmetric problem; for a layer of finite thickness, the expression for displacement (corresponding to equation 2.25) is the same as for a semi-infinite base (corresponding to equation 2.11) with the additional function $F(\lambda u)$. For the same support conditions (2.24a,b), $F(\lambda u)$ is the same as for the axisymmetric problem (2.27, 2.28). Thus it is reasonable to expect that the effect of the kind of support at the lower boundary $(z = h)$ on the nature of the steady state will be similar for two-

dimensional and three-dimensional problems. The two-dimensional problem of a uniform load on a base of finite thickness, rigidly attached, has been solved by Abrahamson and Goodier [2]. This solution gives $g_\infty = 0$, and the resulting steady state is a localized hump near the load (similar to Fig. 2.4b).

These examples suggest general conclusions about the steady state displacement for any load distribution on a base of finite thickness. When the base is rigidly attached at the lower boundary, $g_\infty(\eta) = 0$. The deformation would be localized, forming a hump at the load (Fig. 2.4a). When the lower boundary is not attached (i.e., frictionless support), $g_\infty(\eta) > 0$. There would be general deformation downstream from the load, forming a depression of finite depth (Fig. 2.4b). The overall form of the steady state displacement is thus determined by the way in which the base is supported at the lower boundary. Regardless of the kind of support, a purely viscous (and thus any viscoelastic fluid) material of finite thickness will always reach a steady state.

TABLE 2.1

COEFFICIENTS FOR UNIFORM CIRCULAR LOAD DISPLACEMENT

(Section 2.3)

$$C_k = \frac{1}{\pi} \frac{[\Gamma(k + \frac{1}{2})]^2}{(k!)^2(2k-1)} \quad , \quad D_k = \frac{1}{2\pi} \frac{[\Gamma(k + \frac{1}{2})]^2}{(k!)^2(k+1)} = \frac{2k-1}{2(k+1)} \; C_k$$

k	C_k	D_k	$C_k/(2k+1)$	$D_k/2k$
1	.250000000	.062500000	.083333333	.031250000
2	.046875000	.023437500	.009375000	.005859376
3	.019531250	.012207032	.002790178	.002034506
4	.010681152	.007476806	.001186794	.000934600
5	.006729126	.005046844	.000711738	.000504684
6	.004626274	.003634930	.000355868	.000302910
7	.003375292	.002742424	.000225020	.000195888
8	.002571024	.002142520	.000151236	.000133908
9	.002023490	.001719966	.000106500	.000095554
10	.001633968	.001411154	.000077808	.000070558
Sum	.348046576	.122319176	.098213474	.041381984

$$\sum_{k=1}^{\infty} C_k = 1 - \frac{2}{\pi} = .363380228$$

$$\sum_{k=1}^{\infty} D_k = \frac{2}{\pi} - \frac{1}{2} = .136619772$$

CHAPTER III

MOVING CONTACT PROBLEMS

When a moving body of given shape is pressed into another (stationary) body, the problem is one of "moving contact." There is some load distribution within an area of contact where the deformed surfaces of the two bodies must match. If one or both bodies is viscoelastic, dissipation of energy will produce resistance to the moving body, and in general the contact conditions will change with time.

In this and following chapters, a particular viscoelastic moving contact problem will be considered. A rigid body moves with constant velocity V in the x-direction over the initially flat surface (z=0) of a semi-infinite viscoelastic solid. It is held in contact by a constant normal force N*, which produces a contact area A of unknown shape, extent, and placement. The surfaces are "frictionless" (i.e., no tangential stresses) and non-adhesive, so the load distribution is normal pressure $q(x,y) \geq 0$ within A. The moving contact is thus a moving load problem as discussed in Chapter I, although in the contact problem the load q is initially unknown. It was shown in Section 1.4 that a steady state is always possible; only these will be considered. Then, the contact area and pressure do not change with time. Once they are determined, the "friction" force F^* (which resists the motion) can be found as in Section 1.5.

3.1 Formulation of the Steady State Problem

It is again convenient to consider the rigid body stationary (in x,y,z coordinates), with the base moving in the negative x-direction at velocity V (see Fig. 3.1). For some fixed orientation of the body, its lower surface has a known shape given by $z = \text{constant} + w^*(x-b,y-c)$, where (b,c) are the coordinates of a fixed (but arbitrary) reference point P in the body. The body is held in contact with the moving base by a load N* normal to the initially flat surface of the base (i.e., vertical) and any horizontal load F* (the resisting or "friction" force) that may be necessary. For a given N*, the size, shape, and placement of the contact area A is initially unknown, except that it must of course coincide with some part of the surface of the rigid body. In the actual analysis, it will be convenient to allow the rigid body to rotate through a small angle about the horizontal axis, from the orientation implied by the function

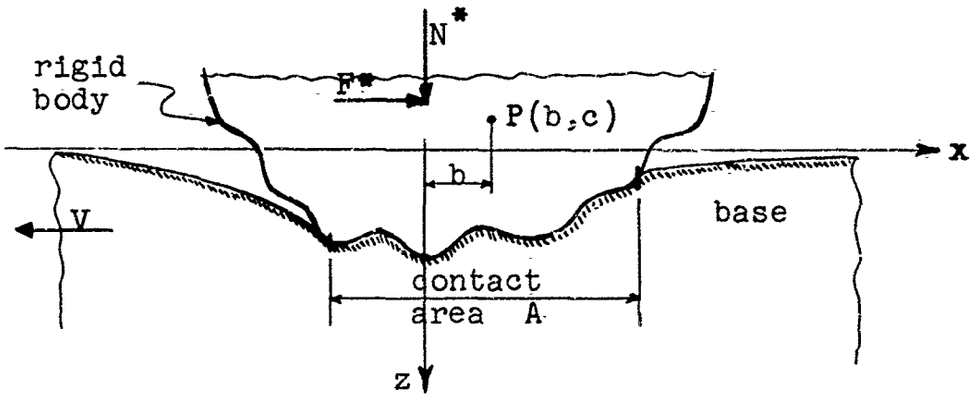

FIG. 3.1

$w^*(x,y)$. The amount and axis of this slight tilt is also initially unknown.

To formulate a definite problem, the conditions of contact must be further specified. There is no adhesion between the contact surfaces so $q(x,y) \geq 0$ inside A. If the surface were sufficiently uneven, breaks in contact would occur within the overall area whenever complete contact required negative pressure (adhesion). It is postulated here that the surface is such as to maintain contact over the full area. This means the area A will be a simply connected region, bounded by a simple closed curve called the "edge" of the contact.

To insure a unique solution to a given contact problem, only smooth contacts will be considered. For a "smooth" contact, by definition, the displacement u_z and its derivatives $\partial u_z/\partial x$ and $\partial u_z/\partial y$ are continuous across the edge of the contact. This requires the pressure $q(x,y)$ to be zero all along the edge[1]. The alternative to smooth contact is a sharp corner at the edge, with infinite pressure there. If the rigid body had such a sharp corner, any vertical load N^* (above a certain minimum) would give proper contact. This possibility is excluded by requiring smooth contact.

---

[1] A finite non-zero pressure at the edge would produce a continuous but vertical slope (see example C, Section 1.6), which would not in general fit the lower surface of the rigid body.

The moving contact is a mixed boundary value problem, since normal displacement is prescribed over part of the surface, and normal stress is prescribed elsewhere. For the quasi-static, steady state problem, the equilibrium and strain-displacement relations to be satisfied are

$$\sigma_{ij,j} = 0 \quad , \quad \epsilon_{ij} = \frac{1}{2}\left(u_{i,j} + u_{j,i}\right) \tag{3.1a}$$

and the stress-strain relations can be written (from Section 1.4)

$$2\mu_o e_{ij}(x,y,z) = \int_o^\infty \frac{dJ(\zeta)}{d\zeta}\, s_{ij}(x+VT\zeta,y,z)\,d\zeta \tag{3.1b}$$

$$3K_c e(x,y,z) = \int_o^\infty \frac{dB(\zeta)}{d\zeta}\, \theta(x+VT\zeta,y,z)\,d\zeta \tag{3.1c}$$

The boundary conditions on $z = 0$ are

$$\tau_{xz}(x,y,0) = \tau_{yz}(x,y,0) = 0 \quad \text{for all } x,y \tag{3.2a}$$

$$\left.\begin{aligned} \sigma_z(x,y,0) &= 0 && \text{outside A} \\ u_z(x,y,0) &= \delta + \alpha x + \beta y + w^*(x-b,y-c) && \text{inside A} \end{aligned}\right\} \tag{3.2b}$$

where α,β,δ are constants initially unknown (α and β are components of the possible small angle of tilt), and A is the initially unknown contact area. The unknown contact pressure inside A is $q(x,y) = -\sigma_z(x,y,0) \geq 0$.

For smooth contact, u_z and its derivatives are continuous, and $q(x,y) = 0$ on the edge of the contact. The load components, from Section 1.5, are

$$N^* = \iint_A q(x,y)dA \; ; \quad F^* = - \iint_A q(x,y) \frac{\partial u_z}{\partial x} dA$$

It is evident from the mixed boundary conditions and the other conditions to be met that solution of a moving problem will in general be very difficult. It seems likely on physical grounds that a solution will exist, provided the lower surface given by $w^*(x,y)$ is sufficiently smooth. This means, for example, that for a given load N^*, there will be a definite area, q, α, β, and δ which allow all the conditions to be satisfied. However, to attempt to find a solution there must be some knowledge or assumption about the contact area. In a general three-dimensional problem, the area is a two-dimensional region, thus encompassing an infinite number of possible shapes, as well as the other unknown parameters of size and placement. The motion of the base introduces an asymmetry not present in stationary contact problems, so that the methods of the Hertz theory for elastic contact problems are not useful here. In view of these difficulties, a solution for even the simplest three-dimensional problems is out of reach at this time.

A considerable simplification results if the problem is two-dimensional, i.e., the rigid body is an infinite cylinder (with arbitrary cross-section). Taking the cylinder axis to be in the y-direction, the problem can be considered in the x,z plane. The area of contact is then simply a line segment, specified by two parameters: its length ℓ, and a distance b fixing its placement on the rigid body surface. The surface is now given by $z = \delta + w^*(x-b)$. For convenience (as in Chapter I) the contact will be taken from $x = 0$ to $x = \ell$. The boundary conditions (3.2a,b) become

$$\tau_{xz}(x,0) = 0 , \qquad -\infty \leq x \leq \infty \tag{3.3a}$$

$$\sigma_z(x,0) = 0 , \qquad x \leq 0 , \; x \geq \ell \tag{3.3b}$$

$$u_z(x,0) = \delta + \alpha x + w^*(x-b) , \; 0 \leq x \leq \ell$$

The unknown pressure is $q(x) \equiv -\sigma_z(x,0)$ for $0 \leq x \leq \ell$. Other conditions to be satisfied are

$$q(x) > 0 , \; 0 < x < \ell ; \quad q(\ell) = q(0) = 0 \tag{3.3c}$$

$$u_z \text{ and } \partial u_z/\partial x \text{ continuous and finite}^1 \text{ at } x=0, \; x=\ell \tag{3.3d}$$

and from (1.45),

$$u_z(x) \sim - \frac{1-\nu_f}{\mu_f} \frac{1}{\pi} N^* \log |x| \quad \text{as} \quad |x| \to \infty \tag{3.3e}$$

---

[1] The displacement u_z must be measured relative to some point near the load (see Section 1.1). This point will usually be taken as x=0, z=0.

The load components (per unit axial length) are

$$N^* = \int_0^{\ell} q(x)dx \quad ; \qquad F^* = -\int_0^{\ell} q(x) \frac{\partial u_z}{\partial x} dx \tag{3.4}$$

Further discussion of moving contacts will be restricted to two-dimensional problems.

3.2 Outline of the Two-Dimensional Solution

For a typical material element at the surface, neither stress nor displacement is known for all time, so the boundary conditions cannot be transformed to give an associated elastic problem. To obtain a solution, the unknown pressure distribution is treated as if it were known. The analysis is carried out to satisfy the prescribed conditions, which then determine the pressure. With given pressure the problem is one of a moving load, and the expressions for steady state displacement given in Chapter I will apply. The following dimensionless quantities (most of them introduced in Chapter I) will be used:

$$\xi \equiv \frac{x}{VT} , \quad \lambda \equiv \frac{\ell}{VT} , \quad \beta \equiv \frac{b}{VT} \tag{3.5a}$$

$$v(\xi) \equiv u_z(x)/VT \; ; \quad w(\xi) \equiv w^*(x)/VT \tag{3.5b}$$

$$Q(\xi) \equiv \frac{1-\nu_o}{\mu_o} \frac{1}{\pi} q(x) \tag{3.5c}$$

$$N = \frac{1-\nu_o}{\mu_o} \frac{1}{\pi} \frac{N^*}{\overline{VT}} = -\int_o^\lambda Q(\xi)d\xi \qquad (3.5d)$$

$$F = \frac{1-\nu_o}{\mu_o} \frac{1}{\pi} \frac{F^*}{\overline{VT}} = -\int_o^\lambda Q(\xi) \frac{\partial v}{\partial \xi} d\xi \qquad (3.5e)$$

Given properties of the viscoelastic base include $\gamma(\zeta)$ (related to the creep functions, equation 1.27), the time parameter and velocity in the combination $\overline{VT}$, and the initial elastic response $(1-\nu_o)/\mu_o$. Also given is the shape of the rigid body surface $w^*(x)$. In an actual problem, the vertical load N^* and the tilt α might be specified, with the extent and placement of the contact to be determined. However, in the analysis it is advantageous to proceed otherwise. Because b enters the problem in a complicated way in the function w^*, it is much easier to solve for α, which occurs only as a linear factor (equation 3.3b). Thus, the extent and placement of the contact region are specified by regarding ℓ and b as known. The tilt α and pressure $Q(\xi)$ are then unknown quantities. After solving for these, the necessary load components N and F can be determined.

Conditions to be satisfied are

$$Q(\xi) > 0\ , \quad 0 \leq \xi \leq \lambda; \quad Q(0) = Q(\lambda) = 0 \qquad (3.6a)$$

$$v(\xi) \text{ and } \partial v/\partial \xi \text{ continuous at } \xi = 0 \text{ and } \xi = \lambda \qquad (3.6b)$$

The displacement $v(\xi)$ is measured from $\xi = 0$, so that here $v(\xi)$ represents what was written $v(\xi)-v(0)$ in Chapter I. Then $v(0) = 0$, so that (3.3b) becomes

$$v(\xi) = \alpha\xi + w(\xi-\beta) - w(-\beta) , \quad 0 \leq \xi \leq \lambda \tag{3.7}$$

The relation between pressure and displacement is given by (1.42a,b) with $\xi_o = 0$. Thus, (3.7) becomes

$$\int_0^\lambda Q(\xi')\left[\log\left|\frac{\xi'}{\xi-\xi'}\right| + \int_0^\infty \gamma(\zeta)\log\left|\frac{\zeta-\xi'}{\zeta+\xi-\xi'}\right| d\zeta\right] d\xi' =$$

$$\alpha\xi + w(\xi-\beta) - w(-\beta) , \quad 0 \leq \xi \leq \lambda \tag{3.8}$$

This is a Fredholm integral equation of the first kind for the unknown pressure $Q(\xi)$. The solution gives $Q(\xi)$ in terms of α, and α is then determined from the conditions of smooth contact (3.6a). The load components are then given by (3.5d,e). Once $Q(\xi)$ is known, the surface displacement outside the contact region is found from (1.42).

To summarize the general analytic procedure for a two-dimensional moving contact problem: given $\gamma(\zeta)$, $w(\xi)$

a) Choose values of λ, β

b) Solve the integral equation (3.8) for $Q(\xi)$

c) Determine α from (3.6a)

d) Find the required N and F from (3.5d,e)

To get numerical values of the actual physical quantities [ℓ, b, q(x), N*, F*], VT and $(1-\nu_o)/\mu_o$ must be given also.

The integral equation (3,8) can be written

$$\int_0^\lambda Q(\xi')[K(-\xi') - K(\xi-\xi')]d\xi' = \alpha\xi + w(\xi-\beta) \ , \ 0 \leq \xi \leq \lambda$$

where

$$K(\xi) \equiv \log|\xi| + \int_0^\infty \gamma(\zeta) \log|\xi+\zeta| \, d\zeta \qquad (3.9)$$

The kernel $K(-\xi')-K(\xi-\xi')$ is the displacement at ξ due to a unit concentrated load at ξ'. If real material properties are used, the creep functions will be available as curves or tabulated data. Then, $\gamma(\zeta)$ is evaluated numerically as outlined in Section 1.3, and $K(\xi)$ would also have to be evaluated numerically. If the material is represented by a mechanical model (general Voigt solid),

$\gamma(\zeta) = \sum_j f_j e^{-b_j(\zeta)}$ from Section 1.3. Then, (3.9) gives

$$K(\xi) = (1 + \sum_j \frac{f_j}{b_j}) \log |\xi| - \sum_j \frac{f_j}{b_j} e^{b_j\xi} E_1(-b_j\xi) \qquad (3.10)$$

The general behavior of $K(\xi)$ is similar to that shown in Fig. 1.13. The function is logarithmically infinite as $|\xi| \to 0$ and as $|\xi| \to \infty$.

With an analytic form for the kernel, there is some hope of obtaining an analytic solution to the integral equation (3.8) for a given $w(\xi)$. The stress-strain laws for materials

represented by mechanical models can be given in differential form as well as the integral form (3.1b,c). This differential form makes it possible to reduce certain viscoelastic problems to "equivalent elastic problems" (abbreviated "EEP") (not to be confused with the "associated elastic problems of Chapter I).

If the EEP can be solved, the viscoelastic problem is reduced to the integration of ordinary differential equations. In moving contact problems, this procedure (called the "EEP method") can be carried out only for very restricted material properties. In these cases, the result is equivalent to analytic solution of (3.8). The results are useful in spite of the restrictions, and indicate what can be expected in more general cases. The next sections will consider the EEP method for steady state moving load and moving contact problems.

3.3 The Equivalent Elastic Problem for a Moving Load (Steady State)

When the stress-strain laws can be given in differential form, such as equations (1.11a,b), an EEP can be formed from the viscoelastic problem. The method will be described here for the steady state moving load problems of Chapter I. Since time appears only in the term $x^*-Vt \equiv x$, $\partial/\partial t$ becomes $-V\,\partial/\partial x$, and the differential operators (1.10b) become

$$P \equiv P_x = \sum_{k=0}^{n} p_k(-V)^k \frac{\partial^k}{\partial x^k} \quad , \quad Q \equiv Q_x = \sum_{k=0}^{m} q_k(-V)^k \frac{\partial^k}{\partial x^k} \tag{3.11}$$

The stress-strain laws (1.11a,b) become[1]

$$P_x[s_{ij}(x,y,z)] = 2\mu_o \, Q_x[e_{ij}(x,y,z)] \tag{3.12a}$$

$$P'_x[\theta(x,y,z)] = 3K_o \, Q'_x[e(x,y,z)] \tag{3.12b}$$

From the actual stresses and strains are obtained "derived stresses and strains," denoted by "~", and defined by

$$\tilde{s}_{ij} \equiv P_x(s_{ij}) \; ; \; \tilde{\theta} = P'_x(\theta) \tag{3.13a}$$

$$\tilde{e}_{ij} \equiv Q_x(e_{ij}) \; ; \; \tilde{e} = Q'_x(e) \tag{3.13b}$$

Then, the stress-strain laws (3.12) become

$$\tilde{s}_{ij} = 2\mu_o \, \tilde{e}_{ij} \; ; \; \tilde{\theta} = 3K_o \, \tilde{e} \tag{3.14}$$

which are the same as the elastic stress-strain laws. The total derived stresses and strains are defined by

$$\tilde{\sigma}_{ij} \equiv \tilde{s}_{ij} + \frac{1}{3}\delta_{ij}\tilde{\theta} = P_x(\sigma_{ij}) + \frac{1}{3}\delta_{ij}(P'_x - P_x)(\theta)$$

$$\tilde{\epsilon}_{ij} \equiv \tilde{e}_{ij} + \frac{1}{3}\delta_{ij}\tilde{e} = Q_x(\epsilon_{ij}) + \frac{1}{3}\delta_{ij}(Q'_x - Q_x)(e)$$

---

[1] For convenience, the initial moduli are introduced as indicated. Then, the P and Q operators are all dimensionless.

Applying the operator P_x to the equilibrium equations gives

$$P_x(\sigma_{ij,j}) = 0 = \tilde{\sigma}_{ij,j} + \frac{1}{3}\delta_{ij}(P_x - P_x')(\theta)$$

Thus, $\tilde{\sigma}_{ij,j} = 0$ in general only if $P_x = P_x'$. Similarly, the derived strains satisfy the compatibility equations in general only if $Q_x = Q_x'$.

If $P_x = P_x'$ and $Q_x = Q_x'$, the viscoelastic material has identical behavior in shear and dilatation, which corresponds to a constant Poisson's ratio ν. This behavior is a considerable restriction on even the idealization of a mechanical model, and is not usually found in real materials such as polymers. However, by making this restriction results can be obtained approximating more realistic behavior, and indicating general features of interest.

It will be assumed in what follows that ν is constant. Then $\tilde{\sigma}_{ij} = P_x(\sigma_{ij})$ and $\tilde{\epsilon}_{ij} = Q_x(\epsilon_{ij})$. The derived stresses satisfy the equilibrium equation $\tilde{\sigma}_{ij,j} = 0$, and the derived strains are compatible. Derived displacements are defined by $\tilde{u}_j = Q_x(u_j)$ and then $\tilde{\epsilon}_{ij} = 1/2(\tilde{u}_{i,j}+\tilde{u}_{j,i})$. Thus, the derived stresses and strains satisfy the same relations as an elastic problem. The viscoelastic problem is reduced to its "equivalent elastic problem" in the derived quantities, with boundary conditions derived by applying P_x to prescribed tractions and Q_x to displacements. The

EEP is a problem in the theory of elasticity, and if it can be solved the derived quantities $\tilde{\sigma}_{ij}$, $\tilde{u}_j$, etc., will be known explicitly.

Since P_x and Q_x are differential operators, each viscoelastic quantity is related by a differential equation (in x, with constant coefficients) to the corresponding derived quantity. For example, $Q_x(u_z) = \sum_{k=1}^{n} q_k(-V)^k \partial^k u_z/\partial x^k = \tilde{u}_z(x)$. Solution of these differential equations admits certain arbitrary functions of y and z, which must be determined to complete the viscoelastic solution. This requires consideration of stated or implied conditions of the viscoelastic solution, such as continuity or behavior at infinity, and the boundary conditions. Every viscoelastic problem will yield only one EEP. But a given EEP may lead to many viscoelastic problems, and the additional conditions are needed to distinguish the proper solution.

It is necessary to be very careful in formulating the EEP from the given viscoelastic boundary conditions. Discontinuities in the x-direction in prescribed boundary functions or their derivatives will become singularities in the EEP boundary conditions after applying the differential operators P_x, Q_x. These singularities must be included in obtaining the elastic solution of the EEP. For example, if a prescribed boundary traction has a finite jump, its first

derivative becomes a concentrated load in the EEP, its second derivative a concentrated couple, and so on.

The EEP method of solving viscoelastic problems is useful principally when it leads to a closed form analytic solution. This effectively limits consideration to low order differential operators, i.e., a mechanical model of few elements. Otherwise, the elastic solution of the EEP would be complicated by the presence of high order singularities, and solution of the differential equations would be difficult. Thus, in addition to the requirement of constant ν, the material behavior is further restricted to a model with a small number of discrete retardation times. Even with these severe restrictions, an analytic solution is useful in studying significant features of the problem and identifying characteristic quantities. This is particularly true for moving contact problems, which will be discussed in the next section.

To demonstrate the method, a simple moving load example will be considered. The two-dimensional problem of a constant load q_o on a length ℓ is treated for the standard linear solid (Fig. 1.4). In dimensionless form with

$$\xi = \frac{x}{VT} \quad , \quad \lambda = \frac{\ell}{VT}$$

the viscoelastic operators are

$$P_\xi = 1 + f - \frac{\partial}{\partial \xi}$$

$$Q_\xi = 1 - \frac{\partial}{\partial \xi}$$

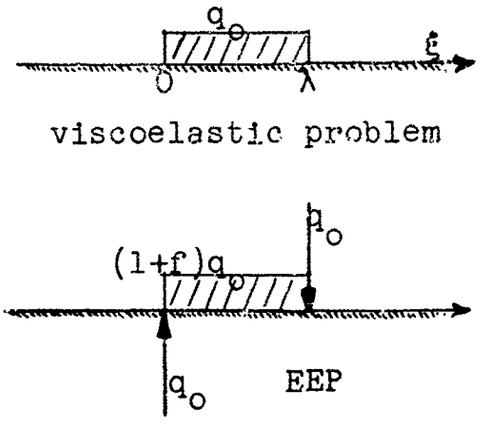

FIG. 3.2

The load can be written

$$q(\xi) = q_o[H(\xi) - H(\xi-\lambda)]$$

The boundary condition is then

$$\tilde{q}(\xi) \equiv P_\xi(q) = q_o(1+f)[H(\xi)-H(\xi-\lambda)] - q_o[\delta(\xi) - \delta(\xi-\lambda)]$$

The discontinuity in the load gives rise to the concentrated forces (Fig. 3.2). For this load, the elastic solution is, with $v(\xi) = u_{\ell}(x)/\sqrt{T}$,

$$\frac{1}{q_o}\tilde{v}(\xi) = (1+f)[\Delta - \xi \log|\xi| - (\lambda-\xi)\log|\lambda-\xi|] + \log|\xi| - \log|\xi-\lambda|$$

where Δ is arbitrary. The viscoelastic solution is determined from

$$\tilde{v} = Q_\xi(v) = v - \frac{\partial v}{\partial \xi} = -e^{\xi}\frac{\partial}{\partial \xi}(e^{-\xi}v)$$

Integrating this with the $\tilde{v}$ given above yields

$$\frac{1}{q_o}v(\xi) = Ae^{\xi} + \Delta + (1+f)[|\xi-\lambda|\log|\xi-\lambda| - \xi\log|\xi|]$$

$$+ f[\log|\xi-\lambda| - e^{\xi-\lambda}\,Ei(\lambda-\xi) - \log|\xi| + e^{\xi}Ei(-\xi)]$$

where A is the arbitrary constant of integration As $|\xi| \to \infty$, $v(\xi) \sim - q_o \lambda (1+f) \log|\xi|$ must be satisfied. This will be true only if $A = 0$. The final result agrees with (1.62) of example c), Section 1.6, with Δ such that $v(0) = 0$.

3.4 EEP Method for Moving Contact Problems

In this section the EEP method is applied to the two-dimensional steady state moving contact problem of Section 3.2. As before, the method is restricted to materials with differential stress-strain laws and constant ν. The differential operators (3.11) expressed in dimensionless form are

$$P_\xi = F_j + \sum_{k=1}^{n} p_k (-1)^k \frac{\partial^k}{\partial \xi^k} \; ; \quad Q_\xi = 1 + \sum_{k=1}^{m} q_k (-1)^k \frac{\partial^k}{\partial \xi^k} \tag{3.15}$$

Within the contact the displacement (3.7) is prescribed, while the pressure $Q(\xi)$ is unknown.

Differentiation does not alter the contact region, so the EEP is again a contact problem. Applying the operator Q_ξ to the prescribed displacement (3.7) gives the EEP boundary condition

$$\tilde{v}(\xi) = Q_\xi[v(\xi)] = v(\xi) - \alpha + \sum_{k=1}^{m} q_k (-1)^k \frac{\partial^k w(\xi-\beta)}{\partial \xi^k} \; , \; 0 \leq \xi \leq \lambda \tag{3.16}$$

Solution of this elastic contact problem gives the pressure $\tilde{Q}(\xi)$. Then,

$$\tilde{Q}(\xi) = P_{\xi}[Q(\xi)] = F_j Q + \sum_{k=1}^{n} p_k (-1)^k \frac{\partial^k Q}{\partial \xi^k} \qquad (3.17)$$

is the differential equation for the actual viscoelastic pressure $Q(\xi)$.

Part of the viscoelastic displacement is purely elastic (see equation 1.58a), while the rest is an integral of the elastic displacement. So the viscoelastic displacement and derivatives will have the same (and no worse) discontinuities as the elastic. By limiting the problem to smooth contact, the viscoelastic displacement and slope will be continuous. However, the second derivative of the displacement, $\partial^2 v/\partial \xi^2$, has a discontinuity of unknown magnitude at each end of the contact ($\xi=0$ and $\xi=\lambda$), and all higher derivatives have singularities there. This means a Q_{ξ} of second order (or higher) will give singularities in displacement of unknown magnitude at $\xi = 0$ and $\xi = \lambda$ in the EEP. Problems with such displacement singularities could be formulated mathematically in elasticity theory, but they would have no direct physical interpretation. It is unlikely that elastic solutions to such problems are available or could be readily obtained.

Thus, to be able to apply the EEP method with any hope of significant results, the material must be further restricted to a model with differential operators no higher than first order. Then, because of the conditions of smooth contact, the displacement in the EEP is continuous, and the

possibility of a concentrated load at the ends of the contact region is eliminated. If smooth contact were not required, the EEP would have infinite jumps in displacement and concentrated loads of infinite magnitude at each end of the contact region.

Consideration is thus limited to a Kelvin solid (no initial elasticity), for which $P_\xi = 1$, or a standard linear solid, for which $P_\xi = 1+f - \partial/\partial\xi$, where $1+f$ = initial elastic modulus/final elastic modulus. For both solids, $Q_\xi = 1 - \partial/\partial\xi$. Even though limited to these two simple models, the EEP method gives results that are useful. The standard linear solid exhibits some significant characteristics of more general viscoelastic solids, so its behavior indicates what might be expected in more general moving contact problems.

From (3.16), the displacement in the EEP is

$$\tilde{v}(\xi) = \alpha\xi + w(\xi-\beta) - w(-\beta) - \alpha - \frac{\partial w(\xi-\beta)}{\partial\xi}, \quad 0 \le \xi \le \lambda \tag{3.18}$$

and $\tilde{v}$ is continuous across the ends of the contact region. This is a contact problem in the plane theory of elasticity, for which general methods of solution are well known. The solution gives the pressure $\tilde{Q}(\xi)$ and the complete displacement $\tilde{v}(\xi)$ except for an arbitrary constant. Thus, $\tilde{Q}(\xi)$ includes a "flat punch" term of arbitrary magnitude

$$\tilde{Q}_{fp} = Q_o / \sqrt{\xi(\lambda-\xi)} \ , \ 0 \leq \xi \leq \lambda \qquad (3.19)$$

which gives constant displacement in the contact region.

For the Kelvin solid, $Q(\xi) = \tilde{Q}(\xi)$ since $P_\xi = 1$. For the standard linear solid, from (3.17)

$$\tilde{Q}(\xi) = (1 + f)\, Q - \frac{\partial Q}{\partial \xi}$$

and thus

$$Q(\xi) = Ae^{(1+f)\xi} + e^{(1+f)\xi} \int_{\xi}^{d} e^{-(1+f)\zeta}\, \tilde{Q}(\zeta)\, d\zeta \qquad (3.20)$$

where A and d are arbitrary constants. The constants, Q_o, and the unknown tilt α, are determined by the smooth contact conditions (3.6a,b) and the asymptotic form of the displacement (from equation 3.3e)

$$v(\xi) \sim -(1+f)\, N \log|\xi| \quad \text{as} \quad |\xi| \to \infty \qquad (3.21)$$

Once $Q'(\xi)$ and α have been found, the solution is essentially complete, and other quantities of interest can be determined. Application of this method to a particular problem, the rolling cylinder, is given in the next chapter.

CHAPTER IV

THE ROLLING CYLINDER PROBLEM

One of the principal problems of moving contact in viscoelasticity is the rolling of a circular cylinder (or sphere) on a flat surface. Osborne Reynolds made an extensive study of the problem in 1876, and since then several other attempts to explain and predict rolling resistance have been made[1]. The most significant recent developments have resulted from the work of Tabor and his colleagues ([4], [16], [30], [31], [32]) since about 1950. The experimental work showed that rolling resistance is nearly independent of surface lubrication, and arises principally from energy dissipation within the rolled material. This has led to two general theories attempting to explain rolling resistance. One, developed chiefly by the Tabor group, makes use of measurements of hysteresis loss in simple loading-unloading cycles, together with the solution for rolling on an elastic base. A similar procedure has been suggested by Drutowski [7]. A second possibility is to consider materials which can, at least approximately, be regarded as linearly viscoelastic. As already explained in Section 1.5, viscoelastic materials dissipate energy, which

---

[1] Discussion and additional references in Bowden and Tabor [4], Kelly [18], Drutowski [6].

gives rise to resistance to moving loads. Flom ([10], [11], [12]) has sought to connect rolling friction with simple energy loss measurements on viscoelastic materials. His tests of hard spheres rolling on several viscoelastic polymers show that the variation of coefficient of friction with velocity of rolling is qualitatively similar to the description of Section 1.5 (Fig. 1.9). There are few other experimental results available for spheres or cylinders rolling on materials of viscoelastic character. Some tests of Tabor [16] on rubber indicate that for cylinders longer than several times the diameter, the behavior is essentially two-dimensional.

This chapter considers in detail the two-dimensional problem of a rigid circular cylinder rolling on a semi-infinite viscoelastic solid. The contact is supposed perfectly lubricated, so there are no tangential forces at the contact surface and there is no distinction between rolling and sliding. This is treated as an example of the general moving contact problem of Chapter III. Several published treatments of the problem are examined. Each involves specific limitations which prevent more general application. A different, less limited, method is proposed and illustrated in the next chapter.

4.1 Formulation of the Rolling Cylinder Problem

The rigid cylinder, of radius R, is considered fixed, and the viscoelastic base moves under it with velocity V. The contact region extends from $x = 0$ to $x = \ell$, and the downstream end $x = 0$ is a distance b from the center of the cylinder (Fig. 4.1). Deformations are assumed small (i.e., $\ell \ll R$), so that within the contact region the surface of the cylinder can be approximated by a parabola[1]:

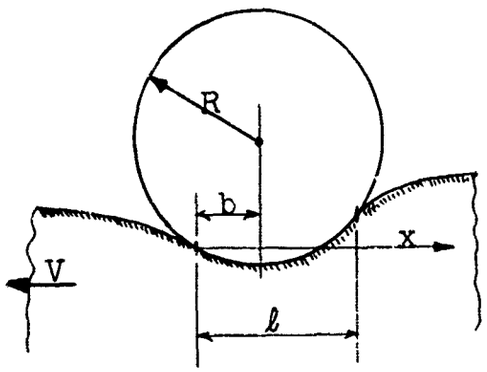

FIG. 4.1

$$w(\xi-\beta) = -\frac{1}{2\rho}(\xi-\beta)^2$$

In this problem $w(\xi-\beta)$ contains a term linear in ξ with unknown magnitude β, so there is no need to introduce the additional tilt α. But now β is to be found, and not, as in Section 3.2, assigned initially. For a given ℓ, variation of b in this special case amounts to a tilt of the contact surface.

The displacement within the contact region is, from (3.7)

$$v(\xi) = \frac{1}{\rho}\left(\beta\xi - \frac{1}{2}\xi^2\right), \quad 0 \le \xi \le \lambda \qquad (4.1)$$

[1] Using quantities defined by (3.5a-e) and $\rho = R/VT$.

It is convenient to introduce new dimensionless quantities

$$Q'(\xi) \equiv \rho\, Q(\xi) = \frac{R}{VT}\,\frac{1-\nu_o}{\mu_o}\,\frac{1}{\pi}\,q(x) \tag{4.2a}$$

$$N' \equiv 2\rho\, N = \frac{R}{VT}\,\frac{1-\nu_o}{\mu_o}\,\frac{2}{\pi}\,\frac{N^*}{VT} = 2\int_o^\lambda Q'(\xi)\,d\xi \tag{4.2b}$$

The integral equation (3.8) then becomes

$$\int_o^\lambda Q'(\xi')[K(-\xi') - K(\xi-\xi')]d\xi' = \beta\xi - \frac{1}{2}\,\xi^2\,,\quad 0 \le \xi \le \lambda \tag{4.3}$$

Proceeding as in Chapter III, the creep function $\gamma(\zeta)$ is given, and a value of the contact length λ is chosen. The solution of (4.3), along with the smooth contact conditions (3.6a,b), gives the pressure $Q'_o(\xi)$ and the parameter β. The total load N' is then found from (4.2b). Rolling resistance is conveniently represented by the coefficient of friction χ. Using (3.5d,e), (4.1), and (4.2a,b),

$$\chi = \frac{F}{N} = \frac{1}{N}\,\frac{1}{\rho}\int_o^\lambda (\xi-\beta)\,Q(\xi)\,d\xi$$

and thus

$$\rho\chi = \frac{2}{N'}\int_o^\lambda \xi\, Q'(\xi)\,d\xi - \beta \tag{4.4}$$

The actual physical and geometrical quantities can be conveniently represented by dimensionless combinations involving only the radius R, actual total load N^*, and initial

elastic constants $(1-\nu_o)/\mu_o$. These combinations, given on the left-hand sides of (4.5a-d), are formed as follows (the quantities on the right-hand sides having been found in the solution for a given λ):

velocity $$\frac{VT}{a_o} = \frac{1}{\sqrt{N^T}} \qquad (4.5a)$$

pressure $$\frac{a_o}{2N^*} q(x) = \frac{VT}{a_o} Q'(\xi) \qquad (4.5b)$$

Coefficient of friction $$\frac{R}{a_o} \chi = \frac{VT}{a_o} \rho\chi \qquad (4.5c)$$

placement $$\frac{b}{a_o} = \frac{VT}{a_o} \beta \qquad (4.5d)$$

where $$a_o = \left[\frac{1-\nu_o}{\mu_o} \frac{2}{\pi} R N^*\right]^{\frac{1}{2}} \qquad (4.6)$$

is one-half the contact length for an elastic solid. It is then possible to exhibit the variation with velocity of $q(x)$, χ, or b, for a given total load and radius. For example, a plot of $R\chi/a_o$ vs VT/a_o shows the variation of coefficient of friction (rolling resistance) with velocity.

In Section 1.4 it was shown that the limiting cases $V \to 0$ $(\lambda \to \infty)$ and $V \to \infty$ $(\lambda \to 0)$ are elastic. This can be used to find the corresponding limiting values of certain quantities in the rolling cylinder problem. For $V \to \infty$, the material exhibits its initial elastic behavior. The solution for given displacement (4.1) is

$$b = \frac{\ell}{2} \; ; \quad q(x) = \frac{\mu_o}{1-\nu_o} \frac{1}{R} \sqrt{x(\ell-x)} \; ; \quad N^* = \frac{\pi}{8} \frac{\mu_o}{1-\nu_o} \frac{\ell^2}{R}$$

For $V \to 0$, the material exhibits its final elastic behavior. The solution is the same as for $V \to \infty$, except that $\mu_o/(1-\nu_o)$ is replaced by $\mu_f/(1-\nu_f) = 1/(1+f)\cdot\mu_o/(1-\nu_o)$, where $f = \int_o^\infty \gamma(\zeta)d\zeta$. Some limiting values are given in Table 4.1.

Table 4.1

Quantity	Limiting Value $\lambda \to 0$, $V \to \infty$	Limiting Value $\lambda \to \infty$, $V \to 0$
$\frac{N'}{\lambda^2} = \frac{2}{\pi} \frac{1-\nu_o}{\mu_o} \frac{R}{\ell} \frac{N^*}{\ell}$	$\frac{1}{4}$	$\frac{1}{4(1+f)}$
$\frac{\beta}{\lambda} = \frac{b}{\ell}$	$\frac{1}{2}$	$\frac{1}{2}$
$\frac{R\chi}{a_o} = \frac{VT}{a_o} \rho\chi$	0	0
$\frac{\ell}{a_o} = \frac{VT}{a_o} \lambda$	2	$2\sqrt{1+f}$
$\frac{Q'}{\lambda} = \frac{1-\nu_o}{\mu_o} \frac{1}{\pi} \frac{R}{\ell} q\,(\max)$	$\frac{1}{2\pi} = .15915...$	$\frac{1}{2\pi} \frac{1}{1+f}$
$Q' \frac{VT}{a_o} = \frac{a_o}{2N^*} q\,(\max)$	$\frac{1}{\pi} = .31831...$	$\frac{1}{\pi} \frac{1}{\sqrt{1+f}}$

4.2 Analytic Solution by the EEP Method

The rolling cylinder problem can be solved by use of the EEP method outlined in Section 3.3. The viscoelastic material must be a standard linear (or Kelvin) solid with constant ν. This is a severe restriction on the material behavior, but it allows a complete analytic solution. The same solution has been previously obtained by Hunter [17]. The EEP method makes more evident the underlying assumptions and conditions of the problem, and is clearer and more direct than the somewhat different procedure of Hunter. The final results of the EEP method are the same as those of Hunter.

Details of the procedure for a standard linear solid are now given. The differential operators are

$$P_\xi = 1 + f - \frac{\partial}{\partial \xi} \quad ; \quad Q_\xi = 1 - \frac{\partial}{\partial \xi}$$

Applying Q_ξ to the displacement (4.1) gives

$$\rho\, \tilde{v}(\xi) = D + (1+\beta)\, \xi - \frac{1}{2}\, \xi^2 \,, \quad 0 \le \xi \le \lambda \qquad (4.7)$$

where D is an arbitrary constant. The elastic contact problem with prescribed displacement (4.7) has a pressure[1]

$$\pi\rho\, \tilde{Q}(\xi) = \frac{A + B(\xi - \frac{\lambda}{2})}{\sqrt{\xi(\lambda - \xi)}} + \sqrt{\xi(\lambda-\xi)} \,, \quad 0 \le \xi \le \lambda \qquad (4.8)$$

---

[1] Muskhelishvili [25], Section 116a.

where A is arbitrary and $B = 1 + \beta - \frac{\lambda}{2}$. From (3.20) and (4.2a), the viscoelastic solution is

$$Q'(\xi) = \frac{1}{\pi} e^{(1+f)\xi} \int_{\xi}^{\lambda} e^{-(1+f)\zeta} \left[\frac{A+B(\zeta - \frac{\lambda}{2})}{\sqrt{\zeta(\lambda-\zeta)}} + \sqrt{\zeta(\lambda-\zeta)} \right] d\zeta \tag{4.9}$$

The upper limit on the integral is here chosen so the condition $Q'(\lambda) = 0$ is satisfied. The condition $Q'(0) = 0$ must also be satisfied. Setting $\xi = 0$ in (4.9), the integral can be evaluated[1]. It must vanish identically, giving the relation

$$A = \frac{\lambda}{2} \frac{I_1(h)}{I_o(h)} \left(B - \frac{1}{1+f} \right) \tag{4.10}$$

where I_1, I_o are modified Bessel functions of the first kind, and

$$h \equiv (1 + f) \frac{\lambda}{2} \tag{4.11}$$

Another relation is needed between A and B. To obtain this, the displacement must be considered. Outside the contact region, the elastic displacement due to the pressure (4.8) is

$$\rho \tilde{v}(\xi) = D + (1+\beta)\xi - \frac{1}{2}\xi^2 - (A + \frac{\lambda^2}{8}) \cosh^{-1} \left| \frac{2\xi}{\lambda} - 1 \right|$$

$$- \left[B \frac{|\xi|}{\xi} - \frac{1}{2} \left| \xi - \frac{\lambda}{2} \right| \right] \sqrt{\xi(\xi-\lambda)}, \quad \xi \leq 0 \text{ or } \xi \geq \lambda \tag{4.12}$$

---

[1] Erdelyi [8], equation 7.12(10).

Since $\tilde{v} = Q_\xi(v) \equiv v - \partial v/\partial\xi$, the viscoelastic displacement is

$$\rho v(\xi) = e^{\xi} \int_{\xi}^{\infty} e^{-\zeta} [\rho \tilde{v}(\zeta)] \, d\zeta + Ce^{\xi}$$

where C is an arbitrary constant (which may have different values inside and outside the contact region) and the upper limit is chosen for convenience. As $|\xi| \to \infty$, this expression gives

$$\rho v(\xi) \sim \rho \tilde{v}(\xi) + C_1 e^{\xi} = C_1 e^{\xi} - (A + \frac{\lambda^2}{8}) \log |\xi| + \text{constant} + \ldots$$

This will have the proper asymptotic form (3.21) only if $C_1 = 0$. Then, substituting for $\rho\tilde{v}$ from (4.7) or (4.12), and choosing $D = -\beta$ gives

$$\rho v(\xi) = \beta\xi - \frac{1}{2}\xi^2 - e^{\xi} I(\xi) , \quad \xi \leq 0 \quad \text{or} \quad \xi \geq \lambda \qquad (4.13a)$$

where

$$I(\xi) \equiv \int_{\xi}^{\infty} \left[(A + \frac{\lambda^2}{8}) \cosh^{-1} \left| \frac{2\zeta}{\lambda} - 1 \right| \right.$$

$$\left. + (B \frac{|\zeta|}{\zeta} - \frac{1}{2} |\zeta - \frac{\lambda}{2}|) \sqrt{\zeta(\zeta-\lambda)} \right] e^{-\zeta} d\zeta \qquad (4.13b)$$

(for $\xi < 0$, the upper limit is 0 rather than ∞)

Inside the contact region, the displacement is

$$\rho v(\xi) = \beta\xi - \frac{1}{2}\xi^2 + [C_2 - I(\lambda)] e^{\xi}$$

Choosing $C_2 = I(\lambda)$ gives the correct displacement (4.1). To meet the condition of continuous displacement at $\xi = \lambda$ requires, on comparing (4.1) and (4.13a), that $I(\lambda) = 0$. Evaluation[1] of the integral $I(\lambda)$ leads to the relation

$$A = \frac{\lambda}{2} \frac{K_1(\lambda/2)}{K_0(\lambda/2)} (1 - B) \qquad (4.14)$$

where K_0, K_1 are modified Bessel functions of the second kind. From the two relations (4.10) and (4.14) A and B can be determined, and then $\beta = B - 1 + \frac{\lambda}{2}$.

Continuity of $v(\xi)$ at $\xi = \lambda$ has been guaranteed, and from (4.13a,b) this is true at $\xi = 0$ also. Since $\tilde{v} = v - \partial v/\partial \xi$ and both v and $\tilde{v}$ are continuous, the slope $\partial v/\partial \xi$ is also continuous. From (3.5d), and since

$$\tilde{Q} = P_\xi(Q) = (1+f)\, Q - \frac{\partial Q}{\partial \xi}$$

the total load is given by

$$(1+f)\, N = (1+f) \int_0^\lambda Q(\xi) d\xi = \int_0^\lambda \tilde{Q}(\xi)\, d\xi + Q(\lambda) - Q(0)$$

Thus, using (4.8), with $Q(\lambda) = Q(0) = 0$,

$$(1+f)\, \rho N = \frac{1}{\pi} \int_0^\lambda \left[\frac{A + B(\xi - \frac{\lambda}{2})}{\sqrt{\xi(\lambda-\xi)}} + \sqrt{\xi(\lambda-\xi)} \right] d\xi = A + \frac{\lambda^2}{8}$$

---

1. Erdelyi [8], equation 7.3(15).

The asymptotic form of the displacement (4.13a,b) as $|\xi| \to \infty$ is

$$v(\xi) \sim -\frac{1}{\rho}\left(A + \frac{\lambda^2}{8}\right) \log |\xi| = -(1+f)\, N \log |\xi| \tag{4.15}$$

which satisfies the condition (3.21). All the conditions of the problem are now satisfied.

This completes the solution for a rolling cylinder on a standard linear solid base. Numerical results are obtained most directly by specifying λ (with a given value of f), then proceeding with evaluation using the following formulas:

1) $$h = \frac{\lambda}{2}(1+f) \tag{4.11}$$

2) $$m = \frac{K_0(\lambda/2) I_1(h)}{K_1(\lambda/2) I_0(h)} \qquad [0 \le m \le 1] \tag{4.16}$$

3) $$A = \frac{\lambda}{2} \frac{f}{1+f} \frac{K_1(\lambda/2)}{K_0(\lambda/2)} \frac{m}{1+m} \tag{4.17a}$$

4) $$B = 1 - \frac{f}{1+f} \frac{m}{1+m} \tag{4.17b}$$

5) $$\beta = \frac{\lambda}{2} - \frac{f}{1+f} \frac{m}{1+m} \qquad \left[\beta \le \frac{\lambda}{2}\right] \tag{4.18}$$

6) $$Q'(\xi) = \frac{1}{\pi} e^{(1+f)\eta\lambda/2} \int_{\eta}^{1} e^{-ht}\left[\frac{A + \frac{\lambda}{2} Bt}{\sqrt{1-t^2}} + \left(\frac{\lambda}{2}\right)^2 \sqrt{1-t^2}\right] dt \tag{4.19}$$

where $\eta = 2\xi/\lambda - 1$

7) $$N' = 2\rho N = \frac{2}{1+f}\left(A + \frac{\lambda^2}{8}\right) \tag{4.21}$$

Evaluation of the coefficient of friction from (4.4) leads to

$$\rho\chi = \frac{f}{1+f} - B\left[1 + \frac{\lambda^2}{8A}\right]^{-1} \qquad (4.21)$$

The surface displacement for the rolling cintact is given by

$$\rho v(\xi) = \beta\xi - \frac{1}{2}\xi^2 - \frac{\lambda}{2} e^{\eta\lambda/2} \int_{\eta}^{0} g(t)\, e^{-\lambda/2\, t}\, dt\,, \quad \xi \leq 0 \qquad (4.22a)$$

$$= \beta\xi - \frac{1}{2}\xi^2 \qquad 0 \leq \xi \leq \lambda \qquad (4.22b)$$

$$= \beta\xi - \frac{1}{2}\xi^2 - \frac{\lambda}{2} e^{\eta\lambda/2} \int_{\eta}^{\infty} g(t)\, e^{-\lambda/2\, t}\, dt\,, \quad \xi \geq \lambda \qquad (4.22c)$$

where

$$g(t) = \left(A + \frac{\lambda^2}{8}\right)\cosh^{-1}|t| + \frac{\lambda}{2}\left(B - \frac{\lambda}{4}\, t\right)\sqrt{t^2 - 1} \qquad (4.23)$$

To obtain the pressure distribution over the contact region a numerical evaluation in step 5) is necessary. Hunter [17] gives a plot of $Q'(\xi)$ for the one case $f = 1$, $\lambda = 1.6$. A sketch of the general case is given in Fig. 4.2, along with an elastic contact for comparison. The effect of viscoelasticity is seen in the non-symm. ·y of contact region and pressure distribution, and the resultant horizontal force.

The variation of rolling resistance with velocity is best presented by plotting $R\chi/a_o$ vs VT/a_o, as suggested

in the preceding section. For a fixed f, solutions for different velocities are obtained by varying λ. The result is a curve of the form of Fig. 1.9, with a single maximum. Typical curves are given by Hunter[1] for f = 1 and f = 9.

In an actual rolling cylinder problem, the physical quantities f,V,T,N*,R, might be specified. To determine the contact region and pressure, a plot of λ vs VT/a_o (for a given f) is useful. The given data determines VT/a_o, and the appropriate λ can be found from the plot. Then the other quantities can be determined by the procedure just given.

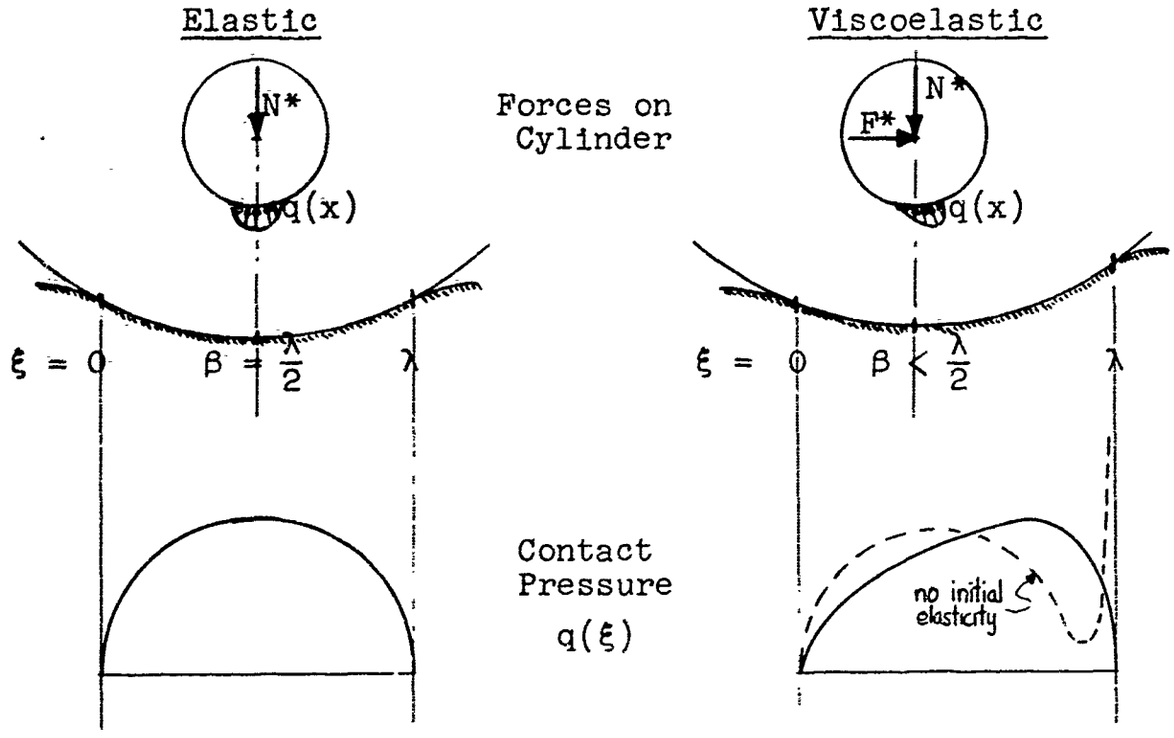

FIG. 4.2

[1] Note that Hunter's a_o is $\sqrt{1+f}$ times the a_o used here.

The solution for a Kelvin solid can be obtained in the same way as for the standard linear solid. There is no initial elasticity so the final elastic response is used. For this material, $P_\xi = 1$ and $Q_\xi = 1 - \partial/\partial\xi$. Only λ need be specified to obtain a solution. The results are summarized below:

1) $$B = \left[1 + \frac{K_o(\lambda/2)}{K_1(\lambda/2)}\right]^{-1} \qquad (4.24)$$

2) $$\beta = B + \frac{\lambda}{2} - 1 \qquad (4.25)$$

3) $$\frac{1-\nu_f}{\mu_f}\,\rho\, q(\xi) = B\sqrt{\frac{\xi}{\lambda-\xi}} + \sqrt{\xi(\lambda-\xi)} \qquad (4.26)$$

4) $$\frac{1-\nu_f}{\mu_f}\,\rho\,\frac{1}{\pi}\,\frac{N^*}{VT} = \frac{\lambda}{2}\left(B + \frac{\lambda}{4}\right) \qquad (4.27)$$

5) $$\rho\chi = \frac{\lambda}{2}\,\frac{6B+\lambda}{4B+\lambda} - \beta = \lambda\,\frac{3\beta+3-\lambda}{4\beta+4-\lambda} - \beta \qquad (4.28)$$

The Kelvin solid is of interest as the limiting case of a standard linear solid with the initial elastic response much smaller than the final response (i.e., very large f). In this limiting case, the pressure is infinite at the upstream end, $\xi = \lambda$ (see Fig. 4.2).

4.3 Direct Analytical Solution (Morland)

Starting from the fundamental field equations (3.1a) and the general stress-strain law in integral form (1.9a,b), viscoelastic problems can be treated directly as boundary value (space) and initial value (time) problems. Morland [24] has investigated the rolling cylinder problem in this way. Conditions to be satisfied are given by (3.3a-e). The general procedure is outlined below, and some details of Morland's solution are given.

At first, the analysis applies to the general two-dimensional problem of a normal load moving on the surface of a semi-infinite base (as in Chapter I). Morland takes a Fourier transform with respect to time. The transformed problem is then essentially an elastic problem, and the solution is expressed as Fourier integrals (in x^*). At this stage the condition of steady state is introduced, and after considerable manipulation the time variable is replaced by the steady state variable $x = x^* - Vt$. The result is then[1] (in the notation of equation 1.29)

$$Q(\xi) = \frac{1}{\pi}\int_0^\infty [f_1(s)\cos s\xi + f_2(s)\sin s\xi]\,ds \qquad (4.29a)$$

---

[1] The whole analysis to this point could be done more directly and simply by considering a moving load, steady state problem from the beginning, including the appropriate stress-strain laws (3.1b,c). Then, a Fourier transform with respect to $\xi(=x/VT)$ gives an elastic problem which leads directly to equations (4.29a,b).

$$v(\xi) = \int_0^\infty \phi(s) \left\{ [f_1(s) + \psi(s) f_2(s)](\cos s\xi - 1) + [f_2(s) - \psi(s) f_1(s)] \sin s\xi \right\} \frac{ds}{s} \tag{4.29b}$$

where $f_1(s) = f_1(-s)$ and $f_2(s) = -f_2(-s)$. The functions $\phi(s)$ and $\psi(s)$ are related to the creep functions and are defined by

$$\phi(s)[1 - i\psi(s)] = 1 + \bar{\gamma}(is) \tag{4.30}$$

where $\bar{\gamma}(s)$ is the Laplace transform of $\gamma(\zeta)$ and $i = \sqrt{-1}$. For a given moving load, f_1 and f_2 are known, and (4.29b) gives the resulting deflection.

The moving contact problem is considered, as before, by assuming some length of contact, and finding the necessary total load. Then, $f_1(s)$ and $f_2(s)$ are unknown functions. Once they have been found, the complete solution can be obtained. It is convenient here to take $\xi = 0$ at the center of the contact region. This region is then $|\xi| \leq \lambda/2$ (see Fig. 4.3). The boundary conditions (3.3) become

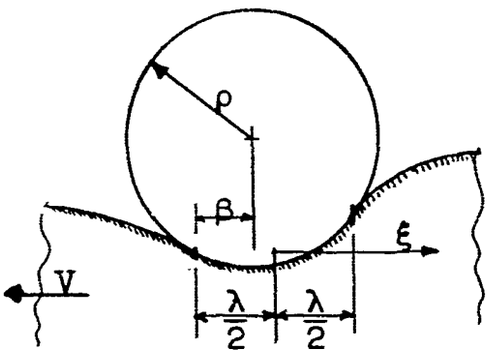

FIG. 4.3

$$Q(\xi) = 0 \ , \ |\xi| \geq \frac{\lambda}{2} \tag{4.31a}$$

$$v(\xi) = \frac{1}{\rho}\left[(\beta - \frac{\lambda}{2})\ \xi - \frac{1}{2}\ \xi^2\right] \ , \quad |\xi| \leq \frac{\lambda}{2} \tag{4.31b}$$

It is necessary to add an additional flat punch pressure, $Q_o[(\lambda/2)^2 - \xi^2]^{-1/2}$, to $Q(\xi)$ given by (4.29a). The resulting displacement is found by the method of Chapter I, and is added to (4.29b). For this, Morland assumes $\gamma(\zeta) = \sum_i f_i e^{-b_i\zeta}$--i.e., a mechanical model--for the viscoelastic behavior. The additional displacement is then

$$v_o(\xi) = \pi Q_o \sum_i \frac{f_i}{b_i} K_o(b_i \frac{\lambda}{2})(1 - e^{b_i\xi}) \ , \quad |\xi| \leq \frac{\lambda}{2} \tag{4.32}$$

With this assumption for $\gamma(\zeta)$,

$$\phi(s) = 1 + \sum_i \frac{f_i b_i}{b_i^2+s^2} \ , \quad \phi(s)\cdot\psi(s) = s \sum_i \frac{f_i}{b_i^2+s^2} \tag{4.33}$$

Satisfying the boundary conditions (4.31a,b) leads to the equations

$$\int_o^\infty [f_1(s) \cos s\xi + f_2(s) \sin s\xi]\ ds = 0 \ , \ |\xi| \geq \frac{\lambda}{2} \tag{4.34a}$$

$$\int_o^\infty \phi[(f_1+\psi f_2)(\cos s\xi - 1) + (f_2 - \psi f_1)\sin s\xi]\frac{ds}{s} + \pi Q_o \sum_i \frac{f_i}{b_i} K_o(b_i \frac{\lambda}{2})(1-e^{b_i\xi})$$

$$= \frac{1}{\rho}\left[(\beta - \frac{\lambda}{2})\ \xi - \frac{1}{2}\ \xi^2\right] \ , \quad |\xi| \geq \frac{\lambda}{2} \tag{4.34b}$$

These are dual integral equations for the unknown functions $f_1(s)$, $f_2(s)$. Morland procedes by splitting each of (4.34a,b) into odd and even parts. Then, a solution is assumed in the form of series of Bessel functions

$$f_1(s) = \pi Q_o \sum_{m=1}^{\infty} a_{2m} J_{2m}(\tfrac{\lambda}{2} s) \; ; \; f_2(s) = \pi Q_o \sum_{m=1}^{\infty} a_{2m-1} J_{2m-1}(\tfrac{\lambda}{2} s)$$

which satisfy (4.34a) identically. Introducing these into the odd and even parts of (4.34b) leads eventually to two infinite sets of equations, which are combined into one infinite set of linear equations for the unknown constants a_m. The coefficients of a_m in the set are integrals of ϕ and ψ with Bessel functions, a typical integral being

$$\int_o^{\infty} \phi(s) \, J_m \, (\tfrac{\lambda}{2} s) \, J_n \, (\tfrac{\lambda}{2} s) \, \frac{ds}{s}$$

The solution of this infinite set of equations, with the additional conditions $q(\pm \lambda/2) = 0$, gives the a_m, Q_o, and β. This formally solves the contact problem, giving f_1 and f_2 as an infinite series. The contact pressure is then given by

$$q(\xi) = \frac{2}{\lambda} \frac{Q_o}{\cos \theta} \left[1 + \sum_{m=1}^{\infty} a_{2m} \cos(2m\theta) + \sum_{m=1}^{\infty} a_{2m-1} \sin\{(2m-1)\theta\}\right]$$

where $\xi = \lambda/2 \sin\theta$. From this it follows that

$$N = \pi Q_o \quad , \quad \rho\chi = \frac{\lambda}{2}\left[1 - \frac{2\beta}{\lambda} + \frac{1}{2}\ a_1\ \right]$$

Thus, for a given λ, the coefficients of a_m must be determined and an infinite set of linear equations solved. Then the pressure, total load, friction coefficient and other quantities of interest can be found. The whole process must be repeated for each value of λ.

To carry out the calculations, Morland makes some simplifying approximations. The material behavior is approximated by assuming ϕ = constant and ψ = constant in the integral part of (4.34b). The coefficient integrals can then be evaluated in closed form. For the "flat punch" displacement (4.32), a different approximation is used by taking a single term in the sum (i.e., standard linear solid with constant ν). The solution is further approximated by using a 9x9 block instead of the infinite set of equations. Even with these approximations, much numerical work is needed to get results for a single value of λ. Morland gives one numerical example and the resulting curve of pressure distribution over the contact region. The results are given below for this example, in which $\lambda = 1$, $f = .5$. Also given are the corresponding results by the method of Section 4.2 (Hunter) for comparison.

Quantity	Method	
	Hunter	Morland
$\frac{VT}{a_o}$	2.40	2.21
β	.446	.490
$\rho\chi$	.067	.072

4.4 Other Treatments of Rolling Contact Problems; Comments

Although each of the methods of Sections 4.2 and 4.3 can be applied only with certain restrictions and approximations, each starts from an "exact" formulation of the rolling contact problem in the sense that the viscoelastic base is treated as a continuum, and the mutual effect of adjacent elements is taken into account. However, only two-dimensional problems can be satisfactorily treated, and analytic solutions are possible only for limited kinds of viscoelastic behavior.

Rolling contact problems have also been discussed by adopting a representation of material behavior which is more widely applicable, but much more approximate. The viscoelastic base is assumed to be made up of independent vertical columns, like a Winkler foundation. Each column is a one-dimensional viscoelastic rod with regard to vertical stress and strain, and the deformation of any one column

has no effect on and is not affected by any other columns. Thus, some of the features of viscoelasticity are present, including delayed recovery and energy dissipation, but the overall behavior of the base as a continuous material is only approximately represented.

With this simplified representation, both three and two-dimensional rolling contact problems can be treated. The base has a finite thickness h, and the vertical displacement of any column is thus $h\epsilon$, where ϵ is the strain. The stress-strain law can be written

$$\sigma(t) = E \int_0^t \dot{G}(t-\tau)\, \epsilon(\tau)\, d\tau \qquad (4.35)$$

where G(t) is the relaxation function. If the surface displacement is prescribed, (4.35) gives the necessary contact pressure. By prescribing a spherical or cylindrical displacement, the rolling contact problem is essentially solved. Due to the delayed recovery behind the roller, the contact region and pressure are not symmetric. This gives a resisting force and a corresponding coefficient of friction, and thus provides some qualitative description of rolling resistance.

Applications of this simplified treatment of rolling contact problems include: Flom and Bueche [13], sphere on a Kelvin solid; May, Morris and Atack [23], cylinder on

Maxwell fluid, standard linear and more general solids; Norman [26], cylinder on a Kelvin solid. Results are qualitatively similar to those of the more "exact" methods of Hunter and Morland. In particular, the coefficient of friction varies with velocity in the manner previously discussed, increasing with velocity to a single maximum, then decreasing to zero. When a mechanical model is used for the material behavior, G(t) is a sum of negative exponentials. Then the results can be expressed in analytic form, in terms of elementary functions.

In summary, this simplified treatment gives some useful results of a qualitative nature for the rolling contact problem, and involves only straightforward (although perhaps tedious) integrations. However, it is a somewhat crude representation of the actual behavior of the base. For the more accurate representation of the base as a continuum, analytic solutions (such as Hunter, Section 4.2, and Morland, Section 4.3) are available only in limited cases of two-dimensional problems. The direct method (Morland) applies in principle for general viscoelastic behavior, but in practice approximations are needed. Even then, an infinite set of equations must be solved, which requires further approximation and much numerical work for each particular example. The EEP method gives a complete closed-form analytic solution, with no approximation in the analysis, and

numerical work is needed only to get the detailed pressure distribution. However, this method can be used only for simple models (standard linear or Kelvin solids, with constant ν) that in some respects represent the behavior of viscoelastic materials. Thus there are significant limitations to each of these methods of obtaining an analytic solution of the rolling contact problem.

CHAPTER V

A NUMERICAL METHOD FOR TWO-DIMENSIONAL MOVING CONTACT PROBLEMS

There is no complete analytic solution of the moving contact problem available for a general viscoelastic material. The EEP method discussed in Chapters III and IV can be used only for a material of very restricted type, represented by a simple model with constant ν. For a rolling cylinder this method allows a complete analytic solution, but for other shapes of contact surface the analysis is much more complicated and does not in general yield closed-form expressions. The direct analytical method discussed in Section 4.3 can in principle be applied to any contact surface on any viscoelastic material. But involved analysis is required, and then much approximation and numerical work is needed to obtain a definite result.

For the general moving contact problem, with arbitrary contact surface on any viscoelastic solid, it is evident that the solution must be obtained numerically. This can best be achieved by using numerical procedures from the beginning, thus avoiding lengthy and elaborate analytical procedures. Creep functions available only as numerical data can be used directly, eliminating the laborious task of trying to represent the data analytically. This chapter presents a numerical method for solving the two-dimensional

steady state moving contact problem (as formulated in Chapter III). The procedure, restricted only by the requirement of smooth contact, is simple and direct, and readily adapted for digital computer. The method is illustrated with the specific problems of a rolling cylinder and a "nearly flat punch".

5.1 Numerical Evaluation of Surface Displacement

The steady state surface displacement due to a two-dimensional pressure distribution $Q(\xi)$ $(0 \leq \xi \leq \lambda)$ moving on a semi-infinite viscoelastic base, given by (1.42a,b), is

$$v(\xi) - v(\xi_a) = \int_0^\lambda Q(\xi')[K(\xi_a-\xi')-K(\xi-\xi')]d\xi' \qquad (5.1)$$

where

$$K(\xi) = \log |\xi| + \int_0^\infty \gamma(\zeta) \log (\xi+\zeta)\, d\zeta \qquad (5.2)$$

and ξ_a is an arbitrary point on the surface (Fig. 5.1). The dimensionless quantities given by (3.5a-e) are used. It is supposed that the pressure is everywhere finite, and that $Q(0) = Q(\lambda) = 0$. This is the case, for example, when $Q(\xi)$ arises from a "smooth" moving contact (defined in Section 3.1).

To evaluate numerically the integral in (5.1), a smooth pressure distribution $Q(\xi)$ on $0 \leq \xi \leq \lambda$ is replaced by n trapezoidal load elements (Fig. 5.1). Within a typical segment $\xi_{k-1} \leq \xi \leq \xi_k$ $(k = 1,2,\ldots,n)$ the pressure is represented by

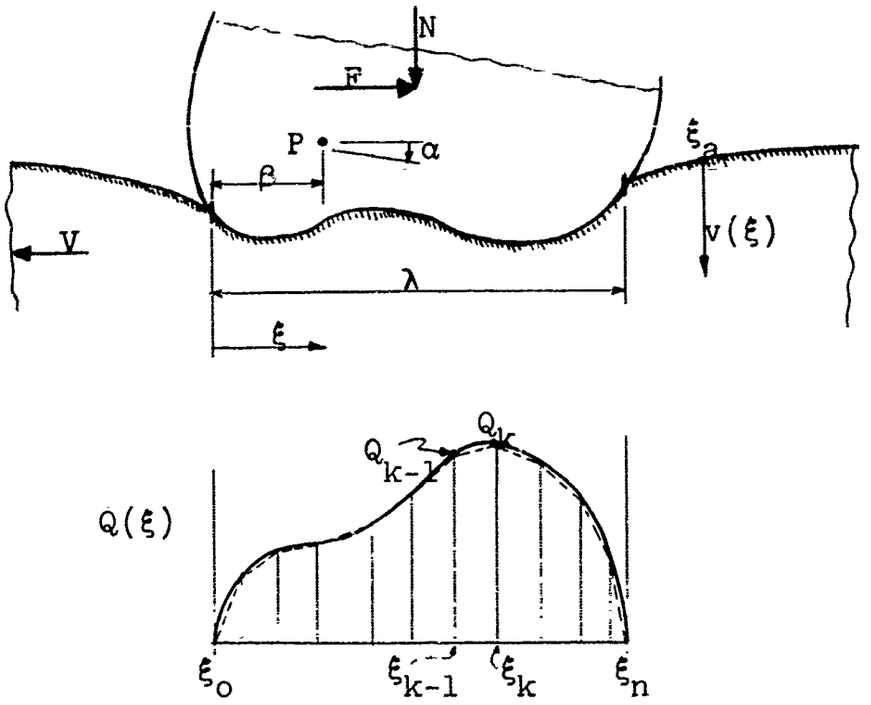

FIG. 5.1

$$Q(\xi) \equiv Q^k(\xi) = \frac{1}{\xi_k - \xi_{k-1}} [Q_k(\xi - \xi_{k-1}) - Q_{k-1}(\xi - \xi_k)] \qquad (5.3)$$

where $Q_k \equiv Q(\xi_k)$, $\xi_o = 0$, $\xi_n = \lambda$. The displacement (5.1) then becomes

$$v(\xi) - v(\xi_a) = \sum_{k=1}^{n} \int_{\xi_{k-1}}^{\xi_k} Q^k(\xi')[K(\xi_a - \xi') - K(\xi - \xi')]d\xi'$$

Substituting for $Q^k(\xi)$ from (5.3) and for $K(\xi)$ from (5.2), and with $Q_o = Q_n = 0$, this can be reduced to

$$v(\xi) - v(\xi_a) = \frac{1}{2} \sum_{k=1}^{n-1} Q_k[\Omega_k(\xi) - \Omega_k(\xi_a)] \qquad (5.4a)$$

$$\Omega_k(\xi) \equiv \left(\frac{1}{\theta_{k+1}} + \frac{1}{\theta_k}\right)K_k(\xi) - \frac{1}{\theta_k} K_{k-1}(\xi) - \frac{1}{\theta_{k+1}} K_{k+1}(\xi) \tag{5.4b}$$

$$K_k(\xi) \equiv \omega(\xi-\xi_k) \quad ; \; \theta_k \equiv \xi_k - \xi_{k-1} \tag{5.4c}$$

$$\omega(\xi) \equiv \xi^2 \log|\xi| + \int_0^\infty \gamma(\zeta)(\xi+\zeta)^2 \log|\xi+\zeta| \, d\zeta \tag{5.4d}$$

The integral in (5.1) is thus replaced by a finite sum. For a given choice of the division points ξ_k, the functions $\Omega_k(\xi)$ depend only on the creep function $\gamma(\zeta)$, and may be regarded as evaluated once for all, for some given viscoelastic material. Then (5.4a) gives the displacement for any pressure distribution in terms of its Q_k values.

The trapezoidal pressure is continuous, but has discontinuous slope $dQ/d\xi$ at each ξ_k. The resulting displacement is consequently continuous with finite slope $dv/d\xi$ everywhere. But, as may be verified from (5.4a), $d^2v/d\xi^2$ will be infinite at each ξ_k. The pressure could be better approximated by polynomials of higher degree, which would give smoother pressure and displacement. But the added smoothness does not justify the increased complexity involved. It is better to use the simple representation given by (5.3), taking more divisions if increased accuracy is desired.

When the pressure $Q(\xi)$ is known, the total load is given by

$$N = \int_0^{\lambda} Q(\xi)\, d\xi$$

Substituting from (5.3) for $Q(\xi)$, this becomes

$$N = \frac{1}{2} \sum_{k=1}^{n-1} Q_k(\xi_{k+1}-\xi_{k-1}) = \frac{1}{2} \sum_{k=1}^{n-1} Q_k(\theta_{k+1}+\theta_k) \qquad (5.5)$$

The displacement at any point on the surface can be determined from (5.4a,b) for any viscoelastic solid. The elastic solid is covered by $\gamma(\zeta) = 0$. If $\gamma(\zeta)$ is in numerical form, determined from measured creep functions (as described in Section 1.3), then the integral in (5.4d) would have to be evaluated numerically. If $\gamma(\zeta)$ has an appropriate analytical form, $\omega(\xi)$ can be expressed analytically. For example, if the viscoelastic material can be represented by a general Voigt solid, so that $\gamma(\zeta) = \sum_{i=1}^{m} f_i e^{-b_i\zeta}$, then

$$\omega(\xi) = \left(1 + \sum_{i=1}^{m} \frac{f_i}{b_i}\right) \xi^2 \log|\xi| + \xi(1+2\log|\xi|) \sum_{i=1}^{m} \frac{f_i}{b_i^2}$$

$$+ \left[\log|\xi| - e^{b_i\xi} E_i(-b_i\xi)\right] \sum_{i=1}^{m} \frac{2f_i}{b_i^3} \qquad (5.6)$$

where $E_i(-x)$ is the Exponential Integral.

5.2 Numerical Procedure for Moving Contact Problems

The moving contact problem was described in Chapter III, and the general procedure for obtaining a solution was outlined in Section 3.2. Values of β and λ (Fig. 5.1) are chosen, and the unknown pressure is found from the integral equation (3.8). Since β and λ are not independent in a particular smooth contact, it is necessary to include an unknown angle of tilt α along with the prescribed contact surface $w(\xi-\beta)$. Then, reasonable values of β and λ can be chosen independently, and the solution will give the necessary tilt for this to be a possible smooth contact.

For a numerical solution, the unknown smooth pressure is approximated by n trapezoidal elements. The number and spacing of the division points ξ_k will be governed by the accuracy desired and the character of the specific problem. Following the procedure of Section 5.1, the integral equation (3.8) becomes

$$\frac{1}{2}\sum_{k=1}^{n-1} Q_k[\Omega_k(\xi)-\Omega_k(\xi_a)] = (\xi-\xi_a)\alpha + w(\xi-\beta) - w(\xi_a-\beta) ,$$

$$0 \le \xi \le \lambda \qquad (5.7)$$

where $\Omega_k(\xi)$ is given by (5.4b-d) and ξ_a is arbitrary. There are n unknown quantities, the $n-1$ pressure ordinates $Q_k = Q(\xi_k)$, $k = 1,2,\ldots,n-1$, and the tilt α.

To solve for these unknowns, the method of collocation is used. If (5.7) is satisfied at each of n points $\xi = \xi_j^*$, $0 \leq \xi_j^* \leq \lambda$ $(j = 1,2,\ldots,n)$, there will be n equations for the n unknowns. Each of the unknowns occurs as a linear factor[1], so the problem is reduced to solving a set of simultaneous linear algebraic equations. For given divisions of the contact region (ξ_k) and given points of collocation (ξ_j^*) there will be a unique solution for the Q_k and α. With this solution the left side of (5.7) will exactly equal the right side only at the points ξ_j^*, but agreement will be close throughout the contact region if these points are suitably chosen.

It is convenient to choose one of the division points ξ_k as the reference point ξ_a, and the remaining ξ_k as the collocation points ξ_j^*. The collocation procedure then insures the prescribed displacement at each end of the contact region and at the n-1 intermediate points at which the pressure is determined. Let

$$A_{jk} \equiv \Omega_k(\xi_j) - \Omega_k(\xi_a) \; ; \; k = 1,2,\ldots,n-1 \qquad (5.8a)$$

$$A_{jn} \equiv \xi_a - \xi_j \qquad (5.8b)$$

$$w_j \equiv w(\xi_j - \beta) - w(\xi_a - \beta) \qquad (5.8c)$$

[1] This is the principal reason why the small tilt α is introduced as an unknown -- because it is a linear term. If the tilt were prescribed or implicit in the function $w(\xi-\beta)$, β could not be prescribed, but would have to be found in the solution. Since β is not a linear factor in general, the whole procedure would be greatly complicated.

where $j = 0,1,\ldots,n$ except $j = a$. Then, (5.7) becomes

$$\frac{1}{2}\sum_{k=1}^{n-1} Q_k A_{jk} + \alpha A_{jn} = w_j \; ; \quad j = 0,1,\ldots,n \text{ except } j = a \tag{5.9}$$

This is the set of n equations to be solved for the n unknowns $Q_k (k = 1,2,\ldots,n-1)$ and α, which gives an approximate solution of the integral equation (3.8). The smooth contact conditions (3.6a,b) are automatically satisfied in this formulation of the problem.

Once the Q_k are known, the total load N is given by (5.5). The coefficient of friction is

$$\chi = \frac{F}{N} = -\frac{1}{N}\int_0^{\lambda} Q(\xi)\,\frac{\partial v}{\partial \xi}\,d\xi = -\alpha - \frac{1}{N}\sum_{k=1}^{n}\int_{\xi_{k-1}}^{\xi_k} Q^k(\xi)\,\frac{\partial w}{\partial \xi}\,d\xi \tag{5.10}$$

The complete numerical procedure for solution of a two-dimensional moving contact problem is summarized below:

Given: $\gamma(\zeta)$-a creep function of the base material (see Section 1.3)

$w(\xi)$-prescribed shape of contact surface

1) Choose values of λ, β.

2) Divide the contact region into n segments at the points $\xi_o = 0$, $\xi_1,\ldots,\xi_k,\ldots,\xi_n = \lambda$. Choose one ξ_k as reference point ξ_a.

3) Determine A_{jk} and w_j from (5.8a-c),(5.4b,c), using (5.4d) for a general viscoelastic material, or (5.6) for a Voigt solid.

4) Solve the set of n simultaneous linear equations (5.9) for α and Q_k ($k = 1,2,\ldots,n-1$). The pressure distribution is then given by (5.3)--straight lines connecting the ordinates Q_k at the points ξ_k.

5) Find the total load N from (5.5), the coefficient of friction from (5.10).

6) Displacements at any points on the surface are found from (5.4a).

For each pair of values of β and λ this procedure gives one solution, with particular values of N and α. If either the actual load N^* or the velocity V is then specified, the other is determined by this solution. This means that if certain values of V, N^*, and α are wanted, trial solutions must be made with various values of β and λ until the desired results are obtained.

The actual numerical calculations are straightforward, and can be programmed for a digital computer. Evaluation of the coefficients A_{jk} will depend on the form in which $\gamma(\zeta)$ is expressed. For a Voigt solid, the general analytic form (5.6) can be used. If the creep functions are given numerically, $\gamma(\zeta)$ can be found as described in Section _.3. Then, the integral in (5.4d) is evaluated numerically. Computer library routines for solving simultaneous linear equations are usually available.

To summarize, this numerical procedure yields a solution to the moving contact problem by representing the unknown

pressure distribution as n trapezoidal elements. The prescribed displacement is then satisfied at certain points in the contact region, leading to n simultaneous equations to be solved for the unknown pressure ordinates. The principal advantages of the method are its simplicity and flexibility, and that it can be used for any viscoelastic (or elastic) solid and for any shape of contact surface subject to the conditions of smooth contact. In the next sections, numerical results are obtained in some specific applications.

5.3 Numerical Solution of the Rolling Cylinder Problem

The numerical method of Section 5.2 will be applied to the rolling cylinder problem as formulated in Section 4.1, where it was indicated that β is to be found and it is not necessary to introduce α. The physical quantities are shown in Fig. I (at the end of the chapter), and the dimensionless quantities are defined there. It is convenient to choose $\xi_a = \xi_o = 0$. Then, using (4.1) and with $Q_k' \equiv Q'(\xi_k)$, (5.7) becomes

$$\sum_{k=1}^{n-1} Q_k' [\Omega_k(\xi) - \Omega_k(0)] = 2\beta\xi - \xi^2 , \quad 0 \leq \xi \leq \lambda \qquad (5.11)$$

Collocating at the points ξ_k, $k = 1,2,\ldots,n$, the set of equations corresponding to (5.9) is

$$\sum_{k=1}^{n-1} Q_k' A_{jk} + 2\beta(-\xi_j) = -\xi_j^2 , \quad j = 1,2,\ldots,n \qquad (5.12)$$

where A_{jk} is given by (5.8a) with $\xi_a = 0$. Once the solution has been obtained, the total load is (from 5.5)

$$N' = \sum_{k=1}^{n-1} Q_k' \, (\xi_{k+1} - \xi_{k-1}) \tag{5.13}$$

and the coefficient of friction is (from 4.4, 4.2a,b, and 5.3)

$$\rho\chi = \frac{1}{N'} \sum_{k=1}^{n-1} Q_k' \, (\xi_{k+1} - \xi_{k-1}) \, \frac{\xi_{k+1} + \xi_k + \xi_{k-1}}{3} - \beta \tag{5.14}$$

From the elastic solution and the existing solutions for standard linear solids (Section 4.2, Fig. 4.2), it is expected that the pressure distribution will be smooth for a general viscoelastic solid. This suggests division of the contact region into equal segments. Then, $\xi_k = k\theta$, where

$$\theta \equiv \xi_k - \xi_{k-1} = \frac{\lambda}{n} \quad , \quad k = 1,2,\ldots,n \tag{5.15}$$

The set of equations (5.12) becomes

$$\sum_{k=1}^{n-1} Q_k' \, A_{jk} - 2\beta\theta j = -j^2\theta^2 \quad , \quad j = 1,2,\ldots n \tag{5.16}$$

where now

$$A_{jk} = \Omega_k(\xi_j) - \Omega_k(0) \tag{5.17a}$$

$$\Omega_k(\xi_j) = \frac{1}{\theta}[2\omega(\xi_j - \xi_k) - \omega(\xi_j - \xi_{k-1}) - \omega(\xi_j - \xi_{k+1})] \tag{5.17b}$$

and $\omega(\xi)$ is given by (5.4d) or (5.6). The total load (5.13) becomes

$$N' = 2\theta \sum_{k=1}^{n-1} Q_k' \tag{5.18}$$

and the coefficient of friction (5.14) becomes

$$\rho\chi = \frac{\Sigma\, Q_k' \xi_k}{\Sigma\, Q_k'} - \beta \tag{5.19}$$

Division into equal segments is used for all rolling cylinder examples given in this chapter.

A particular problem for a given material [given $\gamma(\zeta)$] is fixed by choosing the number of divisions n and the length θ of each segment (or $\lambda = n\theta$). The coefficients A_{jk} are determined from (5.17a,b), and the set of n simultaneous equations (5.16) is solved. This determines Q_k' ($k = 1,2,\ldots,n-1$) and β. From (5.18), (5.19) N' and $\rho\chi$ are found. The results are most conveniently expressed in terms of the quantities defined by (4.5a-d). Each value of λ (or θ) corresponds to a certain V, if N^* is specified, or to a certain N^*, if V is specified. To illustrate the procedure, some specific examples are given in this and the next sections. The numerical work was performed on a digital computer[1], using an existing library routine for solving the simultaneous equations.

[1] The IBM 7090 at the Stanford University Computation Center (using eight significant figures).

A good check on the numerical procedure is provided by the elastic base, for which $\gamma(\zeta) = 0$. The known analytic solution is

$$Q'(\xi) = \frac{1}{\pi}\sqrt{\xi(\lambda-\xi)} \qquad (5.20)$$

$$N' = \frac{\lambda^2}{4} \quad ; \quad \beta = \frac{\lambda}{2}$$

and the pressure distribution is symmetric about $\xi = \lambda/2$. Numerical results for $n = 10$ and $n = 40$ are given in Table 5.1. In each case $\beta = \lambda/2$ exactly (to eight significant figures), and symmetrically located values of Q_k' are identical to at least six significant figures. Values of Q_k' for $n = 10$ are about 2%, those for $n = 40$ about .5%, lower than the exact solution. Values of N' are less than the exact value of 4.8% for $n = 10$, 1.2% for $n = 40$.

When the material is a standard linear solid with constant ν [i.e., $\gamma(\zeta) = fe^{-\zeta}$], results of the numerical method can be compared with the complete analytic solution given in Section 4.2. A few such examples are given in this section to indicate the accuracy of the method. Increasing n beyond a certain value will not necessarily mean more accurate results. When the segments are very short (θ small, n large), increased precision (more significant figures) is necessary, requiring careful attention to the details of calculation, and perhaps more sophisticated numerical

techniques. Trial solutions for several values of n will enable selection of a suitable value of n for a particular class of problems.

Two rolling cylinder problems are solved with n = 10, 20, and 40. In each, $\lambda = 1$ and $\gamma(\zeta) = fe^{-\zeta}$, with f = 1 in one example, f = 10 in the other. Results are given in Table 5.2, and pressure distributions are shown[1] in Fig. II. Numerical values are consistently improved with larger n, the error being roughly halved when n is doubled. Except near the ends, the pressure distributions for all three values of n are nearly the same. On the basis of such examples, n = 20 was chosen for use in all subsequent rolling cylinder examples. Comparison with the analytic solution indicates errors of 2 to 5%. The computer time needed for a typical solution with n = 20 was .1 to .5 minutes.

For a given base material [given $\gamma(\zeta)$], the complete range of rolling cylinder problems is covered by varying λ from 0 to ∞. To illustrate typical results, numerical solutions for some representative values of λ are given in Table 5.3, along with the analytic solution for comparison. In these examples, $\gamma(\zeta) = e^{-\zeta}$ (f=1). Numerical values compare with the exact solution as follows: β - very close agreement; N' - numerical solution consistently 2 to 3% low; $\rho\chi$ - error of 5% or less. The limiting cases $\lambda = 0$ and

[1] Figures labeled with Roman numerals are at the end of the chapter.

$\lambda = \infty$ are the same as the elastic solution (Table 4.1, Section 4.1). These limits are closely approached for $\lambda = .01$ and $\lambda = 100$ respectively. The pressure distributions are shown in Fig. IV. For $\lambda = .01$ and $\lambda = 100$ the pressure is very nearly symmetric, while for $\lambda = 1$ it is noticeably non-symmetric. For large and small λ, β/λ approaches .5, while the lowest value of β/λ occurs for $\lambda = 1$. The variation of coefficient of friction with velocity is shown in Fig. VI, where $R\chi/a_o$ is plotted against VT/a_o (log scale). The friction curve has a pronounced peak, with the maximum occurring for $VT/a_o = 1.42$ ($\lambda = 1.6$).

The results of this set of examples indicate some features which are characteristic of any viscoelastic rolling cylinder problem. The elastic solution is symmetric and gives no resisting force. A viscoelastic material, due to its delayed recovery and energy dissipation, gives rise to asymmetry in the solution and a resisting force (indicated by χ). The asymmetry is evident in two respects (see Fig. 4.2): 1) the contact region is displaced upstream, so that its center ($\xi = \lambda/2$) does not lie directly below the center of the cylinder ($\xi = \beta$); this means β/λ is less than 1/2 (the elastic value), the difference indicating the amount of asymmetry; 2) the pressure distribution is not symmetric in the contact region; the maximum pressure occurs upstream from the center of contact. These features are clearly shown

in the examples just given, particularly for $\lambda = 1$. As the velocity goes from 0 to ∞, the resistance (for a given total load) increases from zero, reaches a maximum for λ near 1, then decreases to zero. This confirms the predictions made in Section 1.5 about the variation of χ with velocity.

The examples give consistently low values of n (about 2 to 3% for n = 20). This error is due principally to an inaccuracy inherent in the approximate representation of the pressure distribution. The pressure elements on each end are triangular (Fig. 5.2), with finite slope at $\xi = 0$ and $\xi = \lambda$. The exact pressure distribution, however, will have a vertical slope at the ends[1]. To compensate for this, the numerical solution tends to give Q_1' and Q_{n-1}' about 2% larger, and the other Q_k' slightly smaller, than their exact values. This tendency can be seen in Table 5.1. Even with this correction, the total load (area under the pressure curve) found in the numerical solution is smaller than the exact value. The difference is indicated by the shaded regions in Fig. 5.2. With smaller segments (larger n), a steeper

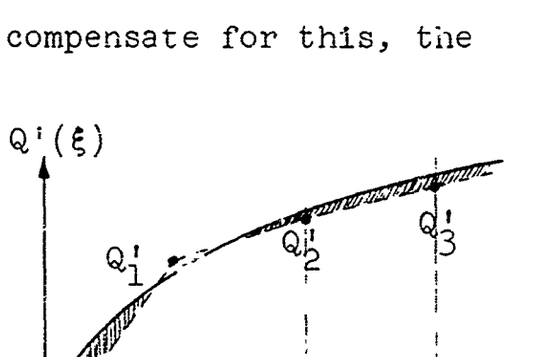

FIG. 5.2

[1] This is true for the elastic solution (5.20), and is also true for viscoelastic solids with initial elastic response.

slope at the end is possible, thus more closely representing the exact pressure distribution. This is evident in Fig. III, where the same problem is solved for different values of n. The numerical procedure could be improved somewhat by using unequal divisions of the contact region. Smaller segments could be used near the ends, since that is where the pressure changes rapidly.

Comparison of the numerical and analytic solutions for these examples shows that the numerical method with n = 20 gives results within a few per cent of the exact values. This suggests that the same procedure could give equally satisfactory results in problems for which no analytic solution can be found. An analytic solution is available only for a standard linear solid with constant ν. Two principal restrictions of this model are 1) similar behavior in shear and dilatation [$B(\zeta) = J(\zeta)$, thus ν = constant], and 2) a single retardation time. Although some general features of rolling cylinder problems are exhibited with this model, other important aspects are not adequately represented. In the next section some examples will be given for which the material behavior is not so restricted.

5.4 Examples of Rolling Cylinder Solutions

More general and realistic viscoelastic behavior is illustrated by simple Voigt solids, each having several retardation times and not restricted to constant ν. Then,

$\gamma(\zeta) = \sum_{i=1}^{m} f_i e^{-b_i \zeta}$, with $m \geq 2$, and $\omega(\xi)$ is again given by (5.6). The numerical procedure of Section 5.3 is used, with the contact region divided into 20 equal segments.

The dilatation behavior of certain viscoelastic materials can sometimes be considered as elastic. In this case, $B(\zeta) = 1$ and ν varies in time, with $\nu_f > \nu_o$. The simplest such material behaves in shear as a standard linear solid, with $J(\zeta) = 1 + f_1(1-e^{-\zeta})$; this will be used for illustration. In addition to f_1, the initial Poisson's ratio ν_o must be specified. For this set of examples, $f_1 = 1$ and $\nu_o = 1/3$, and the final Poisson's ratio is $\nu_f = .412$. Then, from (1.28b)

$$\gamma(\zeta) = .750\, e^{-\zeta} + .027778\, e^{-1.8889\zeta} \qquad (5.22)$$

Results for representative values of λ are given in Table 5.4. The limiting cases $\lambda = 0$ and $\lambda = \infty$ are found from Table 4.1 ($f = .765$ in these examples). The pressure distribution for $\lambda = 1$ is plotted in Fig. V. The variation of friction coefficient with velocity is shown in Fig. VI.

Some corresponding results for the material having the same behavior in shear, but constant ν, are shown in Table 5.3, and Figs. V, VI. Comparison shows the results for the two materials (differing only in dilatational behavior) to be nearly the same. This indicates that in rolling cylinder problems the exact nature of the behavior in dilatation is not a critical feature. With elastic dilatation, the effects

of viscoelasticity (minimum β/λ, maximum $R\chi/a_o$) are again most pronounced for λ in the neighborhood of 1, but the magnitude of these effects is somewhat less than for the material with constant ν.

In all the examples considered thus far, the viscoelastic material has been a model with a single retardation time in shear. For such a material, most of the transition from initial to final elasticity takes place in a short time span (on a log scale), about one decade on each side of the retardation time[1]. This means most of the viscoelastic behavior is concentrated in this short time span. In the rolling cylinder problem, λ is the dimensionless time needed for a given element of material to traverse the contact region. When λ is near 1, the element undergoes most of its transition from initial to final behavior during the time of contact, and the viscoelastic effects are very pronounced. This is somewhat analogous to resonance in damped vibrations. When λ is less than about .1, the contact time is too short for little more than the initial elastic behavior to be effective. Likewise, when λ is larger than about 10, the contact time is long enough that the final elastic behavior predominates. Thus, the asymmetry of the solution is most pronounced for λ in the neighborhood of 1, and the friction-velocity curve has a definite peak in this neighborhood.

---

[1] This retardation time is used to form the dimensionless time variable $\tau = t/T$, so it has the value $\tau = 1$.

These aspects of the results indicate that the model with a single constant retardation time is very artificial. Rather than discrete retardation times, actual materials appear to have a continuous distribution over a large time span. The behavior of an actual material over the full range of contact times ℓ/V can be adequately represented by a single model of discrete retardation times only if there is a broad spectrum of such times. The viscoelastic effects will be significant over a much wider range of λ, but the magnitudes of these effects will be considerably decreased.

This will be illustrated by a simple model with constant ν and five redardation times, τ = .01, .1, 1, 10, and 100. The retardation times have equal weight in the creep behavior, and the final elasticity is the same as for the set of examples of the last section (f=1). Thus,

$$J(\tau) = 2 - .2(e^{-.01\tau} + e^{-.1\tau} + e^{-\tau} + e^{-10\tau} + e^{-100\tau})$$

$$\gamma(\zeta) = .2(.01e^{-.01\zeta} + .1e^{-.1\zeta} + e^{-\zeta} + 10e^{-10\zeta} + 100e^{-100\zeta}) \tag{5.23}$$

The results for λ = 1 are given in Table 5.5, and the pressure distribution shown in Fig. V. For comparison, these include also results previously given for two materials with a single retardation time in shear. A few points on the friction-velocity curve are shown in Fig. VI. Although only five discrete times were used, the results are in

striking contrast to the single time model. For $\lambda = 1$, the 5-time model gives a much more symmetric solution, with β/λ much closer to .5. The friction curve is broad and smooth, with no pronounced peak. The maximum again occurs near $\lambda = 1$, but the curve is relatively flat over the five decades covering the retardation times. The maximum value of the coefficient of friction is considerably reduced, being only about 1/3 of the peak for the single time model with constant ν.

These results and other examples lead to the general conclusion that a single-retardation-time model is not adequate for describing quantitatively the behavior of actual materials when subject to rolling contact over a wide range of contact times. Actual materials with a broad spectrum of retardation times will not produce the pronounced viscoelastic effects of a single-time model. Instead, these examples indicate that the effects will be much reduced in magnitude and spread over a broader range of contact times. This is evident also in the example with elastic dilatation. The difference in shear and dilatation behavior introduces a secondary retardation time of relatively small weight (see 5.22). But even this produces a noticeable decrease in the friction and a more symmetric solution (see Table 5.5). For a given final elasticity f and contact time λ, a model with several retardation times will have a more symmetric

solution and lower friction than the corresponding single-time model. There are definite computational advantages in using a model to represent an actual material, but the model must have at least several retardation times for the results to be at all realistic.

The discussion so far has been concerned principally with those aspects of viscoelastic behavior which are influenced by the retardation times. But also important is the magnitude of the change from initial to final behavior. This is most conveniently indicated by the ratio of final to initial deformation in a creep test. In particular, for moving load or contact problems this ratio is given by $1 + f$, where $f = \int_0^\infty \gamma(\zeta)d\zeta$. Small values of f indicate nearly elastic behavior. Large values of f mean that the final response is much greater than the initial response. The limiting case as $f \to \infty$ is a material with no initial elasticity. This means no free spring in a mechanical model (Fig. 1.3). The simplest such model is a Kelvin solid, consisting of a spring and dashpot in parallel and having one retardation time.

To illustrate the effects of the value of f, a standard linear solid with constant ν is used, thus $\gamma(\zeta) = fe^{-\zeta}$. Fig. III shows the pressure distribution for $f = 10$, $\lambda = 1$. There is a significant peak in the pressure very close to the upstream end of the contact region. The results for

various values of f, with the same contact time $\lambda = 1$, are given in Table 5.6, and the corresponding pressure distributions in Fig. VII. The case $f = 0$ is the elastic solution which is symmetric. As f is increased, the viscoelastic effects become more and more pronounced: β decreases, indicating the contact region is displaced more and more upstream; the maximum pressure increases and the peak shifts closer to the upstream end; the friction increases (although the velocity remains nearly constant). For the limiting case as $f \to \infty$, the Kelvin solid, there is an exact analytic solution given in Section 4.2 (4.24-28). In this limiting case, the pressure peak is infinite and is at the front end of the contact region. Since the Kelvin solid has no initial elasticity, the results in Table 5.6 and Fig. VII are based on the final elastic constants $(1-\nu_f)/\mu_f$ to allow comparison.

These results indicate that for large f the viscoelastic effects (asymmetry, friction coefficient) will be much increased over the effects for small f. In particular, there will be a significant peak in the pressure distribution near the upstream end. The presence of this peak is due to the small initial response relative to the final response when f is large. The deformation near the front of the contact is produced principally by the initial elastic response, while farther downstream the longer time of contact produces a much greater response. Thus, a very high pressure

is needed at the front to produce an initial elastic response comparable in magnitude to the deformation in the rest of the contact region. As f gets larger, a greater pressure is needed, so the peak increases. In the limit $f \to \infty$, there is no initial response, so an infinite pressure is needed. The example used here is a situation most favorable to producing a peak. The time of contact ($\lambda=1$) coincides with the single retardation time of the material, so the viscoelastic effects are exaggerated as explained earlier. With this same material, if $\lambda \gg 1$, the contact time is long enough so the final elastic response is effective over nearly all the contact region. In this case the results are nearly the same as the elastic solution for all values of f. For $\lambda \ll 1$, the short contact time means only the initial elastic response is effective over most of the region. The solutions are thus close to elastic again when f is not too large. However, for very large f the initial response is very small and not significant, so the solution approaches that of the Kelvin solid.

The significance of several rather than just one retardation time in the material behavior has already been discussed. This is particularly evident when f is large. As an example, the results for the 5-retardation-time model used previously, this time with $f = 100$ and $\lambda = 1$, are given in Table 5.6. The solution is considerably more symmetric and

the friction coefficient much less than for the corresponding single-time model. The pressure distribution is very nearly the same shape as the $f = 1$ curve in Fig. VII (with slightly greater ordinates) and there is no pronounced peak.

Actual materials, such as polymers, may have values of f as high as 10^4. However, when f is very large there are difficulties in the numerical calculations due to the sharp peak. Many divisions of short length are needed in the vicinity of the peak. This is evident in Fig. III, where results for different values of n can be compared. But, as mentioned in Section 5.3, other difficulties arise when very short segments are used. Attempts were made to estimate the peak by further theoretical considerations, and so remove it from the numerical calculations, but without success.

5.5 Numerical Solution of the Nearly Flat Punch Problem

As an illustration of another application of the numerical method for moving contacts, the problem of moving "nearly flat" punch is considered in this section. A "flat punch" is a rigid (two-dimensional) body with a plane surface at some angle α pressed into the viscoelastic base (Fig. 5.3) by a force N^*. If the punch is perfectly flat, the contact will be a straight line with

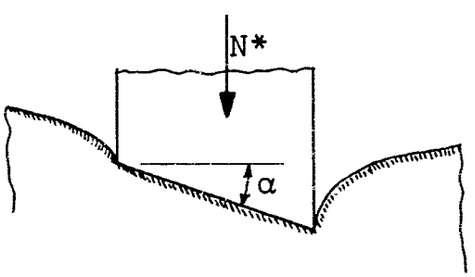

FIG. 5.3

sharp corners at the ends. In this idealized form, the pressure will be infinite and the slope of the deformed surface will be discontinuous at one or both ends of the contact. Real corners, however, will be slightly rounded, not perfectly sharp. The pressure at the corners may be high, but finite, and the contact will be smooth. The important question is how the peak pressures depend on the shape of the rounded corners. Such a "nearly flat punch" may score or gouge the base surface if peak pressures are too high. Avoidance of such damage is a practical problem of frequent occurrence.

Some aspects of the moving contact of a nearly flat punch will be investigated The corners will be assumed to be circular arcs (radius R), with the length of the rounded portion very small relative to the total length of contact (Fig. 5.4). The problem is then treated as one of smooth contact. The length d of the flat portion is fixed. Then, the length of the rounded corner in contact on the left end is b, and for a total contact length ℓ the length of the rounded corner on the right end is $\ell - d - b \equiv \eta b$, with $b \ll \ell$. In general $\eta \neq 1$ because the contact is not symmetric.

The elastic solution for smooth contact of a nearly flat punch (reported elsewhere) shows that, while the pressure is everywhere finite and is zero at the ends, very sharp peaks occur just inside the ends of contact. As the

length of the corners becomes smaller (i.e., $b/d \to 0$), the peak gets sharper, and in the limit the solution becomes that for a perfectly flat punch. This suggests that the viscoelastic solution may also have sharp peaks in the pressure distribution near the ends.

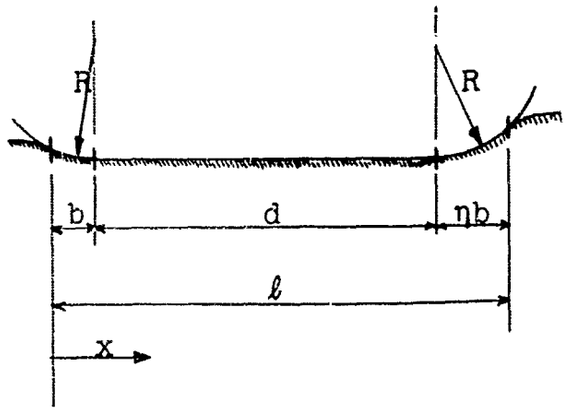

FIG. 5.4

The viscoelastic problem is treated as outlined in Section 5.2. Lengths are expressed as dimensionless ratios to VT:

$$\rho = \frac{R}{VT} \quad , \qquad \delta = \frac{d}{VT} \quad , \qquad \eta = (\lambda-\delta-\beta)/\beta \tag{5.24}$$

The other dimensionless quantities given by (3.5a-d) are used. The shape of the contact surface (with the circular arcs approximated by parabolas) is given by

$$w(\xi-\beta) = -\frac{1}{2\rho}(\xi-\beta)^2 \quad , \qquad 0 \le \xi \le \beta$$

$$= 0 \quad , \qquad \beta \le \xi \le \beta + \delta$$

$$= -\frac{1}{2\rho}(\xi-\beta-\delta)^2 \quad , \qquad \beta + \delta \le \xi \le \lambda$$

The n collocation points are c sen, and, taking $\xi_a = \beta$ (Fig. 5.1), $w(\xi_a-\beta) = 0$. Then, from (5.9),

$$\sum_{k=1}^{n-1} Q_k' A_{jk} + \phi A_{jn} = w_j' \quad , \quad j = 0,1,\ldots,n, \text{ except } j = a \tag{5.25}$$

where

$$Q_k' = \rho Q_k \quad , \quad N' = 2\rho N = \sum_{k=1}^{n-1} Q_k'(\theta_{k+1}+\theta_k),$$

$\phi \equiv 2\rho\alpha$, and

$$\begin{aligned} w_j' \equiv 2\rho w_j &= -(\xi_j-\beta)^2 \quad , \quad 0 \le \xi_j \le \beta \\ &= 0 \quad , \quad \beta \le \xi_j \le \delta + \beta \\ &= -(\xi_j-\beta-\delta)^2 \quad , \quad \beta+\delta \le \xi_j \le \lambda \end{aligned} \tag{5.26}$$

The A_{jk} are given by (5.8a,b) and (5.4b-d) with $\xi_a = \beta$. For a particular problem, values of β and λ are chosen, thus determining η (δ is a given quantity). The solution then gives the pressures Q_k' and the tilt ϕ. To obtain a particular value of ϕ, for example, several trials with different λ and/or β may be necessary

For illustration, the results of one set of examples are given. A standard linear solid with constant ν is used, so $\gamma(\zeta) = e^{-\zeta}$. In these examples, $\delta = .99$ and $\beta = .005$; the only variation is in η (thus λ varies slightly). The division of the contact region and the choice of n is based on the expectation of sharp peaks near the ends and relatively little variation near the center. After some preliminary trials, n = 22 was chosen. A typical division is shown schematically for $\eta = 1.67$:

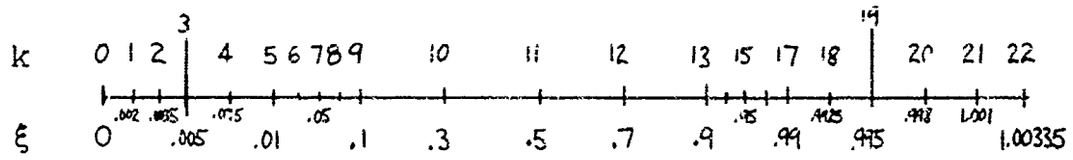

(not to scale)

The results for several values of η are given in Table 5.7, and some pressure distributions are shown in Fig. VIII. The sharp peaks in the pressure are present as anticipated, and the expected asymmetry is shown by the greater height of the upstream peak. Another expectation is verified by the regular change in tilt as the upstream corner is lenghened, other factors being constant. The tilt is nearly zero when $\eta = 1.67$, and the body rotates clockwise as η is increased. The pressure distribution is very little changed near the downstream end, but there is significant change near the upstream end as η is varied. The peak pressure and total load N' increase with η, and the line of action of the vertical resultant moves upstream. For the zero tilt example ($\eta = 1.67$), the line of action of N' is at $\xi = .60$.

These examples indicate the general suitability of the numerical method for viscoelastic moving contact problems of this type. Even with a relatively small n, the important features are evident in the solution. The method can of course be applied for more general viscoelastic materials if desired. The shapes of the rounded corners can also be easily changed. For example, the stress peaks could perhaps be made more nearly equal by using different radii at the

two ends. It is interesting to note that (within the limitations of small displacements and smooth contact) the radius of the rounded corner enters only as a scale factor in the pressure and load expressions. Thus, if b, d, and ηb (Fig. 5.4) are kept the same, the pressure distribution expressed by

$$Q'(\xi) = \frac{R}{VT} \frac{1-\nu_o}{\mu_o} \frac{1}{\pi} q(x)$$

remains unchanged if the radius R is changed. However, the total load changes in proportion to R, so the actual magnitude of the pressure $q(x)$ changes similarly.

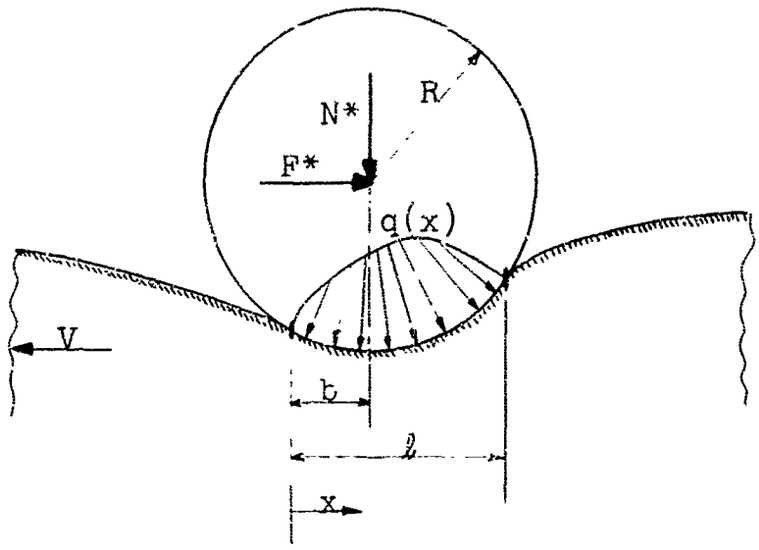

$$a_o = \sqrt{\frac{1-\nu_o}{\mu_o} \frac{2}{\pi} R\, N^*}$$

= half-length of contact on elastic base (μ_o, ν_o)

Material Properties:

μ_o, ν_o - initial elastic constants

T - characteristic time parameter

$\gamma(\zeta)$ - a creep function, defined by eqn. 1.27

Dimensionless Quantities

$$\xi = \frac{x}{VT} \; ; \quad \lambda = \frac{\ell}{VT} \; ; \quad \beta = \frac{b}{VT} \; ; \quad \rho = \frac{R}{VT}$$

$$Q'(\xi) = \frac{1-\nu_o}{\mu_o} \frac{1}{\pi} \frac{R}{VT}\, q(x)$$

$$N' = \frac{1-\nu_o}{\mu_o} \frac{2}{\pi} \frac{R}{VT} \frac{N^*}{VT} = \left(\frac{a_o}{VT}\right)^2$$

$$F' = \frac{1-\nu_o}{\mu_o} \frac{2}{\pi} \frac{R}{VT} \frac{F^*}{VT} \; ; \quad \chi = \frac{F^*}{N^*} = \frac{F'}{N'}$$

FIG. I THE ROLLING CYLINDER PROBLEM

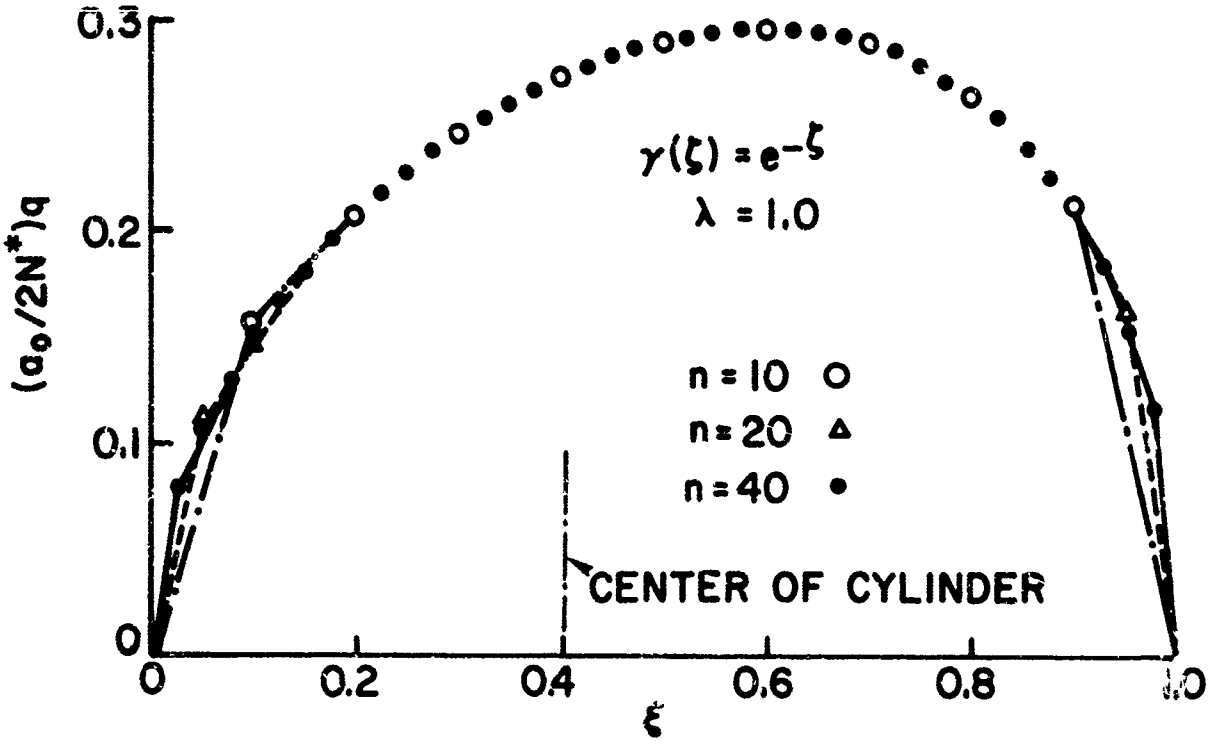

FIG. II ROLLING CYLINDER PRESSURE DISTRIBUTIONS FOR VARIOUS n , f = 1.

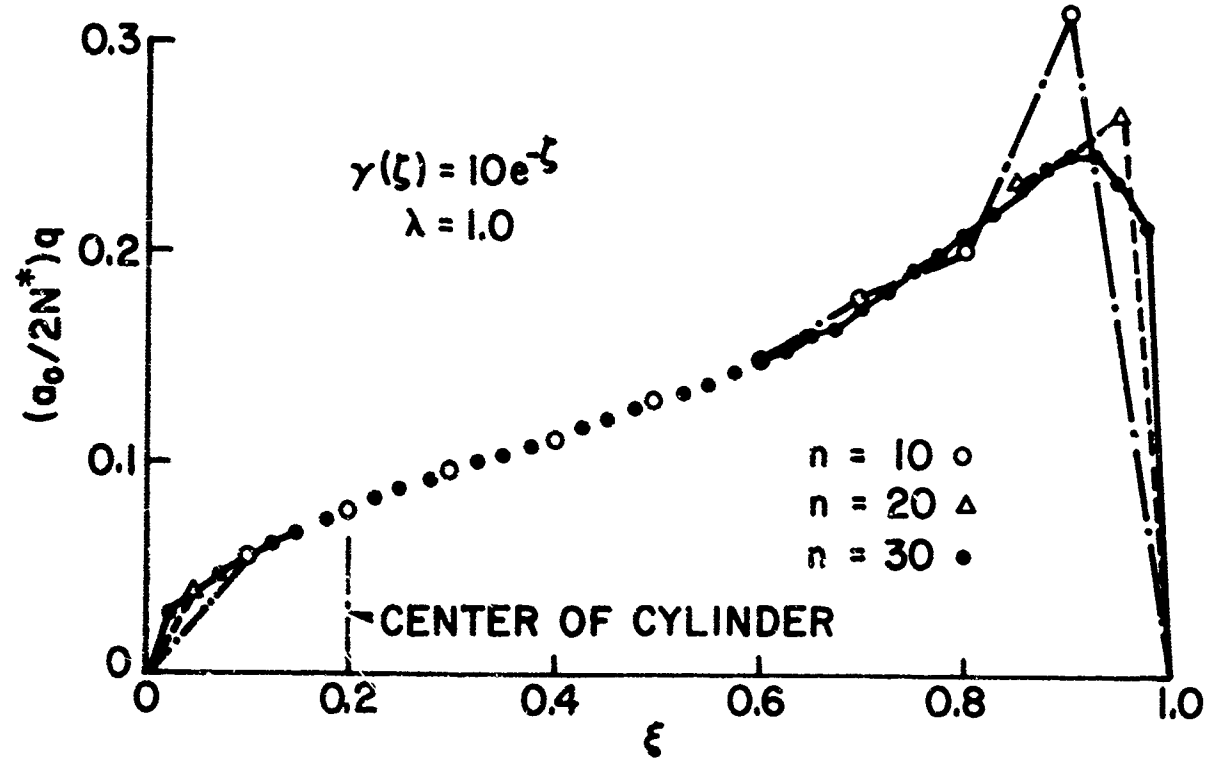

FIG. III ROLLING CYLINDER PRESSURE DISTRIBUTIONS FOR VARIOUS n , f = 10.

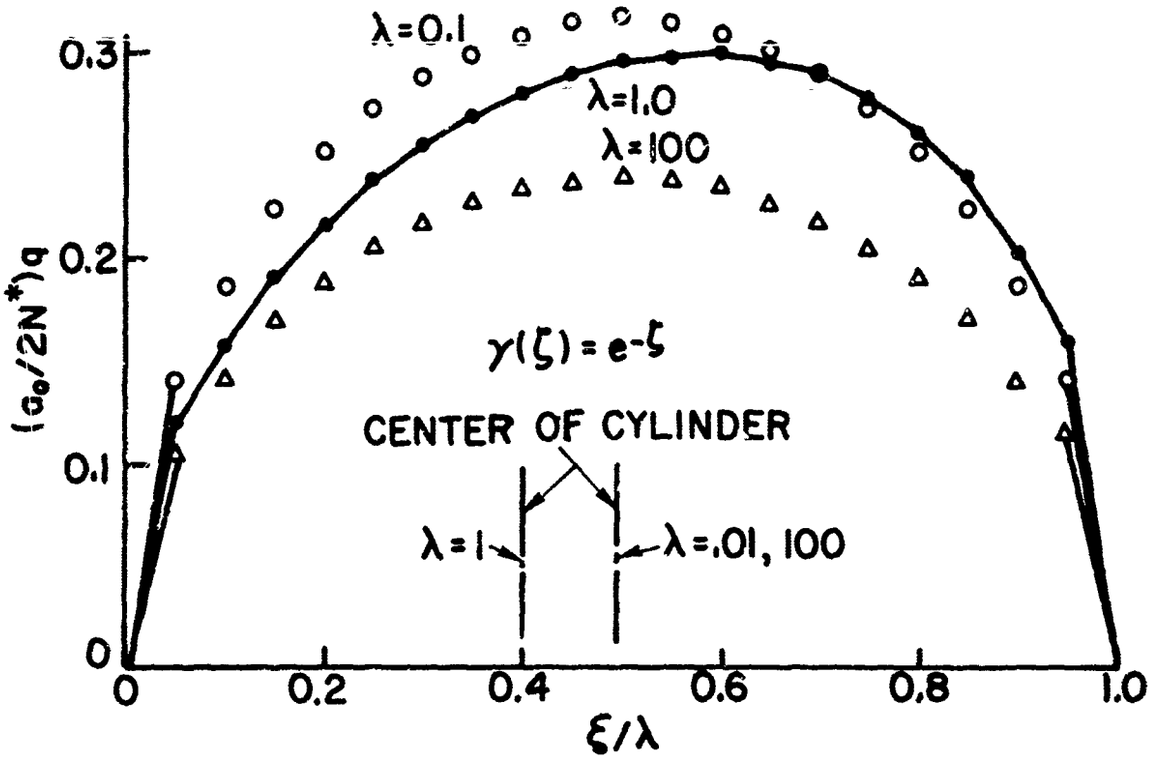

FIG. IV ROLLING CYLINDER PRESSURE DISTRIBUTIONS FOR VARIOUS λ .

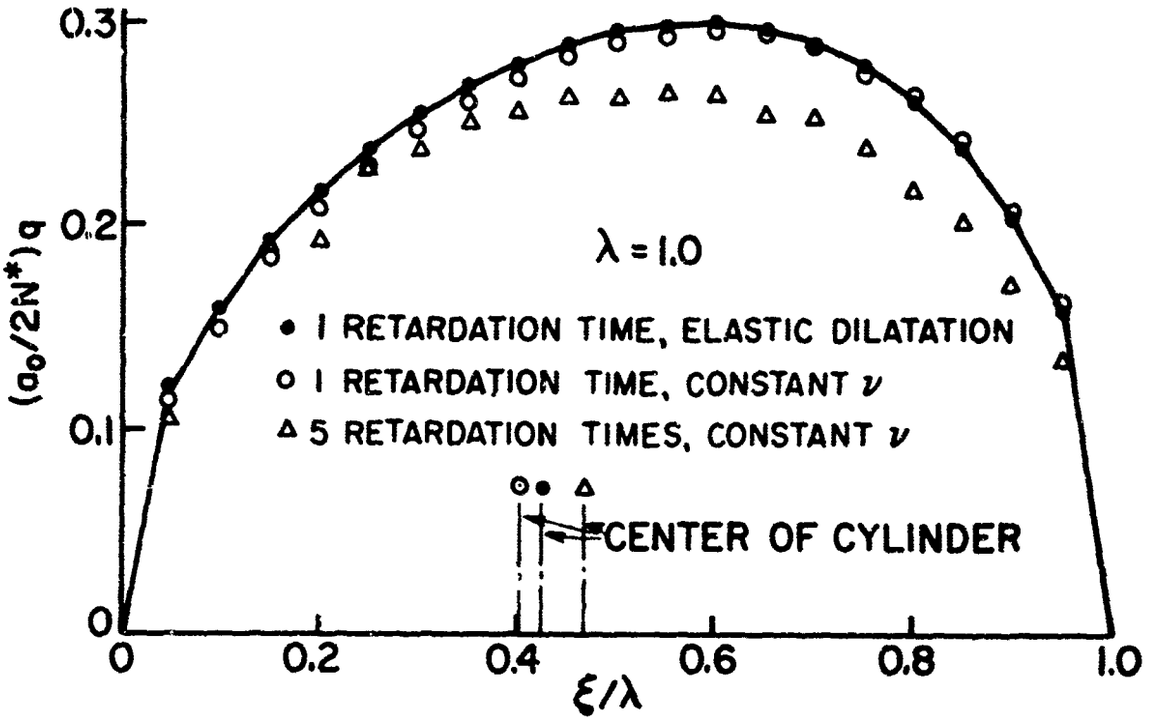

FIG. V ROLLING CYLINDER PRESSURE DISTRIBUTIONS FOR VARIOUS MATERIALS.

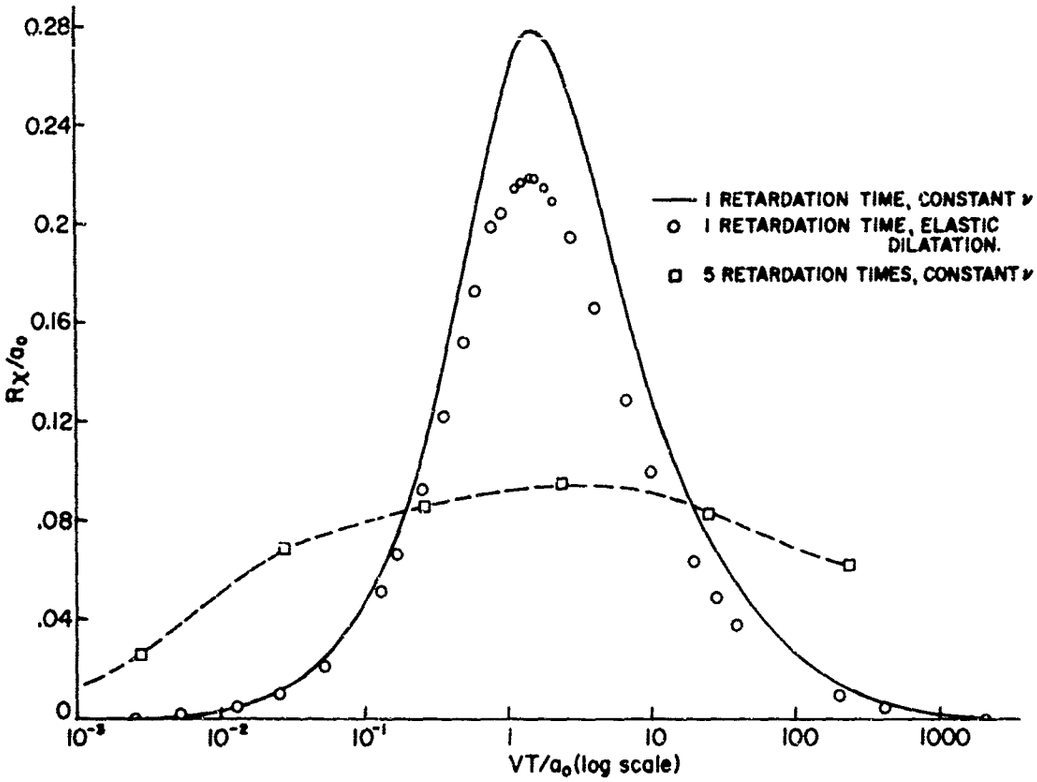

FIG. VI ROLLING RESISTANCE VS. VELOCITY FOR ROLLING CYLINDER.

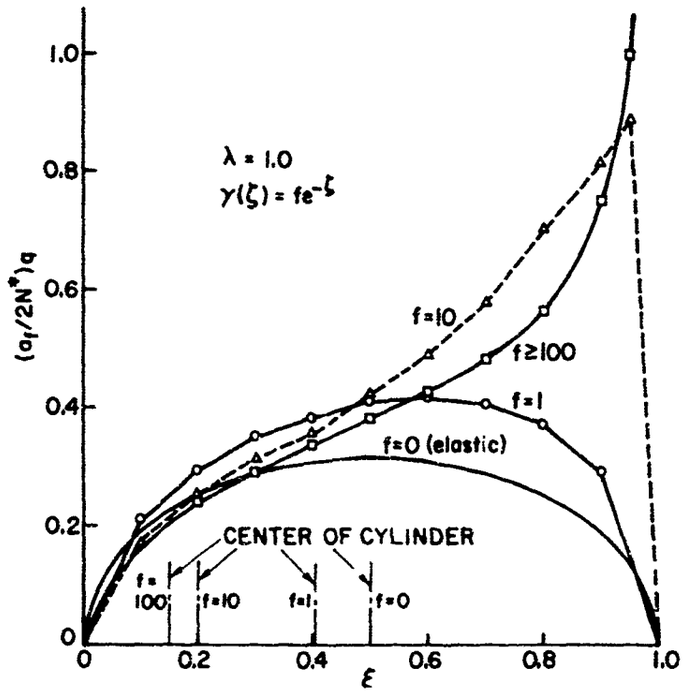

FIG. VII ROLLING CYLINDER PRESSURE DISTRIBUTIONS FOR VARIOUS VALUES OF f .

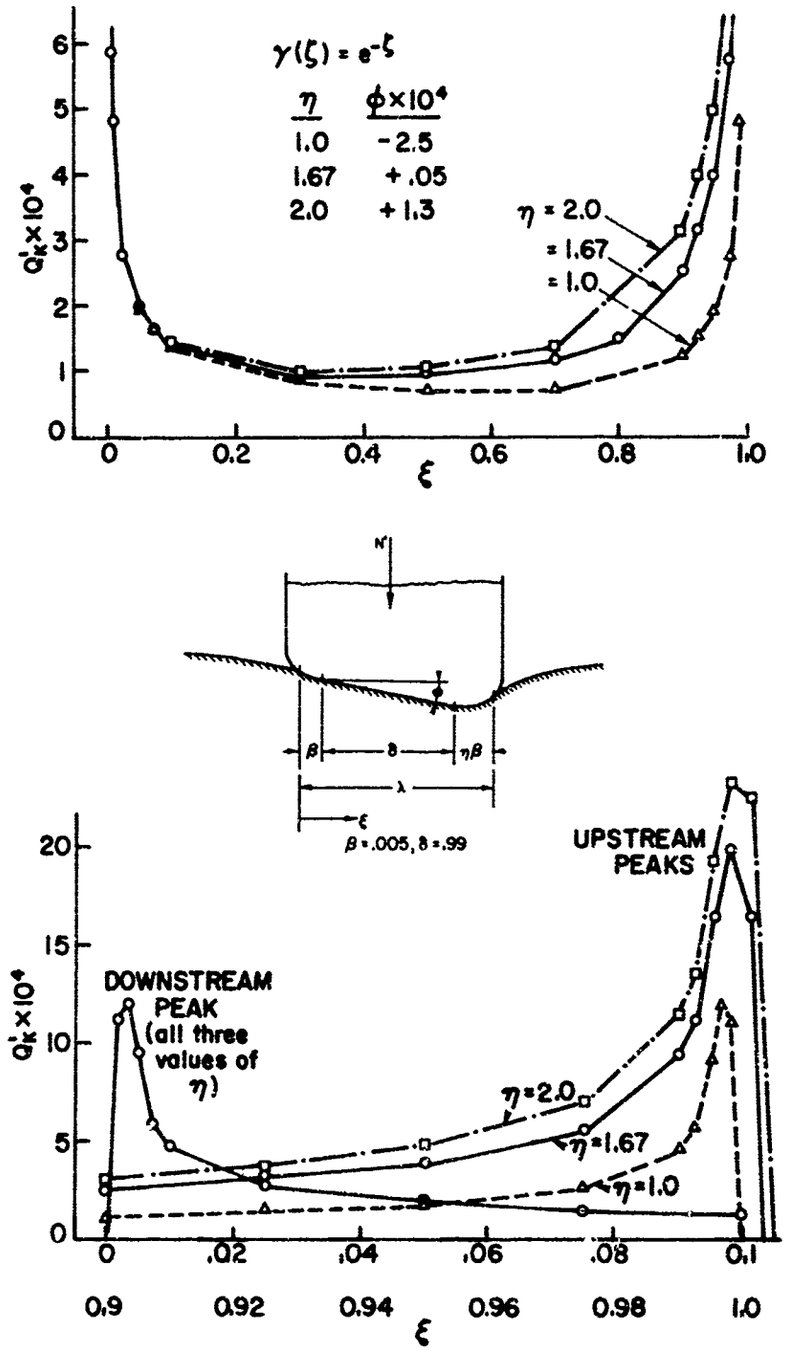

FIG. VIII PRESSURE DISTRIBUTIONS FOR NEARLY FLAT PUNCH.

TABLE 5.1

ROLLING CYLINDER ON ELASTIC BASE,
NUMERICAL AND ANALYTIC SOLUTIONS

Values of Q_k' for $\lambda=10$

	Numerical		Analytic
$40\xi/\lambda$	n=10	n=40	
1		.508	.497
2		.675	.693
3		.825	.839
4	.977	.942	.955
6		1.125	1.134
8	1.234	1.263	1.271
10		1.368	1.379
12	1.429	1.449	1.460
14		1.509	1.518
16	1.529	1.550	1.560
18		1.575	1.584
20	1.561	1.583	1.590
N'	23.80	24.71	25.00
β/λ	.5000	.5000	.5000

TABLE 5.2

ROLLING CYLINDER RESULTS FOR VARIOUS n

$\gamma(\zeta)=fe^{-\zeta}$; $\lambda=1$

	Numerical			Analytic	
	n=10	n=20	n=40		
β/λ	.4025	.4014	.4008	.4003	
N'	.2048	.2097	.2121	.2144	f=1
$\rho\chi$	.1213	.1231	.1239	.1249	
Q'max.	.1350	.1359	.1364		
β/λ	.1981	.1965	.1958	.1952	
N'	.0697	.0712	.0718	.0724	f=10
$\rho\chi$	.4257	.4291	.4308	.4322	
Q'max.	.0835	.0719	.0665		

Corresponding pressure distributions are shown Figures I and II.

TABLE 5.3

ROLLING CYLINDER RESULTS FOR VARIOUS λ

$$\gamma(\zeta)=e^{-\zeta}$$

λ	β/λ	N'/λ^2	$\rho\chi$	VT/a_o	$R\chi/a_o$	$(a_o/2N^*)q$ max	
0	.5000	.2500	0	$2/\lambda$	0	.3183	*
.01	.4932	.2500	.0000670	200.0	.01340		A
	.4934	.2440	.0000692	202.4	.01402	.3186	N
.1	.4612	.2491	.00380	20.0	.0760		A
	.4620	.2430	.00410	20.28	.0832	.3180	N
1	.4003	.2144	.1249	2.16	.270		A
	.4014	.2097	.1231	2.184	.2688	.2967	N
10	.4768	.1377	.4292	.270	.116		A
	.4768	.1343	.4276	.2729	.1167	.2273	N
100	.4975	.1263	.4925	.0281	.0138		A
	.4975	.1227	.4828	.0285	.01378	.2254	N
∞	.5000	.1250	.5000	$2.828/\lambda$	0	.2250	*

A - analytic solution, Section 4.2
N - numerical solution, Section 5.3
* - limiting case, exact solution

Pressure distributions are shown in Figure III.

TABLE 5.4

NUMERICAL RESULTS FOR ROLLING CYLINDERS

Standard linear solid in shear, elastic dilatation

$$\gamma(\zeta) = .750e^{-\zeta} + .02778e^{-1.889\zeta}$$

$$\nu_o = .333 \ , \quad \nu_f = .412 \ , \quad f = .765$$

λ	β/λ	N'/λ^2	VT/a_o	$\rho\chi$	$R\chi/a_o$	$(a_o/2N^*)q_{max}$
0	.500	.250	∞	0	0	.318 (exact)
.01	.495	.244	202	.000054	.0109	.319
.1	.471	.243	20.3	.00317	.0643	.318
.5	.430	.233	4.14	.0403	.167	.312
.75	.423	.225	2.81	.0692	.195	.306
1.0	.422	.217	2.15	.0976	.210	.301
1.6	.427	.200	1.40	.157	.219	.289
2.0	.433	.192	1.14	.189	.215	.282
5.0	.464	.162	.496	.308	.153	.250
10	.480	.150	.258	.364	.0940	.242
100	.498	.139	.0268	.413	.0111	.240
1000	.500	.138	.0027	.415	.0011	.240
∞	.500	.142	0	.432	0	.240 (exact)

TABLE 5.5

ROLLING CYLINDER RESULTS FOR VARIOUS MATERIALS

$\lambda = 1$

a) Standard linear solid, constant ν — $J(\zeta) = 1 + (1 - e^{-\zeta})$; $\gamma(\zeta) = e^{-\zeta}$

b) Standard linear solid in shear, elastic dilatation ($\nu_o = .333$) — $J(\zeta) = 1 + (1 - e^{-\zeta})$; $B(\zeta) = 1$; $\gamma(\zeta) = .750e^{-\zeta} + .02778e^{-1.889\zeta}$

c) Five retardation times in shear, constant ν — $\left.\begin{matrix} J(\zeta) \\ \gamma(\zeta) \end{matrix}\right\}$ see equation (5.23)

	β/λ	N'/λ^2	$\rho\chi$	VT/a_o	$R\chi/a_o$	$(a_o/2N^*)q_{max}$
a)	.4014	.2097	.1231	2.184	.269	.297
b)	.4215	.2171	.0976	2.146	.210	.301
c)	.4694	.1738	.402	2.399	.096	.268

TABLE 5.6

ROLLING CYLINDER RESULTS FOR VARIOUS f

$\lambda = 1$ in all cases

Results are based on the final elastic response: $a_f = a\sqrt{1+f}$

f	β/λ	$(1+f)N'$	$\rho\chi$	VT/a_f	$R\chi/a_f$	$(a_f/2N^*)q_{max}$	
			Single retardation time				
0	.500	.250	0	2.000	0	.318	(exact)
1	.401	.419	.123	1.546	.190	.420	
10	.197	.790	.429	1.129	.434	.892	
100	.149	.872	.524	1.060	.559	3.08	
∞	.143	.893	.538	1.058	.569	∞	(exact)
			Five retardation times				
1	.469	.348	.040	1.696	.068	.379	
100	.401	.576	.133	1.319	.175	.515	

TABLE 5.7

NUMERICAL RESULTS FOR NEARLY FLAT PUNCH

$\beta = .005$, $\delta = .99$, $\gamma(\zeta) = e^{-\zeta}$

$\varphi \times 10^4$	η	λ	$N' \times 10^4$	$Q' \times 10^4$ left max	$Q' \times 10^4$ right max	$Q' \times 10^4$ min
-2.52	1.0	1.000	2.52	11.9	12.0	.71
- .32	1.6	1.003	3.56	12.0	19.1	.91
.05	1.67	1.00335	3.74	12.0	20.1	.93
.53	1.8	1.004	3.97	11.9	21.5	.96
1.3[illegible]	2.0	1.005	4.36	12.0	23.6	.99
6.13	3.0	1.010	6.66	11.9	35.7	1.23

BIBLIOGRAPHY

1. Abrahamson, G. R. "Permanent Periodic Surface Deformations Due to a Traveling Jet," Journal of Applied Mechanics, 28, December 1961, p. 519.

2. Abrahamson, G. R. and Goodier, J. N. "The Hump Deformation Preceding a Moving Load on a Layer of Soft Material," Journal of Applied Mechanics, 28, December 1961, p. 608.

3. Bland, D. R. The Theory of Linear Viscoelasticity, Pergamon, 1960.

4. Bowden, F. P. and Tabor, D. Friction and Lubrication, Methuen, 1956.

5. Corneliussen, A. R. and Lee, E. H. "Stress Distribution Analysis for Linear Viscoelastic Materials," Colloquium on Creep in Structures, ed. N. J. Hoff, Academic Press, 1962.

6. Drutowski, R. C. "Energy Losses of Balls Rolling on Plates," Symposium on Friction and Wear, ed. R. Davies, Elsevier, 1959.

7. Drutowski, R. C. "Linear Dependence of Rolling Friction on Stressed Volume," Symposium on Rolling Contact Phenomena, ed. J. B. Bidwell, Elsevier, 1962.

8. Erdelyi, A., et.al. Higher Transcendental Functions, Bateman Manuscript Project, Vol. II, McGraw-Hill, 1953.

9. Ferry, J. D. Viscoelastic Properties of Polymers, Wiley, 1961.

10. Flom, D. G. "Rolling Friction of Polymeric Materials-Elastomers," Journal of Applied Physics, 31, 1960, p. 306.

11. Flom, D. G. "Rolling Friction of Polymeric Materials-Thermoplastics," Journal of Applied Physics, 32, 1961, p. 1426.

12. Flom, D. G. "Dynamic Mechanical Losses in Rolling Contacts," Symposium on Rolling Contact Phenomena, ed. J. B. Bidwell, Elsevier, 1962.

13. Flom, D. G. and Bueche, A. M. "Theory of Rolling Friction for Spheres," Journal of Applied Physics, 30, 1959, p. 1725.

14. Freudenthal, A. M., Bieniek, M. P., and Henry, L. A. "One-dimensional Response of Linear Viscoelastic Media," International Journal of Mechanical Sciences, 4, May-June 1962, p. 211.

15. Friedman, B. Principles and Techniques of Applied Mathematics, Wiley, 1956.

16. Greenwood, J. A., Minshall, H. and Tabor, D. "Hysteresis Losses in Rolling and Sliding Friction," Proceedings, Royal Society of London, A259, 1960, p. 480.

17. Hunter, S. C. "The Rolling Contact of a Rigid Cylinder with a Viscoelastic Half Space," Journal of Applied Mechanics, 28, December 1961, p. 611.

18. Kelly, J. M. "Moving Load Problems in the Theory of Viscoelasticity," Dissertation, Stanford University, 1962.

19. Lee, E. H. "Stress Analysis in Viscoelastic Bodies," Quarterly of Applied Mathematics, 13, 1955, p. 183.

20. Lee, E. H. "Viscoelastic Stress Analysis," First Symposium on Naval Structural Mechanics, ed. J. N. Goodier and N. J. Hoff, Pergamon, 1960.

21. Lee, E. H. and Rogers, T. G. "Solution of Viscoelastic Stress Analysis Problems Using Measured Creep or Relaxation Functions," Journal of Applied Mechanics, 30, July 1963, p. 127.

22. Love, A. E. H. A Treatise on the Mathematical Theory of Elasticity, 4th edition (1927), Dover, 1944.

23. May, W. D., Morris E. L., and Atack, D. "Rolling Friction of a Hard Cylinder Over a Viscoelastic Material," Journal of Applied Physics, 30, 1959, p. 1713.

24. Morland, L. W. "A Plane Problem of Rolling Contact in Linear Viscoelasticity Theory," Journal of Applied Mechanics, 29, June 1962, p. 345.

25. Muskhelishvili, N. I. Some Basic Problems of the Mathematical Theory of Elasticity, (trans. J. R. M. Radok), Noordhoff, 1953.

26. Norman, R. H. "Rolling Friction of Cylinders on Planes," British Journal of Applied Physics, 13, July 1962, p. 358.

27. Pearson, K. Tables of the Incomplete Beta Function, Cambridge, 1948.

28. Sneddon, I. N. Fourier Transforms, McGraw-Hill, 1951.

29. Staverman, A. J. and Schwarzl, F. "Linear Deformation Behavior of High Polymers," Chapter I in Die Physik der Hochpolymeren, Vol. IV, ed. H. A. Stuart, Springer, 1956.

30. Tabor, D. "The Mechanism of Rolling Friction," Philosophical Magazine (7), 43, 1952, p. 1055.

31. Tabor, D. "The Mechanism of Rolling Friction," Proceedings, Royal Society of London, A229, 1955, p. 198.

32. Tabor, D. and Atack, D. "The Friction of Wood," Proceedings, Royal Society of London, A246, 1958, p. 539.

33. Thomson, W. T. Laplace Transformation, Prentice-Hall, 1961.

34. Tobolsky, A. V. Properties and Structure of Polymers, Wiley, 1960.

35. Watson, G. N. A Treatise on the Theory o. Bessel Functions, 2nd edition, Cambridge, 1958.

Technical Reports Distribution List, Contract Nonr 225(29), Project NR-064-241

Commanding Officer
USNNOEU
Kirtland Air Force Base
Albuquerque, New Mexico
(1) Attn: Code 20 (Dr. J. N. Brennan)

U. S. Atomic Energy Commission
Washington 25, D. C
(2) Attn: Director of Research

Director
National Bureau of Standards
Washington 25, D. C
(1) Attn: Division of Mechanics
(1) Engineering Mechanics Section
(1) Aircraft Structures

Commandant
U. S. Coast Guard
1300 E Street, N.W.
Washington 25, D. C.
(1) Attn: Chief, Testing and Development Div.

U. S. Maritime Administration
Gen. Adminstration Office Building
Washington, D. C.
(1) Attn: Chief, Div. of Preliminary Design

National Aeronautics and Space Administration
1512 H Street, N.W.
Washington, 25, D. C.
(2) Attn: Loads and Structures Div

Director
Langley Aeronautical Lab.
Langley Field, Virginia
(2) Attn: Structures Div.

(1) Director
Forest Products Lab.
Madison, Wisconsin

Civil Aeronautics Administ.
Department of Commerce
Washington 25, D.C.
(1) Attn: Chief, Aircraft Eng. Div.
(1) Chief, Airframe and Equipment Div.

National Sciences Foundation
1520 H Street, N.W.
Washington, D.C.
(1) Attn: Engineering Sciences Div

National Academy of Science
2101 Constitution Avenue
Washington 25, D.C.
(1) Attn: Tech. Dir., Committee on Ships Structural Des.
(1) Executive Sec., Comm. on Undersea Warfare

(1) Director, USAF Project RAND
Via: US Air Force Liaison Off.
The RAND Corporation
1700 Main Street
Santa Monica, California

(1) Dr. H. Norman Abramson
Man., Engineering Analysis
Southwest Research Institute
8500 Culebra Road
San Antonio 6, Texas

(1) Professor Lynn S. Beedle
Fritz Engineering Lab.
Lehigh University
Bethlehem, Pennsylvania

(1) Prof. R. L. Bisplinghoff
Dept. of Aeronautical Eng.
Massachusetts Institute of Technology
Cambridge 39, Massachusetts

(1) Prof. H. H. Bleich
Dept. of Civil Engineering
Columbia University
New York 27, New York

(1) Prof. B. A. Boley
Dept. of Civil Engineering
Columbia University
New York 27, New York

(1) Dr. John F. Brahtz
J. N. Pomeroy and Co.
3625 West 6th Street
Los Angeles 5, Calif.

(1) Prof. G. F. Carrier
Pierce Hall
Harvard University
Cambridge 38, Massachusetts

(1) Prof. J. E. Cermak
Dept. of Civil Engineering
Colorado State University
Fort Collins, Colorado

(1) Prof. Herbert Deresiewicz
Dept. of Civil Engineering
Columbia University
632 W. 125th Street
New York 25, New York

(1) Prof. Lloyd Donnell
Dept. of Mechanics
Illinois Institute of Tech.
Technology Center
Chicago 16, Illinois

(1) Prof. D. C. Drucker
Div. of Engineering
Brown University
Providence 12, Rhode Island

(1) Prof. A. C. Eringen
Dept. of Aeronautical Eng.
Purdue University
Lafayette, Indiana

(1) Prof. W. Flügge
Div. of Engineering Mech.
Stanford University
Stanford, California

(1) Mr. Martin Goland
Southwest Research Institute
8500 Culebra Road
San Antonio 6, Texas

(1) Prof. J. N. Goodier
Div. of Engineering Mech.
Stanford University
Stanford, California

(1) Prof. L. E. Goodman
Eng. Experiment Station
University of Minnesota
Minneapolis, Minnesota

(1) Prof. W. J. Hall
Dept. of Civil Engineering
University of Illinois
Urbana, Illinois

(1) Prof. M. Hetenyi
Div. of Engineering Mech.
Stanford University
Stanford, California

(1) Prof. P. G. Hodge
Illinois Institute of Tech.
Technology Center
Chicago 16, Illinois

(1) Prof. N. J. Hoff
Dept. of Aeronautical Eng.
Stanford University
Stanford, California

(1) Prof. W. H. Hoppmann
Dept. of Mech. Eng.
Johns Hopkins Univ.
Baltimore, Maryland

(1) Prof. Bruce G. Johnston
University of Michigan
Ann Arbor, Michigan

(1) Prof. J. Kempner
Dept. of Aero. Eng. and Appl. Mech.
Polytechnic Institute of Brooklyn
333 Jay Street
Brooklyn 2, New York

(1) Prof. H. L. Langhaar
Dept. of Theoretical and Appl. Mech.
University of Illinois
Urbana, Illinois

(1) Prof. B. J. Lazan, Dir.
Eng. Experiment Station
University of Minnesota
Minneapolis 14, Minn.

(1) Prof. E. H. Lee
Div. of Engineering Mech.
Stanford University
Stanford, California

(1) Prof. George H. Lee
Dir. of Research
Rensselaer Polytechnic Inst.
Troy, New York

(1) Mr. M. M. Lemcoe
Southwest Research Inst.
8500 Culebra Road
San Antonio 6, Texas

(1) Prof. Paul Lieber
Geology Dept.
Rensselaer Polytechnic Inst.
Troy, New York

(1) Midwest Research Institute
4049 Pennsylvania Avenue
Kansas City 2, Missouri
Attn: Library

(1) Prof. Hsu Lo
School of Engineering
Purdue University
Lafayette, Indiana

(1) Prof. R. D. Mindlin
Dept. of Civil Eng.
Columbia University
632 W. 125th Street
New York 25, New York

(1) Dr. A. Nadai
136 Cherry Valley Road
Pittsburgh 21, Pa.

(1) Prof. Paul M. Naghdi
College of Engineering
University of California
Berkeley 4, Calif.

(1) Prof. William A. Nash
Dept. of Eng. Mech.
University of Florida
Gainesville, Florida

(1)Prof. N. M. Newmark
Dept. of Civil Eng.
University of Illinois
Urbana, Illinois

(1)Prof. Aris Phillips
Dept. of Civil Eng.
15 Prospect Street
Yale University
New Haven, Conn.

(1)Prof. W. Prager
Physical Sicences Council
Brown University
Providence 12, R. I.

(1)Prof. E. Reissner
Dept. of Math.
Massachusetts Inst. of Tech.
Cambridge 39, Mass.

(1)Prof. M. A. Sadowsky
Dept. of Mechanics
Rensselaer Polytechnic Inst.
Troy, New York

(1)Dr. Bernard W. Shaffer
Dept. of Mech. Eng.
New York University
University Heights
New York 53, New York

(1)Prof. C. B. Smith
College of Arts and Sciences
Dept. of Math., Walker Hall
University of Florida
Gainesville, Florida

(1)Prof. J. Stallmeyer
Dept. of Civil Engineering
University of Illinois
Urbana, Illinois

(1)Prof. Eli Sternberg
Div. of Mathematics
Brown University
Providence 12, R. I.

(1)Prof. S. P. Timoshenko
School of Engineering
Stanford University
Stanford, Calif.

(1)Prof. A. S. Veletsos
Dept. of Civil Eng.
University of Illinois
Urbana, Illinois

(1)Prof. Enrico Volterra
University of Texas
Austin 12, Texas

(1)Prof. Dana Young
Yale University
New Haven, Conn.

Chief of Naval Research
Dept. of the Navy
Washington 25, D.C.
(2)Attn: Code 438

(1)Commanding Officer
Office of Naval Research
Branch Office
John Crerar Lib. Building
86 E. Randolph Street
Chicago 11, Illinois

(1)Commanding Officer
Office of Naval Research
Branch Office
346 Broadway
New York 13, New York

(1)Commanding Officer
Office of Naval Research
Branch Office
1030 E. Green Street
Pasadena, California

(1)Commanding Officer
Office of Naval Research
Branch Office
1000 Geary Street
San Francisco, Calif.

(2)Commanding Officer
Office of Naval Research
Navy Bo. 100, c/o Fleet P.O.
New York, New York

Director
Naval Research Lab.
Washington 25, D.C.
(6)Attn: Tech. Info. Officer
(1) Code 6200
(1) Code 6205
(1) Code 6250
(1) Code 6260

(5)ASTIA Document Service Center
Arlington Hall Station
Arlington 12, Virginia

(1)Off. of Technical Services
Dept. of Commerce
Washington 25, D.C.

Leg. Ref. Service
Lib. of Congress
Washington 25, D.C.
(1)Attn: Dr. E. Wenk

Off. of the Sec. of Def.
Research and Development Div.
The Pentagon
Washington 25, D.C.
(1)Attn: Technical Library

Chief
Armed Forces Special Weapons
The Pentagon
Washington 25, D.C.
(2)Attn: Technical Inf. Div.
(2) Weapons Effects Div.
(2) Special Field Proj.

Chief
Def. Atomic Support Agency
Washington 25, D.C.
(1)Attn: Document Lib. Br.

Off. of the Sec. of the Army
The Pentagon
Washington 25, D.C.
(1)Attn: Army Library

Chief of Staff
Dept. of the Army
Washington 25, D.C.
(1)Attn: Devel. Branch (Rand D Div.)
(1) Res. Br. (Rand D Div.)
(1) Spec. Weapons Br. (Rand D Div.)

Off. of the Chief of Eng.
Asst. Chief for Mil. Constr.
Dept. of the Army
Bldg. T-7, Gravelly Point
Washington 25, D C
(1)Attn: Library Branch
(1) Structural Br. (Eng. Div.)
(1) Planning and Dev. Div.
(1) Eng. Div. (P , Eng., and Contracts)
(1) Prot. Constr. Br. (P., Eng., and Contracts)
(1) Struc. Br. (P., Eng., and Contracts)

(1) Commanding Officer
Eng. Research and Devel. Lab.
Fort Belvoir, Va.

Office of the Chief of Ord.
Dept. of the Army
Washington 25, D.C.
(1)Attn: Res. and Mat. Br. (Ord. R and D. Div.)

Off. of the Chief Sig. Off.
Dept. of the Army
Washington 26, D C.
(1)Attn: Eng. and Tech. Div.

Commanding Officer
Watertown Arsenal
Watertown, Mass.
(1)Attn: Lab. Div.

Commanding Officer
Frankford Arsenal
Bridesburg Station
Philadelphia 37, Pa.
(1)Attn: Lab. Div.

Office of Ord. Res.
2127 Myrtle Drive
Duke Station
Durham, N.C
(1)Attn: Div. of Eng. Sci.

Commanding Officer
Squier Signal Lab.
Fort Monmouth, N. J.
(1)Attn: Comp. and Mat. Br.

Chief of Naval Operations
Dept. of the Navy
Washington 25, D.C.
(1)Attn: Op 37

(1)Commandant, Marine Corps
Headquarters, U. S. M C.
Washington 25, D.C

Chief, Bureau of Ships
Dept. of the Navy
Washington 25, D C
(2)Attn: Code 327
(2) Code 420
(2) Code 423
(2) Code 442

Chief, Bureau of Naval Weap.
Dept. of the Navy
Washington 25, D.C
(3)Attn: DLI-31

Chief, Bur. of Yards and Docks
Dept. of the Navy
Washington 25, D.C.
(1)Attn: Code D-210
(1) Code D-213
(1) Code D-220
(1) Code D-222
(1) Code D 410
(1) Code D-410C
(1) Code D-440
(1) Code D-500

Commanding Officer and Dir.
David Taylor Model Basin
Washington 7, D.C.
(1)Attn: Code 140
(1) Code 600
(1) Code 700
(1) Code 720
(1) Code 725
(1) Code 731
(2) Code 740

Commander
U. S Nav. Ord. Lab.
White Oak, Maryland
(2)Attn: Tech. Lib.
(1) Tech. Eval. Dept.

(1)Director
Materials Lab.
New York Nav. Shipyard
Brooklyn 1. New York

(2) Office-in-Charge
Nav. Civ. Eng. Res. & Eval. Lab.
U. S. Nav. Constr. Batt. Center
Fort Hueneme, Calif.

Director
Nav. Air Exper. Station
Nav. Air Mat. Center
Naval Base
Philadelphia 12, Pa.
(1) Attn: Mat. Lab.
(1) Structures Lab.

Officer-in-Charge
Underwater Expl. Res. Div.
Norfolk Naval Shipyard
Portsmouth, Va.
(2) Attn: Dr. A. H. Keil

(1) Commander
U. S. Nav. Proving Grounds
Dahlgren, Va.

(1) Superintendent
Naval Gun Factory
Washington 25, D.C.

Commander
Naval Ord. Test Station
Inyokern, China Lake, Calif.
(1) Attn: Physics Div.
(1) Mech. Br.

Commander
Nav. Ord. Test Station
Underwater Ord. Div.
3202 E Foothill Boul.
Pasadena 8, Calif.
(1) Attn: Structures Div.

(1) Commanding Officer & Dir.
Nav. Eng. Exper. Station
Annapolis, Maryland

(1) Superintendent
Nav. Post Grad. School
Monterey, Calif.

Commandant
Marine Corps Schools
Quantico, Va.
(1) Attn: Dir., Marine Corps Develop. Center

Commanding General
U. S. Air Force
Washington 25, D.C.
(1) Attn: Res. & Dev. Div.

Commander
Air Mat. Command
Wright-Patterson Air Force Base
Dayton, Ohio
(1) Attn: MCREX-B
(1) Structures Div.

Commander
U. S. Air Force Inst. of Tech.
Wright-Patterson Air Force Base
Dayton, Ohio
(1) Attn: Chief, Appl. Mech. Gr.

Commander
Wright Air Dev. Center
Wright-Patterson AFB
Dayton, Ohio
(1) Attn: Dyn. Br.
(1) Aircraft Lib.
(1) WCLSY

Director of Intelligence
Headquarters, USAF
Washington 25, D.C.
(1) Attn: P.V. Br. (Air Targets (Div.)

Commander
Air Res. and Dev. Command
P. O. Box 1395
Baltimore 3, Maryland
(1) Attn: RDMPE